國立臺灣大學理學院物理學系
博士論文
Department of Physics
College of Science
National Taiwan University
Doctoral Thesis

統計物理在化學主方程式、艾根模型及表面機械研磨處理的應用
Application of Statistical Physics in Chemical Master Equation, Eigen Model, and Surface Mechanical Attrition Treatment

黃冠榮
Guan-Rong Huang

指導教授：胡進錕博士
Advisor: Chin-Kun Hu , Ph.D.

中華民國 104 年 9 月
September, 2015

致謝

　　在台大五年多來，我能夠完成這篇論文，首先必須感謝我所有的指導教授：David Saakian，黃志青，余瑞琳和胡進錕博士。在論文研究問題的討論和修改，總是能給予許多的方向。讓我在每次討論中總是學到新的知識，觀念和方法。

　　感謝每次解析計算的討論中，David 教授總是一再的講解生物演化和化學主方程式的解析計算方法直到我可以完全理解。以及不遺餘力對於論文每個方程式的檢查與校正。感謝黃志青老師在材料科學計算中給予理論的方向，論文的修改和實驗數據的講解，其中，我也感謝在中山大學共同研究的時期，黃幫實驗室給予的照顧：生活起居和實驗數據的討論。特別是蔡濰猷學弟的幫忙，讓我心無旁騖專心做研究。感謝余瑞琳老師在數值方法上的指導，總是耐心地解說每一個步驟每一個原理，讓我在論文的數值計算部分，可以順利完成。感謝胡進錕博士提供我足夠的兼任助理薪水，讓我能夠專心在台大學習研究，以及在每篇論文的修改與審視和論文投稿的協助。

　　另外，我也感謝在博士班各位同學們互相支援幫助，感謝我的家人在博士班求學過程中全力支持。最後，感謝神讓我有這機會完成這篇論文。

Abstract

In macro, the method and concept of statistical physics can be a powerful tool in analytical and numerical computation and applied to many fields such as chemical reaction, bio-evolution, and material science. In our work, the methods of statistical physics: chemical master equation (CME), Hamilton-Jacobi equation (HJE), and canonical ensemble are used to calculate various physical quantities. Our work is organized in three topics: the CME with the Gaussian and compound Poisson noise, bio-evolution of Eigen model, and energy conversion in the surface mechanical attrition treatment (SMAT) experiment.

In the CME part, the chemical reaction among DNA, mRNA, and protein can be regarded as a stochastic process. We consider the CME with compound Poisson and Gaussian noises and obtain the exact solution of steady-state probability density function (PDF) verified by the algorithm of forward finite difference in large-scale time. Without Gaussian white noise, the solution of CME (set diffusion coefficient $\epsilon = 0$) can be returned to that of CME derived by Long Cai, et al.

In the bio-evolution part, we use the method of expansion in $O(\frac{1}{N})$ to obtain the HJE for probability distribution in Hamming class which is applied to calculate the correction of $O(\frac{1}{N})$ accuracy for the steady-state probability distribution in Hamming class and mean fitness in Eigen model. The steady-state distributions of $O(\frac{1}{N})$ correction are well-consistent with the Runge-Kutta simulation with relative errors less than 1 %, while the mean fitness

of $O(\frac{1}{N})$ is the same one derived by Michael Deem, et al. in quantum field theory.

In the SMAT part, we consider the collisions among the 304-steel balls, motor top, and chamber bottom, where the chamber or motor can be treated as a hot reservoir. Since we assume that all the collisions among them are elastic except the ball-sample collisions, the balls with negligible potential among them can be regarded as the canonical ensemble. By this concept, we construct the link for energy conversion among the motor top, sample bottom, and balls, where the kinetic energy, heat energy, and internal energy are included in the energy conversion. We also introduce the one-dimensional heat equation with uniform-distributed heat source to obtain the temperature distribution of sample, and we use this temperature distribution of sample to connect the Zenner-Hollmann parameter and the heat energy and surface hardness of sample.

Key words: chemical master equation, Gaussian white noise, compound Poisson noise, bio-evolution, Eigen model, SMAT, collision, energy conversion

Contents

List of Figures

List of Tables

Chapter 1

Introduction

This chapter is organized as the three following topics: the chemical master equation, bio-evolution, and SMAT experiment in a brief and general introduction. It makes the connection and correspondence among the techniques and concepts of statistical physics. Each section states the topic background and physical meaning of each equation.

1.1 Chemical Master Equation

The coupled chemical differential equations which are equivalent to a number of chemical reactions are common model to describe the chemical reactions among molecules, where such equations are described by variables: time-dependent concentration of each molecule and constants of temperature-dependent reaction rate. The changes of concentrations with time can be modelled by differential equations with the large number of each interacting molecules. In the same circumstance, two or more reactions can take place simultaneously. The meaning for the collection of coupled ordinary differential equations is that these reactions occur concurrently in the solution.

For the small number of interacting molecules, however, the simple deterministic process breaks down. Molecules are collided by stochastic process (drift or diffusion) described well by Ito lemma, so chemical reactions can't well described by some simultaneous processes. With the introduction of probability density function (PDF), $P(x,t)$, in terms of concentration for each molecule at a given time, the time-evolution of PDF

represents that reactions take place randomly among any possible reactions.

In recent years, biophysicists have paid more attention to stochastic dynamics in cell biology [1–6]. Friedman, Cai and Xie (FCX) obtained an partial differential equation (PDE) to describe the steady-state PDF of protein concentration for living cells in gene expression problem [1]. Losick and Desplan found that noises can induce cells to switch between different gene states in their experiments [2]. Thus, the PDF of stochastic process is a tool to describe stochastic reactions in cell biology.

From Itδ's lemma [7], the total differential of concentration

$$dx = b(x)dt + \sqrt{2\epsilon}dB, \tag{1.1}$$

, where B is the Brownian motion, we can derive the corresponding Kolmogorov forward equation (KFE), i.e. the chemical master equation (CME),

$$\frac{\partial P(x,t)}{\partial t} = \epsilon\frac{\partial^2 P(x,t)}{\partial x^2} - \frac{\partial}{\partial x}[b(x)P(x,t)], \tag{1.2}$$

obeyed by PDF related to large deviation function or WKB expansion in quantum mechanics, $P(x,t) = e^{\frac{-1}{\epsilon}u_\epsilon(x,t)}$. The equation for large deviation function is:

$$\begin{aligned}
\frac{\partial u_\epsilon(x,t)}{\partial t} &= -[(\frac{\partial u_\epsilon(x,t)}{\partial x})^2 + b(x)\frac{\partial u_\epsilon(x,t)}{\partial x}] \\
&+ \epsilon[\frac{\partial^2 u_\epsilon(x,t)}{\partial x^2} + \frac{db(x)}{dx}],
\end{aligned} \tag{1.3}$$

which reduces to Hamilton-Jacobi equation (HJE) with $\epsilon = 0$, where x is the time-dependent concentration, and ϵ is a small perturbed constant. In classical mechanics (CM), the right-handed term is negative Hamiltonian, and $u_\epsilon(x,t)$ is the generating function for corresponding canonical transformation (CT).

For correspondence, we can consider a chemical reaction whose concentration x described by ordinary differential equation (ODE),

$$\frac{dx}{dt} = b(x), \tag{1.4}$$

where the ODE can be re-written into Itõ's lemma by the introduction of B white noise after diffusive perturbation. Equation (1.4) is equivalent to Eq. (1.1) with $\epsilon = 0$, and the $u(x,t) = \lim_{\epsilon \to 0} u_\epsilon(x,t)$ is called the principal function furnishing the entire family of orbits corresponding to Hamiltonian system in phase space. The corresponding Hamiltonian has the form,

$$H(q,p) = p^2 + b(q)p, \tag{1.5}$$

which follows the equation of motion,

$$\dot{q} = \frac{\partial H}{\partial p} = 2p + b(q)$$
$$\dot{p} = -\frac{\partial H}{\partial q} = -p\frac{db(q)}{dq}, \tag{1.6}$$

and has the following Lagrangian,

$$L(q,\dot{q}) = [p\dot{q} - H(q,p)]_{p=\frac{1}{2}(\dot{q}-b(q))} = \frac{1}{4}(\dot{q} - b(q))^2, \tag{1.7}$$

which corresponds to the action functional,

$$S_0[q(t); (0, q(0)) \to (t, q(t))] = \int_0^t d\tau \frac{1}{4}[\frac{dq(\tau)}{d\tau} - b(q(\tau))]^2. \tag{1.8}$$

This is equivalent to path integral in quantum mechanics by making the integration path along imaginary axis in complex plane, and the probability of the system is proportional to e^{-S_0/ϵ_0} which is exactly the probability for a path in stochastic dynamics in Eq. (1.4) with $\epsilon = 0$. For finite ϵ, the action functional generalized by Onsager and Machlup is $S_\epsilon = S_0 + \frac{\epsilon}{2}b'(q)$ [8–10].

On the other hand, the corresponding CME can be obtained by the chemical system with n molecules,

$$\frac{\partial P(n,t)}{\partial t} = N[R_+(n-1)P(n-1,t)$$
$$+ R_-(n+1)P(n+1,t) - [R_+(n) + R_-(n)]P(n,t)], \tag{1.9}$$

where N is a large integer and a maximal allowed number of molecules, R_+ is the growth rate, and R_- is the degradation rate. And the equation should be modified at the border. Let us use the variable, $x = \frac{n}{N}$, to re-write Eq. (1.9) in terms of x as

$$
\begin{aligned}
\frac{1}{N}\frac{\partial P(x,t)}{\partial t} &= R_+(x - \frac{1}{N})P(x - \frac{1}{N}, t) \\
&+ R_-(x + \frac{1}{N})P(x + \frac{1}{N}, t) - [R_+(x) + R_-(x)]P(x,t). \quad (1.10)
\end{aligned}
$$

With the largeness of N, x becomes continuous from discrete. By using the ansatz (Or WKB method),

$$
P(x,t) = exp[Nu(x,t)], \quad (1.11)
$$

to construct a equation for $P(x,t)$. By using HJE with $N \to \infty$ [11–15], the partial differential equations can be solved exactly as the following steps:

$$
\begin{aligned}
\frac{\partial u}{\partial t} + H(x, u') &= 0, \\
H(x, u') &= [R_+(x) - R_-(x)]u',
\end{aligned}
$$

and the corresponding equation of motion for x:

$$
\begin{aligned}
\dot{x}(t) &= \frac{\partial H}{\partial u'} \\
&= R_+(x) - R_-(x) = b(x), \quad (1.12)
\end{aligned}
$$

where $u' = \frac{\partial u}{\partial x}$. The distribution variance has been derived in [15]:

$$
b^2(x) \int_{x_0}^{x} \frac{c(y)}{b^3(y)}, \quad (1.13)
$$

where $c(y) = R_+(y) + R_-(y)$. With these results, we can formulate new CME with different process or noise.

The rest of CME topic is organized as follows: Firstly, we use HJE as a tool to investigate the physical of chemical system and solve the CME. Secondly, we introduce the drift-diffusion process to generalize PDF for chemical reactions [16, 17], which de-

scribes how to make the correspondence probability of chemical reaction by path integral and formulate CME with white noise [18]. Finally, we introduce the hybrid model of Gaussian and Poisson noise solved exactly and verified by the forward finite difference simulation [19], and we make conclusion about this hybrid model.
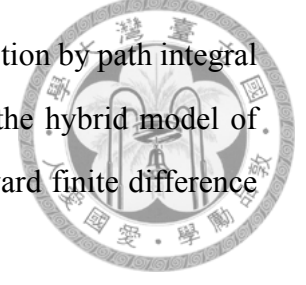
1.2 Bio-evolution

It's widely acknowledged that DNA can carry hereditary code to determine the life performance, and it has the important influence on the reproduction and survival for each specie. As we all know that the positive self-regulation or mutation of gene can help species adapt to their surroundings for survival, and such processes called bio-evolution. Exact bio-evolution results, the mean fitness, steady state distribution , and dynamics for genes are obtained by the tool of statistical physics and mathematics [20], HJE method, partial differential equation, and numerical simulation, which makes possibility to realize the mechanism of virus or cancer evolution.

In past decades, the bio-evolution process of virus is described very well by the Eigen and Crow-Kimura models for large population size or genome size [20–27]. In the two models, the fractions of population for different types p_i are described by a set of deterministic partial differential equations. The corresponding HJE for the two models can be obtained by expanding p_i in the order of $O(\frac{1}{N})$, $p_i = \exp(Nu_i)$, where N is the genome length. Since N is possibly $40 \sim 100$ [28], it's important to investigate the finite population effect of $\frac{1}{N}$ in a small N genome.

For the sake of simplicity, we can assume there are two different genotypes (denoted as ± 1) for each nucleotide, and the N-nucleotide genome has 2^N types. We have the following system of equations in Eigen model for each probability p_i,

$$\frac{\partial p_i}{\partial t} = \sum_{j=1}^{2^N} (Q_{ij}) r_j p_j - p_i (\sum_{j=1}^{2^N} r_j p_j),$$ (1.14)

where the p_i satisfies $\sum_i p_i = 1$, the mean fitness r_i is the mean number of offspring per unit cycle for type i sequence, and mutation matrix with the mean nucleotide incorporation

fidelity q is expressed as:

$$Q_{ij} = q^{N-d_{ij}}(1-q)^{d_{ij}}, \qquad (1.15)$$

where d_{ij} is the Hamming distance (HD) between two sequences, S_i and S_j, defined as:

$$d_{ij} = (N - \sum_{l=1}^{N} s_i^l s_j^l)/2, \qquad (1.16)$$

where s_i^l is the spin with possible values ± 1 at l-th site in S_i. To simplify the HD between sequences, we can choose a reference sequence S_0 with all spins being $+1$. Without loss of generality, sequences with the same number of -1 spin are assumed to have the same probability, namely, it's symmetrical distribution. Thus, 2^N types are divided into $N + 1$ Hamming class, and the HD can be written as

$$d_{l0} = (N - \sum_{i=1}^{N} s_l^i)/2 = l, \qquad (1.17)$$

where $0 \leq l \leq N$ and l is the number of -1 spin for a sequence. With symmetrical distribution, we can also assume the mean fitness r_i in terms of m is symmetrical,

$$r_i = f(m), \qquad (1.18)$$

where $m = 1 - \frac{2l}{N}$ between ± 1 called magnetization and $f(m)$ is called the fitness function. Therefore, the original Eigen model with 2^N equations is transformed into Eigen model with $N + 1$ equations with which is easy to be treated. This model with $p_i = exp[Nu(m,t) + u_1]$ expansion is lead to HJE equation as we did in CME and other high order of $\frac{1}{N}$ equations on which the work of finite correction is based.

The rest of bio-evolution topics is organized as follows: Firstly, we introduce Crow-Kimura model and derive its some properties. Secondly, HJE is obtained by WKB expansion of p_i to investigate the characteristic of Crow-Kimura model, and then we develop HJE method and derive some useful formula from Crow-Kimura model which can be a useful tool for the finite correction of Eigen model. Finally, we solve Eigen model with $N + 1$ class in $O(\frac{1}{N})$ accuracy, and it's verified by the numerical simulation, Runge-Kutta

method.

1.3 SMAT modelling

In traditional engineering treatments, shot peening by using steel balls to bombard onto metal surfaces has been adopted to leave compressive residual strains within the affected region in promoting the fatigue properties [29, 30]. The balls have typical diameters of $0.1 \sim 2\ mm$ and gain their speed by compressed air. Normally, these balls bombard the metal surfaces in the frequency range of $20 \sim 100\ Hz$ and speed range of $50 \sim 100\ m/s$.

A new physical treatment named ultrasonic surface mechanical attrition treatment (SMAT) was firstly introduced in 1999 [31, 32]. The SMAT balls are accelerated and bombarded by the ultrasonic motor on the chamber bottom, as shown in Fig. 1.1 (a). The diameter and speed of flying balls and the bombarding frequency are in the range, $1 \sim 10\ mm$, $1 \sim 20\ m/s$, and $10 \sim 100\ kHz$ [33], respectively. The most important feature is that the incident direction onto the metal surface can be designed to vary with time lapse in making smaller grain size of metallic materials. This will lead to promising properties of metals such as grain refinement and gradient structure. And researchers have made extensive uses of this SMAT treatment on various metallic materials including pure iron [34], stainless steel [35], and pure copper [36] in making gradient and nano-crystalline structure [37–40].

Although SMAT has gradually developed into a matured engineering surface treatment, never before has SMAT been treated with rigorous analytical modelling. Therefore, a systematic SMAT model is actually needed. Here, we consider the interaction between flying balls and chamber imagined as a canonical ensemble, where chamber is reservoir giving balls the kinetic, internal, and heat energy. The chamber volume is much greater than balls volume, so collision frequency between balls is small compared to that between balls and chamber and balls interaction can be neglected. The motion of motor top is characterized by longitudinal harmonic motion,

$$v_m = 2A\pi\nu sin(2\pi\nu t), \tag{1.19}$$

where v_m is the velocity of motor top, A is the amplitude, and ν is the angular frequency. To construct the relation of energy conversion between motor top and balls, the ball-motor collision can be counted as elastic collision. Thus, the induced velocity of ball, v_b, is described by

$$v_b = \frac{2m_m v_m}{m_b + m_m} \approx 2v_m, \ m_m >> m_b,\ \ \ (1.20)$$

where m_b and m_m are the mass of each ball and motor. On the other hand, the ball-sample collision is assumed to be inelastic collision with restitution constant e obeying conservation of momentum,

$$e = \frac{v'_s - v'_b}{v_b - v_s}, m_s v_s + m_b v_b = m_s v'_s + m_b v'_b, \ \ \ (1.21)$$

where m_s and v_s are sample mass and velocity, respectively.

The kinetic energy of flying balls is not conserved due to the inelastic ball-sample collision. The kinetic energy loss for flying balls and sample in the SMAT chamber can be mainly converted into three parts as indicated in Fig. 1.1 (b). Firstly, it is the strain energy of sample due to the formation of dislocations and vacancies [41–43]. Secondly, it is the heat energy of sample, where the heat flow and its temperature distribution are both important factors for the resulting metal micro-structure [44]. Recrystallization might be taken place in the sample while the experienced temperature reaches some critical values. Finally, it would be the sonic energy and heat energy in the chamber originated from the inelastic collisions between flying balls.

In SMAT topics, we have established connections among the parameters of flying balls, the ball size, flying speed, the bombarding frequency and amplitude of motor motion, the height of chamber, and the energy and power of sample. During the SMAT processing time, we can find the input energy and power of sample through these connections. The condition for the frequency of flying ball reaching a stead speed can also be obtained in this approach. For the heat energy of sample, we have introduced the one-dimensional heat equation with the uniformly-distributed heat source to estimate the heat flow and temperature distribution of sample which are hard to be measured in the SMAT

experiment. With the temperature distribution of sample, we can make connection among the strain rate, hardness, and grain size of sample. With these connections and modelling, one can find an optimized approach to the mechanical performance of metal surface via the SMAT experiment.
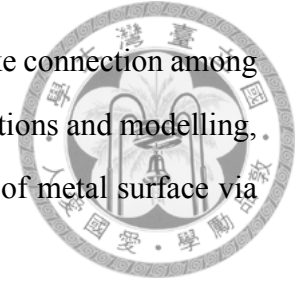
Chapter 2

Basic theory for CME, Bio-evolution, and SMAT

2.1 Hamilton-Jacobi Equation

In Classical Mechanics (CM) [45], theoretical physicists use independent variable of position x and momentum p for each particle in constructing Hamiltonian to characterize the particle dynamics, where the correspond equation of motion constructed by Hamiltonian for x and p is the Hamilton equation. To simplify the equation of motion, we prefer the physical system in which all of the generalized coordinates or all of the canonical momentums are cyclic, namely, Hamiltonian with respect to x and p is a constant. To achieve the goal, a canonical transformation (CT) under which the equation of motion is invariant should be found, and any CT corresponds to a generating function consisted of half new and half old generalized coordinates. Here comes the Hamilton-Jacobi equation (HJE) which generating function satisfies.

In stochastic dynamics, a fictitious Hamiltonian which is similar to that of CM as a tool to formulate the Lagrangian and the action functional by using the WKB expansion, $P(x_t, t) = e^{-\frac{1}{\epsilon} u_\epsilon(x_t, t)}$ with small ϵ, where ϵ results from diffusion. And such WKB expansion we use in bio-evolution is $P(x, t) = e^{Nu(x,t)}$ with large N, where the N is genome length or population size. It's obviously that both expansions are mathematically equiva-

lent for small ϵ or large N. In our work for CME or bio-evolution, we put such expansion into the equation of motion (KFE or evolution model) with condition $\epsilon \to 0^+$ or $N >> 1$ to get the HJE for u. As $\epsilon \to 0^+$ or $N >> 1$, $\lim_{\epsilon \to 0^+} u_\epsilon(x_t, t)$ is called the large deviation rate function in probability theory [46] or the principal function in CM [45]. The large deviation rate function asymptotes the behaviour of $P(x_t, t)$ as $\epsilon \to 0^+$ or $N \to \infty$, and the principal function furnishes the entire family of orbits corresponding to a Hamiltonian system in phase space.

In our research, HJE in chemical reaction derives the path probability of each reaction while HJE in bio-evolution derives a series of equation for finite correction of $O(\frac{1}{N})$. Here we give some derivation and introduction to HJE in CM.

2.1.1 Canonical Transformation

In CM, the form of Hamilton's equations are invariant under canonical transformation (CT) and Hamilton's principle states that the most possible track of classical system makes the corresponding action functional minimized. Thus, we have the variation of action functional is 0 over the most possible track:

$$\delta \int_{t_1}^{t_2} L(q, \dot{q}, t) dt = 0,$$
$$\delta \int_{t_1}^{t_2} L'(q, \dot{q}, t) dt = 0,$$
$$\delta \int_{t_1}^{t_2} [p_i \dot{q}_i - H(q, p, t)] dt = 0,$$
$$\delta \int_{t_1}^{t_2} [P_i \dot{Q}_i - K(q, p, t)] dt = 0,$$

which implies:

$$\lambda[p_i \dot{q}_i - H(q, p, t)] = P_i \dot{Q}_i - K(q, p, t) + \frac{dF}{dt},$$

where q and p are old generalized coordinates, Q and P are new generalized coordinates, L, L', H, and K are the corresponding Lagrangian respectively, λ is a scale constant, and F is corresponding generating function in terms of half new and half old coordinates. For

the $\lambda = 1$ case, it's the case called CT in CM. With $\lambda = 1$, the equation becomes:

$$p_i \dot{q}_i - H(q, p, t) = P_i \dot{Q}_i - K(q, p, t) + \frac{dF}{dt},$$ (2.1)

where F called the generating function has four basic forms by [45],

$$\begin{cases} F = F_1(q, Q, t) \\ F = F_2(q, P, t) - P_i Q_i \\ F = F_3(p, Q, t) + p_i q_i \\ F = F_4(p, P, t) + p_i q_i - P_i Q_i \end{cases}.$$ (2.2)

2.1.2 Hamilton-Jacobi Equation

We start the derivation of Hamilton-Jacobi equation (HJE) from Eq. (2.1) and put the generating function F_2 in Eq. (2.2) to arrive:

$$\begin{aligned} p_i \dot{q}_i - H(q, p, t) &= P_i \dot{Q}_i - K(Q, P, t) + \frac{dF}{dt} \\ &= P_i \dot{Q}_i - K(Q, P, t) + \frac{\partial F_2}{\partial t} + \frac{\partial F_2}{\partial q_i} \dot{q}_i + \frac{\partial F_2}{\partial p_i} \dot{p}_i - \dot{P}_i Q_i - P_i \dot{Q}_i \\ &= -K(Q, P, t) - \dot{P}_i Q_i + \frac{\partial F_2}{\partial t} + \frac{\partial F_2}{\partial q_i} \dot{q}_i + \frac{\partial F_2}{\partial p_i} \dot{p}_i. \end{aligned}$$

Then we rearrange it and have the equation:

$$[H(q, p, t) + \frac{\partial F_2}{\partial t} - K(Q, P, t)] + (\frac{\partial F_2}{\partial q_i} - p_i) \dot{q}_i + (\frac{\partial F_2}{\partial P_i} - Q_i) \dot{P}_i = 0,$$ (2.3)

where $\dot{q}_i$ and $\dot{P}_i$ are separated independently. Since the three terms in Eq. (2.3) are independent of each other, the three terms must be 0 to hold the equality. Therefore,

$$\frac{\partial F_2}{\partial q_i} = p_i, \frac{\partial F_2}{\partial P_i} = Q_i,$$

$$H(q, p, t) + \frac{\partial F_2}{\partial t} = K(Q, P, t).$$ (2.4)

To make all generalized coordinates cyclic, we can set $K(Q, P, t) = 0$. And the corresponding Hamilton's equations are:

$$\dot{Q}_i = \frac{\partial K}{\partial P_i} = 0,$$
$$\dot{P}_i = -\frac{\partial K}{\partial Q_i} = 0,$$

which means that all generalized coordinates are constants of motion. On the other hand, making $K(Q, P, t) = 0$ gives the corresponding equation for F_2:

$$H(q, p, t) + \frac{\partial F_2}{\partial t} = 0,$$
$$\rightarrow H(\vec{q}, \frac{\partial F_2}{\partial \vec{q}}, t) + \frac{\partial F_2}{\partial t} = 0, \tag{2.5}$$

where Eq. (2.5) is called Hamilton-Jacobi equation and F_2 is the Hamilton's principal function in CM which is the counterpart of $u(x, t)$ in stochastic dynamics. To investigate the physical meaning of F_2, we can take its total differential with respect to t:

$$
\begin{aligned}
\frac{dF_2}{dt} &= \frac{\partial F_2}{\partial q_i}\dot{q}_i + \frac{\partial F_2}{\partial P_i}\dot{P}_i + \frac{\partial F_2}{\partial t} \\
&= p_i\dot{q}_i - H(q, p, t) = L(q, \dot{q}, t),
\end{aligned}
$$

and then we integrate $\frac{dF_2}{dt}$ back with respect to t:

$$F_2 = \int_{t_0}^{t} L(q, \dot{q}, t')dt',$$

which states that the Hamilton's principal function F_2 is equivalent to action functional. Thus, in physics, solving the HJE is equivalent to solve the variation equation of action functional, Euler-Lagrange equation.

2.1.3 HJE Application in CME

The HJE method in CM has been well developed for hundreds years, and it is a power and analytical tool to investigate the characteristic of physical system in macro. Thus, we

want to develop the HJE method in CME to help us realize the mechanism of chemical system. As stated in previous sections, the principal function $u(x,t)$ in stochastic dynamics is similar to the role of generating function in CM. Here we introduce a fictitious Hamiltonian corresponding to HJE in CM. In the introduction of CME, we have the following CME for general chemical system with n molecules:

$$
\frac{\partial P(x,t)}{N \partial t} = R_+(x - \frac{1}{N})P(x - \frac{1}{N}, t) + R_-(x + \frac{1}{N})P(x + \frac{1}{N}, t)
$$
$$
- [R_+(x) + R_-(x)]P(x,t), \qquad (2.6)
$$

where N is the maximally-allowed number of molecule, $x = \frac{n}{N}$, and R_+ and R_- are the rate of generation and degradation. By Taylor expansion with largeness of N at x and $P(x,t) = \exp[Nu(x,t)]$, we have:

$$
R_+(x - \frac{1}{N}) \approx R_+(x) - \frac{1}{N}\frac{\partial R_+(x)}{\partial x},
$$
$$
R_-(x + \frac{1}{N}) \approx R_-(x) + \frac{1}{N}\frac{\partial R_-(x)}{\partial x},
$$
$$
P(x \mp \frac{1}{N}, t) \approx P(x,t) \mp \frac{1}{N}\frac{\partial P(x,t)}{\partial x}
$$
$$
= P(x,t)[1 \mp \frac{\partial u(x,t)}{\partial x}],
$$
$$
\frac{\partial P(x,t)}{\partial t} = N\frac{\partial u(x,t)}{\partial t}P(x,t).
$$

Put these expansions above into Eq. (2.6) to get the equation of zero order in $\frac{1}{N}$:

$$
\frac{\partial u}{\partial t}P(x,t) = [R_+(x)(1 - \frac{\partial u}{\partial x}) + R_-(x)(1 + \frac{\partial u}{\partial x}) - (R_+(x) + R_-(x))]P(x,t), \quad (2.7)
$$

and divide both sides of Eq. (2.7) by $P(x,t)$ and let $u' = \frac{\partial u}{\partial x}$ to obtain:

$$
\frac{\partial u}{\partial t} + [R_+(x) - R_-(x)]u' = \frac{\partial u}{\partial t} + H(x, u') = 0. \qquad (2.8)
$$

Equation (2.8) has the exact form of HJE, where u corresponds to generating function in CT and H corresponds to Hamilton in CM. Thus, the fictitious Hamiltonian and equation

of motion are shown as:

$$H(x, u') = [R_+(x) - R_-(x)]u',$$
$$\dot{x}(t) = \frac{\partial H(x, u')}{\partial u'} = R_+(x) - R_-(x) = b(x),$$

where $b(x) = R_+(x) - R_-(x)$. It is reasonable for chemical reaction of zero order whose concentration obeys the ordinary differential equation. And the variance of $P(x, t)$ has been derived in [15]:

$$b^2(x) \int_{x_0}^{x} \frac{c(y)}{b^3(y)} dy, \tag{2.9}$$

where $c(y) = R_+(y) + R_-(y)$ and x_0 is the reference point. Therefore, each chemical system actually corresponds to a fictitious Hamiltonian system derived from CME of each chemical system.

2.2 Diffusion Process

Stochastic or random process is always related to diffusion process which can be traced back to Brownian motion. The random motion of particles suspended in water and reported by Robert Brown in 1827 is known as Brownian motion or Wiener process, which is the most important case in stochastic process. Some scientists in earlier periods considered that Brownian motion is caused by living cells, and Poincaré thought this motion violates the second law of thermodynamics. Now scientists consider that such molecule motion is induced by the continuous collision of molecules around them. For general situation, a specific molecule undergoes 10^{20} collisions per second. In 1905, Albert Einstein described Brownian motion in term of PDF equation by the kinetic molecular theory. He proved that the PDF motion satisfied the following partial differential equation (PDE),

$$\frac{\partial P}{\partial t} = D \frac{\partial^2 P}{\partial x^2}, \tag{2.10}$$

where the positive D is a diffusion coefficient and x is the particle position. By changing of variables, $y = \frac{x}{\sqrt{2D}}$, the PDE equation can be transformed into the form of heat equation:

$$\frac{\partial P}{\partial t} = \frac{1}{2}\frac{\partial^2 P}{\partial x^2},\qquad(2.11)$$

whose well-known solution is

$$P(x,t) = \frac{1}{\sqrt{4\pi Dt}}exp[-\frac{(x-x_0)^2}{4Dt}],\qquad(2.12)$$

where x_0 is the mean position of particle, t is the time, and it is Gaussian distribution for any given time.

Kiyoshi Itõ, a Japanese mathematician, came up a good idea to describe the drift-diffusion process by Itõ's lemma:

$$dX_t = \mu(X_t, t)dt + \sigma(X_t, t)dB_t,\qquad(2.13)$$

which states that the random variable dB_t makes an impact on other deterministic variables in a small time interval Δt; the expectation value $E[dX_t]$ is unchanged for an entire cycle. The derivatives of Itõ's lemma is the stochastic differential equation which is widely used in financial and biological physics. From Itõ's lemma, we also derive the equation of motion for PDF, Kolmogorov forward equation (KFE), which is substantial to many fields related to stochastic process.

2.2.1 Brownian Motion

Brownian motion is the process of foundation for various stochastic processes, and here we derive it from central limit theorem. Considering one particle, it undergoes a collision to step Δx displacement after a time-interval Δt which is independent of the particle position. Also we consider the probabilities of stepping Δx and $-\Delta x$ are p and $1-p$ respectively. With largeness of container volume, particles are far away from container border. The particle motion can be treated as the independent 1D-random walk. The

particle location at a specific time t, $X(t)$, is expressed as:

$$X(t) = \Delta x(I_1 + I_2 + ... + I_{[\frac{t}{\Delta t}]}),$$ (2.14)

where the I_i is 1 or -1 depending on i-th displacement which is $+\Delta x$ or $-\Delta x$, $[\,]$ is the Gauss function, and the corresponding probabilities for different displacement ($\pm\Delta x$) are:

$$P(I_i = 1) = p, P(I_i) = 1 - p.$$ (2.15)

To simplify the derivation of Brownian motion, we can set the following variables:

$$\Delta x = \sigma\sqrt{\Delta t}, p = \frac{1}{2} + \frac{\sqrt{\Delta t}}{2\sigma}\mu,$$
$$n = \lim_{\Delta t \to 0}[\frac{t}{\Delta t}] = \lim_{\Delta t \to 0}\frac{t}{\Delta t}.$$ (2.16)

We can prove Eq. (2.16) by sandwich theorem:

$$\frac{t}{\Delta t} \geq [\frac{t}{\Delta t}] \geq \frac{t}{\Delta t} + 1,$$
$$\because \lim_{\Delta t \to 0}\frac{t}{\Delta t} + 1 = \lim_{\Delta t \to 0}\frac{t + \Delta t}{\Delta t} = \lim_{\Delta t \to 0}\frac{t}{\Delta t},$$
$$\therefore \lim_{\Delta t \to 0}[\frac{t}{\Delta t}] = \lim_{\Delta t \to 0}\frac{t}{\Delta t}.$$ (2.17)

We have the expectation value of $I_i\Delta x$,

$$
\begin{aligned}
E[I_i\Delta x] &= p \times \Delta x + (1 - p) \times (-\Delta x) \\
&= (\frac{1}{2} + \frac{\sqrt{\Delta t}}{2\sigma}\mu - \frac{1}{2} + \frac{\sqrt{\Delta t}}{2\sigma}\mu)\sigma\sqrt{\Delta t} \\
&= \mu\Delta t,
\end{aligned}
$$ (2.18)

and the variance of $I_i\Delta x$,

$$
\begin{aligned}
V[I_i\Delta x] &= E[(I_i\Delta x)^2] - E^2[I_i\Delta x] \\
&= E[\Delta x^2] - \mu^2(\Delta t)^2 = (\sigma^2 - \mu^2\Delta t)\Delta t,
\end{aligned}
$$

where μ and σ are both time-independent constants. For $p = \frac{1}{2}$ case, the $E[I_i \Delta x] = 0$ and $V[I_i \Delta x] = \sigma^2 \Delta t$. Therefore, the expectation value and variance of $X(t)$ for $p = \frac{1}{2}$ case are:
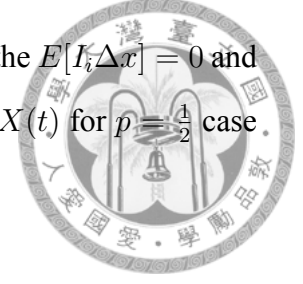
$$E[X(t)] = nE[I_i \Delta x] = 0,$$

$$V[X(t)] = n\sigma^2 \Delta t = \sigma^2 t,$$

and the position distribution of particle can be derived from central limit theorem as $\Delta t \to 0$:

$$
\begin{aligned}
z &= \frac{X(t) - n\mu\Delta t}{\sigma\sqrt{n\Delta t}} = \frac{X(t) - X_0}{\sigma\sqrt{t}} \to \frac{1}{\sqrt{2\pi}}e^{\frac{-z^2}{2}}, \\
&\to \frac{1}{\sqrt{2\pi}}\exp\left[-\frac{(X(t) - X_0)^2}{2\sigma^2 t}\right] \to \mathbf{N}(X_0, \sigma t),
\end{aligned}
\tag{2.19}
$$

where $\mathbf{N}(X_0, \sigma t)$ is the Gaussian distribution with expectation value $X_0 = \mu t$ and variance $\sigma^2 t$ for a given time t. The motion with $\mu = 0$ and $\sigma^2 = 1$ is called standard Brownian motion (SBM). Since any Brownian motion can be transformed into SBM, only SBM have to be taken into account. Thus, such SBM lead to the important conclusion that each particle position is normally distributed with expectation value 0 and variance 1.

2.2.2 Itõ's Lemma

In previous sections, the deterministic term μ which is so-called drift term is interfered by non-deterministic term σ which is so-called diffusion term, and any drift-diffusion process is well described by Itõ's lemma. In physics, we also have the corresponding counterpart that the specific track of each quantum particle is unpredictable due to the wave-particle property, so do we have deterministic term (mean particle position) and non-deterministic term (track). For the total differential of any function $f(x, t)$ in terms of x and t with the influence of B_t, the useful consequence,

$$df(x, t) = (\mu\frac{\partial f}{\partial x} + \frac{\sigma^2}{2}\frac{\partial^2 f}{\partial x^2} + \frac{\partial f}{\partial t})dt + \sigma\frac{\partial f}{\partial x}dB_t, \tag{2.20}$$

can be derived from Itô's lemma. Before proving the formula above, we need to prove the equality:

$$dB_t^2 = dt. \tag{2.21}$$

To prove this, we at first set S with $t_n = t$ as:

$$S = \lim_{n\to\infty} \sum_{k=1}^{n} (B_{t_k} - B_{t_{k-1}})^2, \tag{2.22}$$

where $B_{t_k} - B_{t_{k-1}}$ is Brownian motion in the time interval, $\Delta t = t_k - t_{k-1}$, and $B_{t_k} - B_{t_{k-1}} = dB_{t_k}$ and $\Delta t = t_k - t_{k-1} = dt$ in the case of $n \to \infty$. Then we take the expectation of S:

$$
\begin{aligned}
E(S) &= \lim_{n\to\infty} \sum_{k=1}^{n} (B_{t_k} - B_{t_{k-1}})^2 \\
&= \lim_{n\to\infty} \sum_{k=1}^{n} E[(B_{t_k} - B_{t_{k-1}})^2]] \\
&= \lim_{n\to\infty} \sum_{k=1}^{n} (t_k - t_{k-1}) = t, \tag{2.23}
\end{aligned}
$$

and the variance of S:

$$
\begin{aligned}
V(S) &= \lim_{n\to\infty} \sum_{k=1}^{n} V[(B_{t_k} - B_{t_{k-1}})^2] \\
&= \lim_{n\to\infty} \sum_{k=1}^{n} \{ E[(B_{t_k} - B_{t_{k-1}})^4] - E^2[(B_{t_k} - B_{t_{k-1}})^2] \} \\
&= \lim_{n\to\infty} \sum_{k=1}^{n} [3(t_k - t_{k-1})^2 - (t_k - t_{k-1})^2] \\
&= \lim_{n\to\infty} \sum_{k=1}^{n} 2(t_k - t_{k-1})^2,
\end{aligned}
$$

where here we have used the result, $\int_{-\infty}^{\infty} x^4 \mathbf{N}(0, \Delta t) dx = 3\Delta t^2 = 3(t_k - t_{k-1})^2$. We can derive $V(S) = 0$ as follows:

$$
\begin{aligned}
V(S) &= \lim_{n \to \infty} \sum_{k=1}^{n} 2(t_k - t_{k-1})^2 \\
&\leq \lim_{n \to \infty} 2 \max_{k}(t_k - t_{k-1}) \sum_{k=1}^{n} (t_k - t_{k-1}) \\
&= 2t \lim_{n \to \infty} \max_{k}(t_k - t_{k-1}) = 0.
\end{aligned} \tag{2.24}
$$

As $n \to \infty$, the corresponding integral to $E(S)$ is:

$$
E(S) = \int_0^t dB_{t'}^2 = t, \tag{2.25}
$$

which states $dB_t^2 = dt$, and $V(S) = 0$ implies that dB_t^2 is a measurable variable. Thus, we can immediately deduce that $dB_t^2 = dt$. On the other hand, we have the corresponding counterpart in quantum mechanics, Heisenberg Uncertainty Principal, which states: If two physical observables are measured simultaneously, their commutator is 0. Here comes the simple proof from this principle,

$$
\begin{aligned}
&[dB_t^2, dt] = 0 \to dB_t^2 = cdt, \\
&dt = E[dB_t^2] = cE[dt] = cdt, \\
&\to c = 1, \quad \therefore dB_t^2 = dt, \# \tag{2.26}
\end{aligned}
$$

where c is a phase constant. Now we turn to derive Eq. (2.20) by this equality. We have the following Taylor expansion near (x, t) point,

$$
\begin{aligned}
f(x + \Delta x, t + \Delta t) &\approx f(x, t) + \frac{\partial f}{\partial x} \Delta x + \frac{\partial f}{\partial t} \Delta t \\
&+ \frac{1}{2!} \frac{\partial^2 f}{\partial x^2} (\Delta x)^2 + \frac{\partial f}{\partial x} \frac{\partial f}{\partial t} \Delta t \Delta x + \frac{1}{2!} \frac{\partial^2 f}{\partial t^2} (\Delta t)^2.
\end{aligned}
$$

From Eq. (2.13), we also have:

$$
\Delta x = \mu \Delta t + \sigma \Delta B_t.
$$

Subtract $f(x, t)$ from the both sides of Taylor expansion to obtain the Δf:

$$
\begin{aligned}
\Delta f &= f(x + \Delta x, t + \Delta t) - f(x, t) \\
&\approx \frac{\partial f}{\partial x}(\mu \Delta t + \sigma \Delta B_t) + \frac{\partial f}{\partial t}\Delta t + \frac{1}{2}\frac{\partial^2 f}{\partial x^2}(\mu \Delta t + \sigma \Delta B_t)^2 \\
&+ \frac{\partial f}{\partial x}\frac{\partial f}{\partial t}(\mu \Delta t + \sigma \Delta B_t)\Delta t + \frac{1}{2}\frac{\partial^2 f}{\partial t^2}(\Delta t)^2 \\
&\approx (\mu\frac{\partial f}{\partial x} + \frac{\partial f}{\partial t})\Delta t + \frac{\sigma^2}{2}\frac{\partial^2 f}{\partial x^2}\Delta B_t^2 + \sigma\frac{\partial f}{\partial x}\Delta B_t,
\end{aligned}
$$
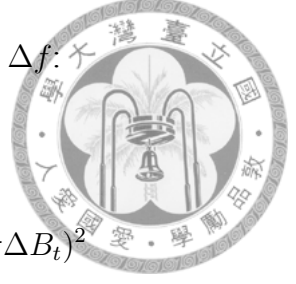
where the approximation has ignored the high order terms, and take the expectation of Δf:

$$
E[\Delta f] \approx (\mu\frac{\partial f}{\partial x} + \frac{\partial f}{\partial t} + \frac{\sigma^2}{2}\frac{\partial^2 f}{\partial x^2})\Delta t.
$$

Under the condition of $\Delta t \to 0$, the higher order terms of Δt disappears. And the random part of f changes is:

$$
\Delta f - E[\Delta f] \approx \sigma\frac{\partial f}{\partial x}\Delta B_t.
$$

Thus, the total differential of f is obviously:

$$
df = (\mu\frac{\partial f}{\partial x} + \frac{\partial f}{\partial t} + \frac{\sigma^2}{2}\frac{\partial^2 f}{\partial x^2})dt + \frac{\partial f}{\partial x}dB_t. \# \tag{2.27}
$$

From this equation, it's not hard to discover that if dx is a drift-diffusion process, then so does the $f(x, t)$ be.

2.2.3 Kolmogorov Forward Equation

As we all know that in classical or quantum mechanics, we need a universal equation of motion for physical observable to describe the system characteristic, and Kolmogorov forward equation (KFE) is the equation of motion for PDF in drift-diffusion process, which is the foundation of CME. Here we start with an arbitrary fixed function $f(x)$ on the interval $[a, b]$ to check how the following expectation will change over an infinitesimal

increment of time Δt:

$$E_f(t) = \int_a^b f(x)P(x,t)dx,$$

$$\Delta E_f(t) = E_f(t + \Delta t) - E_f(t)$$

$$= \int_a^b f(x)\frac{\partial P(x,t)}{\partial t}\Delta t dx. \tag{2.28}$$

With the Eq. (2.20) aid, we can obtain:

$$\Delta E_f(t) \approx \int_a^b dx P(x,t)\int_{\Delta B_t}[(\mu\frac{\partial f}{\partial x} + \frac{\sigma^2}{2}\frac{\partial^2 f}{\partial x^2})\Delta t + \sigma\frac{\partial f}{\partial x}]\Delta B_t,$$

and take its integration over all Brownian paths for every x at a given time t to arrive:

$$\Delta E_f(t) \approx \int_a^b P(x,t)(\mu\frac{\partial f}{\partial x} + \frac{\sigma^2}{2}\frac{\partial^2 f}{\partial x^2})\Delta t dx, \tag{2.29}$$

where the contribution of Brownian motion is 0 by its definition. From Eq. (2.29) and Eq. (2.30), we have:

$$\int_a^b P(x,t)(\mu\frac{\partial f}{\partial x} + \frac{\sigma^2}{2}\frac{\partial^2 f}{\partial x^2})dx = \int_a^b f(x)\frac{\partial P(x,t)}{\partial t}dx,$$

$$\int_a^b [\frac{\partial P(x,t)}{\partial t}f(x) - P(x,t)(\mu\frac{\partial f}{\partial x} + \frac{\sigma^2}{2}\frac{\partial^2 f}{\partial x^2})]dx = 0. \tag{2.30}$$

Without loss of generality, we can set the following boundary conditions for $f(x)$,

$$f(a) = f(b) = f'(a) = f'(b) = 0.$$

In physical world, physical observables always disappear at boundaries. If $f(x)$ didn't satisfy the boundary condition, we could let $a \to -\infty$ and $b \to \infty$ to make $P(\pm\infty, t) = 0$, where it's equivalent to set $f(\pm\infty) = 0$. Next, we can apply integration by part into each

term of Eq. (2.30):

$$
\begin{aligned}
\int_a^b \mu \frac{\partial f}{\partial x} P(x,t) dx &= [\mu f(x) P(x,t)]\Big|_a^b - \int_a^b f(x) \frac{\partial}{\partial x}[\mu P(x,t)] dx \\
&= -\int_a^b f(x) \frac{\partial}{\partial x}[\mu P(x,t)] dx,
\end{aligned} \tag{2.31}
$$

$$
\begin{aligned}
\int_a^b \frac{\sigma^2}{2} P(x,t) \frac{\partial^2 f}{\partial x^2} dx &= [\frac{\sigma^2}{2} P(x,t) \frac{\partial f}{\partial x}]\Big|_a^b - \int_a^b \frac{\partial f}{\partial x} \frac{\partial}{\partial x}[\frac{\sigma^2}{2} P(x,t)] dx \\
&= -f(x) \frac{\partial}{\partial x}[\frac{\sigma^2}{2} P(x,t)]\Big|_a^b + \int_a^b f(x) \frac{\partial^2}{\partial x^2}[\frac{\sigma^2}{2} P(x,t)] dx \\
&= \int_a^b f(x) \frac{\partial^2}{\partial x^2}[\frac{\sigma^2}{2} P(x,t)] dx.
\end{aligned} \tag{2.32}
$$

Then, we put Eqs. (2.31-32) results into Eq. (2.30) to obtain:

$$
\int_a^b f(x) [\frac{\partial P(x,t)}{\partial t} + \frac{\partial}{\partial x}[\mu P(x,t)] - \frac{\partial^2}{\partial x^2}[\frac{\sigma^2}{2} P(x,t)]] dx = 0.
$$

Since $f(x)$ is an arbitrary function over interval $[a,b]$, the terms inside the integration should be 0,

$$
\frac{\partial P(x,t)}{\partial t} + \frac{\partial}{\partial x}[\mu P(x,t)] - \frac{\partial^2}{\partial x^2}[\frac{\sigma^2}{2} P(x,t)] = 0, \# \tag{2.33}
$$

where the PDE of second order, Eq. (2.33), is called Kolmogorov forward equation (KFE) or Fokker-Planck equation.

2.3 Bio-evolution Model

In statistical physics of magnetism, statistical physicists make a good use of Ising model with letters to investigate the phase transition of magnetism. And in bio-evolution model, bio-physicists apply Ising model with two-letters (± 1) to investigate the evolution dynamics and steady-state distribution for different genotypes. Usually, scientists in evo-

lution consider the N-length genome with two-letters ($\pm\ 1$) as shown in the illustration:

$$(+,+,+,+,-,-,-,+),\ N = 7,$$

$$(+,+,-,-,+,+,-,+,+),\ N = 8,$$

$$\Rightarrow (s_1^i, s_2^i, ..., s_k^i, ..., s_N^i), \tag{2.34}$$

where s_k^i with ± 1 possible values is the k-th spin in type i sequence or configuration. For a given length N, the genome or sequence has 2^N possible configurations. To express the gene distribution well, biologists introduce the gene frequency to describe the dynamics of genome evolution through selection or mutation. The gene frequency has two expressions: absolute or relative frequency. Take the $N = 2$ genome with two-letters and 4 possible configurations for an example:

$$i = 0 : (+,+),\ i = 1 : (-,+),\ i = 2 : (+,-),\ i = 3 : (-,-),$$

$$(+,+), (+,+), (+,+), (+,-), (+,-), (-,-), (-,-), (-,-),$$

where the absolute frequency p_i for type $0 \sim 3$ is $p_0 = 3, p_1 = 0, p_2 = 2$, and $p_3 = 3$ and the relative frequency P_i for type $0 \sim 3$ is $P_0 = \frac{3}{8}, P_1 = 0, P_2 = \frac{1}{4}$, and $P_3 = \frac{3}{8}$. Therefore, the relation between p_i and P_i is:

$$P_i = \sum_{j=0}^{2^N} \frac{p_i}{p_j}. \tag{2.35}$$

The gene adaptivity to their surroundings make an impact on the number of gene offspring in which scientists are interested, so they define the fitness r_i for type i sequence which is the mean number of gene offspring per unit cycle. To model the interaction between different sequences, the Hamming distance (HD) between different sequences i and j is defined as:

$$d_{ij} = (N - \sum_{k=1} s_i^k s_j^k)/2. \tag{2.36}$$

It's not hard to find that Hamming distance is the spin difference between any two sequences.
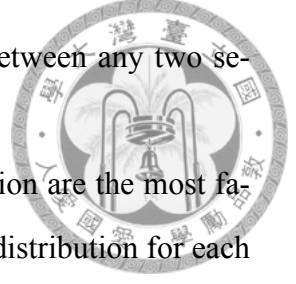
Crow-Kimura and Eigen model which describe molecular evolution are the most famous model in bio-evolution governing the dynamics of probability distribution for each type of sequence. This section introduces briefly the two models in mathematical expression and explains each term defined in two models in a detail.

2.3.1 Crow-Kimura Model

Crow and Kimura in 1968 proposed firstly the Crow-Kimura model formulated by molecular evolution for i and j type sequence, and the model is:

$$\frac{\partial P_i}{\partial t} = P_i(r_i - \sum_{j=1}^{2^N} r_j P_j) + \sum_{j=1}^{2^N} m_{ij} P_j,$$

(2.37)

where P_i satisfies $\sum_{i=1}^{2^N} P_i = 1$ and the element of mutation matrix m_{ij} is:

$$\begin{cases} m_{ij} = \gamma_0, \ d_{ij} = 1, \\ m_{ii} = -N\gamma_0, \ d_{ii} = 0, \\ m_{ij} = 0, \ d_{ij} > 1, \end{cases}$$

(2.38)

where γ_0 is the transition rate of mutation. For a given sequence with genome length N, it has N neighbourhoods with HD $d_{ij} = 1$, so the sum of all transition rate for any sequence is zero:

$$N \times \gamma_0 + (-N\gamma_0) = 0.$$

With such m_{ij} matrix, it means that only one-step mutation takes place in the evolution. Just like in Ising model, the gene mutation only happens for the two parallel site with different spins as indicated in the following:

$$(+,-)(+,+) \Rightarrow (+,+)(+,+) \ or \ (+,-)(+,-).$$

As a matter of fact, Crow-Kimura model is equivalent to Ising model with two-valued (±1) spin.

To simplify the Crow-Kimura model, the second term on the right-handed side of Eq. (2.37) called dilution term,

$$-P_i \sum_{j=1}^{2^N} r_j P_j,$$

can be ignored by the non-linear transformation of Eq. (2.35) in mapping P_i into p_i. We have the following equation for the fitness:

$$r_i = \frac{n_i}{\Delta t}, \tag{2.39}$$

where n_i is the number of gene offspring for type i and Δt is time of a cycle, and the change of p_i with respect to Δt is:

$$
\begin{aligned}
\frac{\partial p_i}{\partial t} &= \frac{\Delta p_i}{\Delta t} = \frac{[n_i p_i + (\sum_j m_{ij} \Delta t p_j) + p_i] - p_i}{\Delta t} \\
&= \frac{n_i p_i}{\Delta t} + \sum_j m_{ij} p_j \\
&= r_i p_i + \sum_j m_{ij} p_j.
\end{aligned}
\tag{2.40}
$$

With Eq. (2.39-40) aid, we can verify that Eq. (2.37) is equivalent to Eq. (2.40):

$$\frac{\partial P_i}{\partial t} = \frac{1}{\sum_j p_j} \frac{\partial p_i}{\partial t} - \frac{p_i}{(\sum_j p_j)^2} \sum_j \frac{\partial p_j}{\partial t},$$

$$P_i\left(r_i - \sum_{j=1}^{2^N} r_j P_j\right) + \sum_{j=1}^{2^N} m_{ij} P_j$$

$$= \frac{r_i p_i}{\sum_j p_j} - \frac{p_i}{(\sum_j p_j)^2} \sum_{j=1}^{2^N} r_j p_j + \frac{1}{\sum_j p_j} \sum_{j=1}^{2^N} m_{ij} p_j.$$

Therefore, the right-handed side of Eq. (2.37) becomes:

$$\frac{1}{\sum_j p_j}\left(r_i p_i + \sum_{j=1}^{2^N} m_{ij} p_j\right) - \frac{p_i}{(\sum_j p_j)^2}\left(\sum_{j=1}^{2^N} r_j p_j + \sum_{j=1}^{2^N} \sum_{i=1}^{2^N} m_{ji} p_i\right),$$

$$= \frac{1}{\sum_j p_j}\left(r_i p_i + \sum_{j=1}^{2^N} m_{ij} p_j\right) - \frac{p_i}{(\sum_j p_j)^2} \sum_{j=1}^{2^N} r_j p_j, \# \tag{2.41}$$

where recall that the total sum of m_{ji} is $\sum_j m_{ij} = 0$.

In addition, Crow-Kimura model is invariant under the transformation for fitness:$r_i \rightarrow r'_i = r_i + c$, where c is an arbitrary constant. This can be proved by taking summing all i-index on the both sides of Eq. (2.37):

$$\sum_{i=1}^{2^N} \frac{\partial P_i}{\partial t} = \sum_{i=1}^{2^N} P_i[(r_i + c) - \sum_{j=1}^{2^N} (r_j + c - c)P_j] + \sum_{i=1}^{2^N} \sum_{j=1}^{2^N} m_{ij}P_j,$$

$$\sum_{i=1}^{2^N} \frac{\partial P_i}{\partial t} = \sum_{i=1}^{2^N} P_i[r'_i - \sum_{j=1}^{2^N} r'_j P_j)] + \sum_{i=1}^{2^N} \sum_{j=1}^{2^N} m_{ij}P_j + c(\sum_{j=1}^{2^N} P_j - \sum_{i=1}^{2^N} P_i),$$

$$\sum_{i=1}^{2^N} \frac{\partial P_i}{\partial t} = \sum_{i=1}^{2^N} P_i[r'_i - \sum_{j=1}^{2^N} r'_j P_j)] + \sum_{i=1}^{2^N} \sum_{j=1}^{2^N} m_{ij}P_j,$$

$$\rightarrow \frac{\partial P_i}{\partial t} = P_i[r'_i - \sum_{j=1}^{2^N} r'_j P_j)] + \sum_{j=1}^{2^N} m_{ij}P_j.\#$$

This result means that we can choose any value for r_i at reference point without changes of Crow-Kimura model.

2.3.2 Eigen Model

The quasispecies or Eigen model in 1977 was firstly formulated by Manfred Eigen and put forward by Peter Schuster from Eigen's initial work. The Eigen model with genome length N without degradation term is the following equation:

$$\frac{\partial P_i}{\partial t} = \sum_{j=1}^{2^N} Q_{ij} r_j P_j - P_i(\sum_{j=1}^{2^N} r_j p_j), \tag{2.42}$$

where P_i is the relative frequency for type i sequence and the element of mutation matrix is:

$$Q_{ij} = q^{N-d_{ij}} (1-q)^{d_{ij}}, \tag{2.43}$$

where q is the mean nucleotide incorporation fidelity and d_{ij} is Hamming distance between type i and j sequence. It's obvious to find that $Q_{ij} \neq 0$ for any value of d_{ij}. With such mutation matrix, it means that multiple-step mutation takes place in a given sequence. The $1 - q$ meaning in such transition process is the probability to copy a nucleotide without

error. As shown in previous section, the second term on the right-handed side of Eq. (2.42) called dilution can be ignored by the mapping: $P_i = \sum_j \frac{p_i}{p_j}$, which lead to the equation:

$$\frac{\partial p_i}{\partial t} = \sum_{j=1}^{2^N} Q_{ij} r_j p_j. \tag{2.44}$$
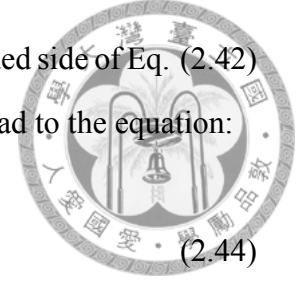
2.4 Collision and Heat Equation

In the SMAT experiment, engineers are interested in energy conversion from kinetic energy to strain and heat energy in a SMAT sample. The energy conversion enhances the mechanical properties of sample such as the hardness and fatigue improvement on the sample surface. The energy conversion at first in SMAT is the kinetic transferring between 304 steel balls and motor top. Since the motor mass is millions-time ball mass, the ball-motor collision can be taken as elastic. After balls accelerated by motor, the collision between 304 steel balls and sample bottom will take place in a short time. Since the sample mass is not as large as motor mass, the ball-sample collision should be counted as inelastic. This is key to the loss of kinetic energy for balls which will transform into the heat and internal energy of sample. The resulting heat energy will increase the probability of sample recrystallization which is an important process related to the strain and hardness of sample. Thus, it's necessary to model the heat equation of sample to estimate the distribution of sample temperature and heat flow in sample.

2.4.1 Collision

The conservation of momentum for a physical system has been widely used for hundreds years in collisions. We can write down the equation for two-particle collision:

$$m_1 v_1 + m_2 v_2 = m_1 v_1' + m_2 v_2',$$
$$m_1 (v_1 - v_1') = -m_2 (v_2 - v_2'), \tag{2.45}$$

where m_1 and m_2 is the mass of particle 1 and 2, v_1 and v_2 is the velocity of particle 1 and 2 before collision, and v_1' and v_2' is the velocity of particle 1 and 2 after collision. If the total kinetic energy is conserved after collision, Eq. (2.45) should add the following constraint:

$$\frac{1}{2}m_1 v_1^2 + \frac{1}{2}m_2 v_2^2 = \frac{1}{2}m_1 v_1'^2 + \frac{1}{2}m_2 v_2'^2,$$
$$m_1(v_1^2 - v_1'^2) = -m_2(v_2^2 - v_2'^2). \tag{2.46}$$

Such collisions with the Eq. (2.46) constraint are named elastic collision. And we can investigate the relation between $v_{1,2}$ and $v_{1,2}$ by dividing Eq. (2.46) by Eq. (2.45) to obtain:

$$v_1 + v_1' = v_2 + v_2',$$
$$v_1 - v_2 = v_2' - v_1',$$
$$\rightarrow \frac{v_2' - v_1'}{v_1 - v_2} = 1. \tag{2.47}$$

Thus, scientists in classical physics introduced the restitution constant $e = \frac{v_2' - v_1'}{v_1 - v_2}$ to judge whether the collision is elastic or not. With the introduction of e, v_1' and v_2' can be obtained as a function of e, $m_{1,2}$, and $v_{1,2}$ as follows:

$$v_2' = e(v_1 - v_2) + v_1',$$
$$m_1 v_1' = -m_2 v_2' + m_1 v_1 + m_2 v_2$$
$$= (m_1 - em_2)v_1 + (1 + e)m_2 v_2 - m_2 v_1'.$$

Therefore,

$$v_1' = \frac{m_1 - em_2}{m_1 + m_2}v_1 + \frac{(1+e)m_2}{m_1 + m_2}v_2,$$
$$v_2' = \frac{(1+e)m_1}{m_1 + m_2}v_1 + \frac{m_2 - em_1}{m_1 + m_2}v_2, \tag{2.48}$$

where $0 \le e < 1$ corresponds to the inelastic collision and $e = 1$ corresponds to elastic collision:

$$v_1' = \frac{m_1 - m_2}{m_1 + m_2}v_1 + \frac{2m_2}{m_1 + m_2}v_2,$$
$$v_2' = \frac{2m_1}{m_1 + m_2}v_1 + \frac{m_2 - m_1}{m_1 + m_2}v_2. \tag{2.49}$$

Therefore, the loss of kinetic energy for two particles due to inelastic collision between them is:

$$\Delta E_k = \frac{1}{2}m_1 v_1^2 + \frac{1}{2}m_2 v_2^2 - \frac{1}{2}m_1 v_1'^2 - \frac{1}{2}m_2 v_2'^2.$$

2.4.2 Heat Equation

Considering the heat transfer in Fig. (2.1), we can use the law of energy conservation to derive one-dimension heat equation. In Fig. (2.1), A is the cross-sectional area of sample and z is the distance from sample bottom. Let us start to consider three kinds of heat flow: the input, output, and heat generation. The generation of heat energy per unit volume and time, heat source, is denoted as $\dot{q}$, so the energy generation in Adz volume is:

$$Q_g = \dot{q}Adz. \tag{2.50}$$

The input flow at z is:
$$Q_i = -Ak\frac{dT}{dz},$$

where k is the thermal conductivity of sample, the output flow at $z + dz$ is:

$$\begin{aligned}
Q_o &= Q_i + \frac{dQ_i}{dz}dz \\
&= -Ak\frac{dT}{dz} - \frac{d}{dz}(Ak\frac{dT}{dz})dz,
\end{aligned}$$

and the change of internal energy in Adz volume with respect to time is:

$$Q_t = \rho C A \frac{dT}{dt} dz,$$

where ρ is the sample density, C is the specific heat of sample, and t is the time. Since the net of heat flow must be 0, $Q_i + Q_g = Q_o + Q_t$, we have the followings:

$$-Ak\frac{dT}{dz} + \dot{q}Adz = -Ak\frac{dT}{dz} - \frac{d}{dz}(Ak\frac{dT}{dz})dz + \rho C A \frac{dT}{dt} dz,$$

$$\rightarrow \frac{1}{A}\frac{d}{dz}(Ak\frac{dT}{dz}) + \dot{q} = \rho C \frac{dT}{dt}, \tag{2.51}$$

where Eq.(2.51) is called one-dimension heat equation. By solving this equation, the distribution of sample temperature and heat energy can be estimated.

Chapter 3

Advanced Theory for CME, Bio-evolution, and SMAT

In this chapter, we use the basic theory in Ch. 2 to derive important and useful results in the CME, Bio-evolution, and SMAT modelling.

For CME part, we at first solve the CME in linear-drift Gaussian process, and then the probability of chemical reaction for each stochastic path is obtained by path integral formalism through the solution of linear-drift Gaussian process. And the CME with compound Poission noise, Van Kampen model, is derived by the expansion of characteristic function for PDF.

For bio-evolution part, we modify the Crow-Kimura and Eigen model based on the following assumptions. Firstly, each sequence with the same number of -1 spin has the same probability, namely, the distribution is symmetrical. Secondly, the mean fitness is also assumed to be symmetrical. This two assumptions make tremendous difference in Crow-Kimura and Eigen model which simplify the equation in a large scale. In next step, we introduce HJE method to investigate the probability distribution of gene and to obtain the mean fitness of zero order of $\frac{1}{N}$. With the bulk equation of probability distribution, the equation of $O(\frac{1}{N})$ for probability distribution is constructed, where we derive the mean fitness of $O(\frac{1}{N})$ and correction term u_1 of $O(\frac{1}{N})$ for probability distribution.

For SMAT part, we model the motor motion as longitudinal harmonic motion in which

we can derive the average velocity of motor. Through the average velocity of motor and Taylor expansion, the average velocity and period of flying balls without interaction is constructed to estimate the loss of kinetic energy and power for balls. With the known loss, the strain energy and power of sample can be obtained by the law of energy conservation.
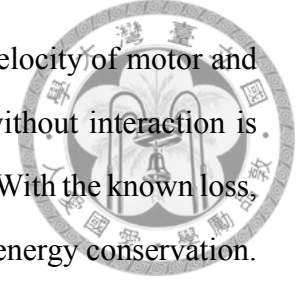
3.1 Formalism of Chemical Master Equation

Scientists are always interested in the probability of chemical reaction for a given stochastic process, and the mean, maximum, and fluctuation of physical observables are connected to this probability. In this section, the solution of linear-drift Gaussian process is used to construct the probability of chemical reaction by path integral. In our CME research, we work with CME with Gaussian and compound Poission noise. Thus, we also derive the CME with compound Poission noise by the expansion of characteristic function for PDF.

3.1.1 Solution of Linear-Drift Process

Consider Eq. (2.35) with the following functions:

$$\mu = -bx, \sigma = \sqrt{2\epsilon},$$

where b and ϵ are both constants, the drift term μ is linear in x. Therefore, Eq. (2.35) with such functions is so-called linear-drift Gaussian process. The corresponding KFE has the form:

$$\frac{\partial P(x,t)}{\partial t} = \frac{\partial}{\partial x}[bxP(x,t)] + \epsilon\frac{\partial^2 P(x,t)}{\partial x^2},$$

which is also called Fokker-Planck equation in physics. Using the WKB expansion,

$$P(x,t) = \exp\left[-\frac{1}{\epsilon}u_\epsilon(x,t)\right],$$

we have the following partial derivatives for $P(x, t)$:

$$\frac{\partial P(x, t)}{\partial t} = \frac{-1}{\epsilon} \frac{\partial u_\epsilon(x, t)}{\partial t} P(x, t),$$

$$\frac{\partial P(x, t)}{\partial x} = \frac{-1}{\epsilon} \frac{\partial u_\epsilon(x, t)}{\partial x} P(x, t),$$

$$\frac{\partial^2 P(x, t)}{\partial x^2} = \frac{-1}{\epsilon} \frac{\partial^2 u_\epsilon(x, t)}{\partial x^2} P(x, t) + \frac{1}{\epsilon^2} (\frac{\partial u_\epsilon(x, t)}{\partial x})^2 P(x, t).$$

The set of derivatives maps the equation of $P(x, t)$ into the equation of $u_\epsilon(x, t)$:

$$\frac{\partial u_\epsilon}{\partial t} = -[(\frac{\partial u_\epsilon}{\partial x})^2 - bx \frac{\partial u_\epsilon}{\partial x}] + \epsilon[\frac{\partial^2 u_\epsilon}{\partial x^2} - b]. \tag{3.1}$$

To solve Eq. (3.1), we can set the change of variable as a function of t,

$$u_\epsilon(x, t) = a(t) + \frac{(x - \mu(t))^2}{2\sigma^2(t)}, \tag{3.2}$$

to arrive the following differential equation:

$$\begin{aligned}
\frac{\partial u_\epsilon}{\partial t} &= \frac{a(t)}{dt} - \frac{x - \mu(t)}{\sigma^2(t)} \frac{d\mu(t)}{dt} - \frac{(x - \mu(t))^2}{\sigma^3(t)} \frac{d\sigma(t)}{dt} \\
&= -[\frac{(x - \mu(t))^2}{\sigma^4(t)} - bx \frac{x - \mu(t)}{\sigma^2(t)}] + \epsilon[\frac{1}{\sigma^2(t)} - b] \\
&= -\frac{(x - \mu(t))^2}{\sigma^4(t)}[1 - b\sigma^2(t) - b \frac{\sigma^2(t)\mu(t)}{x - \mu(t)}] + \epsilon[\frac{1}{\sigma^2(t)} - b]. \tag{3.3}
\end{aligned}$$

Divide the both sides of Eq. (3.3) by $\frac{(x - \mu(t))^2}{\sigma^4(t)}$ to have:

$$\begin{aligned}
& \frac{\sigma^4(t)}{(x - \mu(t))^2} \frac{da(t)}{dt} - \frac{\sigma^2(t)}{(x - \mu(t))} \frac{d\mu(t)}{dt} - \sigma(t) \frac{d\sigma(t)}{dt} \\
&= -[1 - b\sigma^2(t) - b \frac{\sigma^2(t)\mu(t)}{(x - \mu(t))}] + \epsilon[\frac{\sigma^2(t)}{(x - \mu(t))^2} - b \frac{\sigma^4}{(x - \mu(t))^2}]. \tag{3.4}
\end{aligned}$$

We can find that only the $\sigma(t) \frac{d\sigma(t)}{dt}$ in Eq. (3.4) is not multiplied by $\frac{1}{(x - \mu(t))}$, so we can let

$$\sigma(t) \frac{d\sigma(t)}{dt} = 1 - b\sigma^2(t),$$

$$\frac{d\sigma^2(t)}{dt} = 2[1 - b\sigma^2(t)]. \tag{3.5}$$

Put Eq. (3.5) into Eq. (3.4) and divide both sides of Eq. (3.4) by $-\frac{\sigma^2(t)}{(x-\mu(t))}$ to get:

$$-\frac{\sigma^2(t)}{(x-\mu(t))}\frac{da(t)}{dt} + \frac{d\mu(t)}{dt}$$
$$= -b\mu(t) + \epsilon\left[\frac{1}{(x-\mu(t))} + \frac{b\sigma^2(t)}{(x-\mu(t))}\right]. \tag{3.6}$$
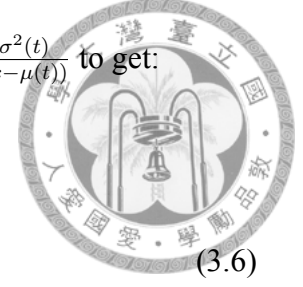
Similarly, the $\frac{d\mu(t)}{dt}$ in Eq. (3.6) is not multiplied by $\frac{1}{(x-\mu(t))}$, we can let

$$\frac{d\mu(t)}{dt} = -b\mu(t). \tag{3.7}$$

Finally, put Eq. (3.7) into Eq. (3.6) and divide both sides of Eq. (3.5) by $-\frac{\sigma^2(t)}{(x-\mu(t))}$ to obtain:

$$\frac{da(t)}{dt} = \epsilon\left[\frac{1}{\sigma^2(t)} - b\right]. \tag{3.8}$$

Thus, the Eq. (3.5) can be solved by the following integration:

$$\int_0^t \frac{d\sigma^2(t')}{\frac{1}{b} - \sigma^2(t')}dt' = \int_0^t 2dt',$$

$$\ln\left|\frac{1}{b} - \sigma^2(t')\right|\Big|_0^t = -2bt,$$

$$\sigma^2(t) = \frac{1}{b} + \left[\sigma^2(0) - \frac{1}{b}\right]\exp\left(-2bt\right), \tag{3.9}$$

and so does the Eq. (3.7):

$$\int_0^t \frac{d\mu(t')}{\mu(t')}dt' = -\int_0^t bdt'$$

$$\ln|\mu(t)| - \ln|\mu(0)| = -bt,$$

$$\mu(t) = \mu(0)\exp\left(-bt\right). \tag{3.10}$$

From Eq. (3.5), we also have:

$$\frac{1}{\sigma^2(t)}\frac{d\sigma^2(t)}{dt} = d\ln|\sigma^2(t)| = 2\left[\frac{1}{\sigma^2(t)} - b\right].$$

Thus, the solution of Eq. (3.8) can be obtained by the integration:

$$\int_{a(0)}^{a(t)} da(t') = \frac{\epsilon}{2} \int_{\sigma^2(0)}^{\sigma^2(t)} d\ln|\sigma^2(t')|,$$

$$a(t) = a(0) + \frac{\epsilon}{2} \ln\left[\frac{\sigma^2(t)}{\sigma^2(0)}\right]. \tag{3.11}$$

We can find that the ϵ term only contributes to $a(t)$, and the diffusive term $\sigma^2(t)$ is not influenced by ϵ. With the aid of Eq. (3.9-10), the solution of Fokker-Planck equation for PDF is:

$$
\begin{aligned}
P(x,t) &= \exp\left[\frac{-1}{\epsilon} u_\epsilon(x,t)\right] \\
&= \exp\left[-\frac{a(t)}{\epsilon} - \frac{(x-\mu(t))^2}{2\epsilon\sigma^2(t)}\right] \\
&= \sqrt{\frac{\sigma^2(0)}{\sigma^2(t)}} e^{-\frac{a(0)}{\epsilon}} \exp\left[-\frac{(x-\mu(t))^2}{2\epsilon\sigma^2(t)}\right] \\
&= \frac{A}{\sqrt{\pi\epsilon\sigma^2(t)/2}} \exp\left[-\frac{(x-\mu(t))^2}{2\epsilon\sigma^2(t)}\right],
\end{aligned}
\tag{3.12}
$$

where $A = \sqrt{\frac{\pi\epsilon\sigma^2(0)}{2}} \exp\left[-\frac{a(0)}{\epsilon}\right]$. The PDF of Eq. (3.12) is always Gaussian distribution for any given time, and that's the reason we call dB_t is Gaussian white noise. For a small ϵ, the PDE of Eq. (3.12) decreases quickly from the mean value $\mu(t)$. And for $\epsilon \to 0^+$ case, the PDF of Eq. (3.12) becomes the delta function with its center at $x = \mu(t)$, and this means physically only the path, $x = \mu(t)$, will take place in this process.

3.1.2 Path Integral Formalism in Stochastic Process

In the former section, we have the solution of PDF in linear-drift Gaussian process. In this section, we apply the solution and start from the Lagrangian L and action functional S_0 as mentioned in CME introduction:

$$L(q,\dot{q}) = [p\dot{q} - H(q,p)]_{p=\frac{1}{2}(\dot{q}-b(q))} = \frac{1}{4}(\dot{q} - b(q))^2,$$

$$S_0[q(t); (0, q(0)) \to (t, q(t))] = \int_0^t d\tau \frac{1}{4}\left[\frac{dq(\tau)}{d\tau} - b(q(\tau))\right]^2,$$

to get PDF for each path of chemical reaction in linear-drift process. Let us consider the initial condition for PDF with linear drift $-bx$ and diffusion term ϵ:

$$P(x', 0) = \delta(x'),$$
$$\to \sigma^2(0) = 0, \mu(0) = 0.$$

And remember that the zero order equation of chemical system obeys the ordinary differential equation:

$$\frac{dx'}{dt} = b(x') = -bx',$$
$$\to x'(t) = x'(0)e^{-bt},$$

which means that the expectation value of x obeys this ordinary differential equation. The transient PDF of Fokker-Planck equation with linear drift $-bx$ obeys the Markov process:

$$
\begin{aligned}
P(x, \Delta t | x', 0) &= \frac{P(x - x', \Delta t)P(x', 0)}{P(x', 0)} = P(x - x', \Delta t) \\
&= \sqrt{\frac{2}{\pi\epsilon\sigma^2(\Delta t)}} \exp\left[-\frac{(x - x'e^{-b\Delta t})^2}{2\epsilon\sigma^2(\Delta t)}\right] \\
&\approx \frac{1}{\sqrt{\frac{\pi\epsilon}{2b}(1 - e^{-2b\Delta t})}} \exp\left[-\frac{(x - x'e^{-b\Delta t})^2}{2(\epsilon/b)(1 - e^{-2b\Delta t})}\right] \\
&\approx \frac{1}{\sqrt{\frac{\pi\epsilon}{2b}[2b\Delta t - 2b^2(\Delta t)^2]}} \exp\left[-\frac{(x - x' + bx'\Delta t)^2}{4\epsilon\Delta t}\right] \\
&= \frac{1}{\sqrt{\pi\epsilon\Delta t(1 - b\Delta t)}} \exp\left[-\frac{(x - x' + bx'\Delta t)^2}{4\epsilon\Delta t}\right] \\
&= \frac{1}{\sqrt{\pi\epsilon\Delta t}} \exp\left[\frac{(x - x' + bx'\Delta t)^2}{4\epsilon\Delta t} - \frac{1}{2}\ln\left(1 - \frac{db(x)}{dx}\Delta t\right)\right], (3.13)
\end{aligned}
$$

where we have set $A = 1$ and used the Taylor expansion:

$$
\begin{aligned}
e^{-2b\Delta t} &\approx 1 - 2b\Delta t + \frac{(2b\Delta t)^2}{2!}, \\
\sigma^2(\Delta t) &= \frac{1}{b}(1 - e^{-2b\Delta t}) \\
&\approx \frac{1}{b}(1 - 1 + 2b\Delta t + \frac{(2b\Delta t)^2}{2!}) \\
&= 2\Delta t(1 - b\Delta t).
\end{aligned}
$$

And the trajectory of PDF for any generalized drift $b(x)$ following the Fokker-Planck equation is:

$$
\begin{aligned}
&P(x_n, n\Delta t; x_{n-1}, (n-1)\Delta t; ...; x_1, \Delta t | x_0, 0) \\
&= \frac{1}{\sqrt{\pi\epsilon\Delta t}} \prod_{k=1}^{n} \exp\left[-\frac{(x_k - x_{k-1} - b(x_{k-1})\Delta t)^2}{4\epsilon\Delta t} - \frac{1}{2}\ln\left(1 + \frac{db(x_j)}{dx}\Delta t\right)\right] \\
&\approx \mathbf{A} \exp\left[-\frac{1}{4\epsilon} \int_0^t \left[(\frac{dx(t)}{dt} - b(x(t)))^2 + 2\epsilon\frac{db(x)}{dx}\right]dt'\right] \\
&= \mathbf{A} \exp\left[-\frac{1}{\epsilon}(S_0 + \frac{\epsilon}{2}\int_0^t \frac{db(x)}{dx}dt')\right],
\end{aligned} \tag{3.14}
$$

where $\mathbf{A} = \frac{1}{\sqrt{\pi\epsilon\Delta t}}$ is an appropriate constant for normalization, $t = n\Delta t$ with $n >> 1$, and we have used the Taylor expansion:

$$
\ln(1 + y) = \sum_{k=1}^{\infty} (-1)^{k+1}\frac{y^k}{k} \approx y, \ for \ y << 1. \tag{3.15}
$$

For the $\epsilon \to 0^+$ or non-diffusion case, the only trajectory obeyed by the chemical reaction is:

$$
\frac{dx(t)}{dt} = b(x(t)),
$$

which states that the chemical reaction without ϵ term is deterministic.

3.1.3 Formalism for CME with Compound Poisson Noise

In previous sections, only Gaussian white noise used in a long time interval is taken into account, however, chemical reactions often take place in a short time interval, where
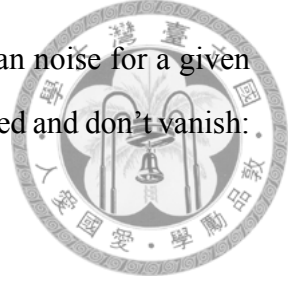
the compound Poisson noise is useful. Let us consider a non-Gaussian noise for a given time t, $\Lambda(t)$, whose higher cumulants are supposed to be delta-correlated and don't vanish:

$$
\begin{cases}
< \Lambda(t) >= \Gamma_1 \\[2mm]
< \Lambda(t)\Lambda(t') >= \Gamma_2\delta(t - t') \\[2mm]
< \Lambda(t)\Lambda(t')\Lambda(t'') >= \Gamma_2\delta(t - t')\delta(t - t'') \\[2mm]
< \Lambda(t_1)\Lambda(t_2)...\Lambda(t_m) >= \Gamma_m\delta(t_1 - t_2)\delta(t_1 - t_3)...\delta(t_1 - t_m)
\end{cases}
, m \geq 1,
$$

where $< \quad >$ is the notation for taking expectation value and Γ_k are constants for $1 \leq k \leq m$. Since such distribution of $\Lambda(t)$ has singularities, we can define the integral process:

$$
Z(t) = \int_0^t \Lambda(t')dt',
$$

which makes the increment of Z independent of the previous Z and is only dependent on the time interval τ:

$$
\begin{aligned}
z &= Z(t + \tau) - Z(t) \\
&= \int_0^{t+\tau} \Lambda(t')dt' - \int_0^t \Lambda(t')dt' \\
&= \int_t^{t+\tau} \Lambda(t')dt'.
\end{aligned}
$$

Common processes with independent increments for a short time interval can be generated by compound Poisson processes in the following steps. Put a stochastic set of dots on time axis making noise:

$$
f_n(t_1, t_2, ..., t_n) = \rho^n,
$$

$$
f_n(t_1, t_2, ..., t_n)dt_1 dt_2...dt_n
$$

$$
\equiv \; the \; probability \; between \; \vec{t} \; and \; \vec{t} + d\vec{t},
$$

where ρ is the probability per unit time, $\vec{t} = (t_1, t_2, ..., t_n)$, and $d\vec{t} = (dt_1, dt_2, ..., dt_n)$. Assume that Z increases in an amount z at each dot, which is random with probability

39

density $w(z)$. The n random dots in time interval τ is assumed to be Poissonian with average value $\rho\tau$, so the distribution of z is:

$$T_\tau(z) = \sum_{n=0}^{\infty} \frac{(\rho\tau)^n}{n!} e^{-\rho\tau} w(z) * w(z) * ... * w(z),$$

where $*$ is the notation for convolution and the $w(z)$ product is the convolution of n factors for $w(z)$. Hence its characteristic function in probability theory can be written as:

$$\int e^{ikz} T_\tau(z) dz = \sum_{n=0}^{\infty} \frac{(\rho\tau)^n}{n!} e^{-\rho\tau} \int w(z) * w(z) * ... * w(z) dz.$$

This characteristic function can be simplified by applying Fubini's theorem,

$$\int\int_{A\times B} g(x)h(y) dx dy = \int_A g(x) dx \int_B h(y) dy, \tag{3.16}$$

into the characteristic function:

$$\sum_{n=0}^{\infty} \frac{(\rho\tau)^n}{n!} e^{-\rho\tau} \int w(z) * w(z) * ... * w(z) dz$$
$$= \sum_{n=0}^{\infty} \frac{(\rho\tau)^n}{n!} e^{-\rho\tau} [\int e^{ikz} T_\tau(z) dz]^n$$
$$= e^{-\rho\tau} \exp\left[\rho\tau \int e^{ikz} w(z) dz\right]$$
$$= \exp\left[\rho\tau \int (e^{ikz} - 1) w(z) dz\right],$$
$$\rightarrow \int e^{ikz} T_\tau(z) dz = \exp\left[\rho\tau \int (e^{ikz} - 1) w(z) dz\right], \tag{3.17}$$

where we have used the following equality:

$$\int e^{ikz} w(z) * w(z) dz$$
$$= \int w(y) dy \int e^{ikz} w(z - y) dz$$
$$= \int w(y) dy \int e^{ik(z+y)} w(z) dz$$
$$= \int e^{iky} w(y) dy \int e^{ikz} w(z) dz$$
$$= [\int e^{ikz} w(z) dz]^2.$$

Differentiate Eq. (3.17) with respect to τ to obtain the CME:

$$
\begin{aligned}
\frac{\partial}{\partial \tau} \int e^{ikz} T_\tau(z) dz &= \int e^{ikz} \frac{\partial T_\tau(z)}{\partial \tau} dz \\
&= \frac{\partial}{\partial \tau} \exp\left[\rho\tau \int (e^{ikz} - 1)w(z)dz\right] \\
&= \rho \int (e^{ik\eta} - 1)w(\eta)d\eta \times \exp\left[\rho\tau \int (e^{ikz} - 1)w(z)dz\right] \\
&= \rho \int (e^{ik\eta} - 1)w(\eta)d\eta \int e^{ikz} T_\tau(z)dz \\
&= \rho \int\int e^{ik(\eta+z)} T_\tau(z)w(\eta)d\eta dz - \rho \int w(\eta)d\eta \int e^{ikz} T_\tau(z)dz \\
&= \rho \int\int e^{ikz} T_\tau(z-\eta)w(\eta)dz d\eta - \rho \int e^{ikz} T_\tau(z)dz \\
&= \rho \int e^{ikz} \left[\int T_\tau(z-\eta)w(\eta)d\eta - T_\tau(z)\right]dz.
\end{aligned}
$$

Since ρ and k are both arbitrary, we have the equation:

$$
\begin{aligned}
&\int e^{ikz} \left[\frac{\partial T_\tau(z)}{\partial \tau} - \rho\left(\int T_\tau(z-\eta)w(\eta)d\eta - T_\tau(z)\right)\right]dz = 0, \\
&\rightarrow \frac{\partial T_\tau(z)}{\partial \tau} = \rho\left[\int T_\tau(z-\eta)w(\eta)d\eta - T_\tau(z)\right].
\end{aligned} \tag{3.18}
$$

Equation (3.18) is the CME induced by compound Poisson noise with independent increments in a short time interval. Finally, we can rewrite $T_\tau(z)$ as $P(x, t)$ and the drift term $\mu(x)$ can be added to Eq. (3.18):

$$
\frac{\partial P(x, t)}{\partial t} = -\frac{\partial}{\partial x}[\mu(x)P(x, t)] + \rho\left[\int P(x-\eta, t)w(\eta) - P(x, t)\right], \tag{3.19}
$$

which is Van Kampen model with compound Poisson noise.

3.2 Formalism of Bio-evolution Model in Hamming Class

Crow-Kimura and Eigen model in Eq. (2.40) and Eq. (2.42) having 2^N equations are not easy to handle in a large N. We need to develop a method to simplify the equations in Crow-Kimura and Eigen model, so we here apply HJE into these models based on the two following assumptions. Firstly, each sequence with the same number of -1 spin has the same probability, namely, the distribution is symmetrical. Secondly, the fitness is also

assumed to be symmetrical. Finally, the general formula for correction term u_1 for PDF and mean fitness in bio-evolution are derived through HJE method.

3.2.1 Crow-Kimura Model in Hamming Class

The equation of motion for probability in Crow-Kimura model is:

$$\frac{\partial p_i}{\partial t} = r_i p_i + \sum_j m_{ij} p_j, \tag{3.20}$$

where p_i is the relative frequency for type i sequence and recall that m_{ij} is the mutation matrix:

$$\begin{cases} m_{ij} = \gamma_0, \ d_{ij} = 1, \\ m_{ii} = -N\gamma_0, \ d_{ii} = 0, \\ m_{ij} = 0, \ otherwise. \end{cases}$$

Since we have assumed that the distribution is symmetrical, the 2^N-type probability can be divided into $N + 1$ classes called Hamming class as illustrated as follows:

$$(+, +, +, +, +, +), N = 6, \ l = 0 \ class,$$
$$(+, +, +, -, +, +), N = 6, \ l = 1 \ class,$$
$$(+, -, +, +, +, +), N = 6, \ l = 1 \ class,$$
$$(+, -, +, -, +, +), N = 6, \ l = 2 \ class,$$

where l is the number of -1 spin for a sequence and $0 \leq l \leq N$. To make convenience, we define the magnetization of l-th Hamming class as:

$$m = 1 - \frac{2l}{N},$$

where $-1 \leq m \leq 1$ and m becomes continuous from discrete as $N \to \infty$. The symmetrical fitness function can be written as:

$$r_i = Nf(m), \qquad (3.21)$$
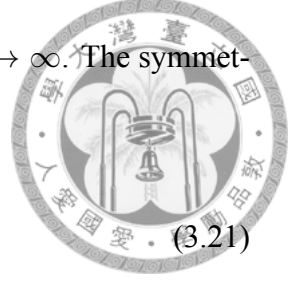
where i is belong to the l-th Hamming class. Based on the symmetrical distribution, we are interested at the total probabilities of l-th Hamming class. For a given sequence with l number of -1 spin, l-th class has N_l possible states and

$$N_l = \frac{N!}{l!(N-l)!}. \qquad (3.22)$$

Hence, the total probabilities P_l for l-th Hamming class is:

$$P_l = N_l p_l = \frac{N!}{l!(N-l)!} p_l.$$

We can chose a special sequence S_0 with all spins being $+1$ as a reference to simplify the Hamming distance as:

$$
\begin{aligned}
d_{i0} &\equiv d = (N - \sum_{k=1}^{N} s_i^k s_0^k)/2 \\
&= (N - \sum_{k=1}^{N} s_i^k)/2 \\
&= N(1 - m)/2 = l.
\end{aligned}
\qquad (3.23)
$$

There are two possible transitions of one-step for p_l as illustrated as follows:

$$p_l : (+,+,+,+,+,-,-,....,-) \to p_{l+1} : (+,+,+,+,-,-,-,....,-),$$

$$p_l : (+,+,+,+,+,-,-,....,-) \to p_{l-1} : (+,+,+,+,+,+,-,....,-).$$

There are l possible transitions from p_l to p_{l-1} and $N - l$ possible transitions from p_l to p_{l+1}. Therefore, Eq. (3.20) is transformed into the equation for Hamming class probability

p_l:

$$
\begin{aligned}
\frac{\partial p_l}{\partial t} &= N f(m) p_l + \sum_{j=1, d=l\pm 1}^{2^N} \gamma_0 p_j + m_{ii} p_l \\
&= N p_l [f(m) - \gamma_0] + \gamma_0 [l p_{l-1} + (N-l) p_{l+1}].
\end{aligned}
\tag{3.24}
$$

And we have the total probabilities for $l + 1$ and $l - 1$ Hamming class:

$$
P_{1+1} = N_{1+1} p_{1+1}, p_{1+1} = \frac{P_{l+1}}{N_{l+1}},
$$

$$
P_{1-1} = N_{1-1} p_{1-1}, p_{1-1} = \frac{P_{l-1}}{N_{l-1}}.
$$

Therefore, we can gain the equation for total probabilities of Hamming class by multiplying the both sides of Eq. (3.24) by N_l:

$$
\begin{aligned}
\frac{\partial P_l}{\partial t} &= N P_l [f(m) - \gamma_0] + \gamma_0 [\frac{l N_l}{N_{l-1}} P_{l-1} + \frac{(N-l) N_l}{N_{l+1}} P_{l+1}] \\
&= N P_l [f(m) - \gamma_0] + \gamma_0 [(N-l+1) P_{l-1} + (l+1) P_{l+1}],
\end{aligned}
\tag{3.25}
$$

where we have used the two equalities:

$$
\frac{l N_l}{N_{l-1}} = l \frac{(l-1)!(N-l+1)!}{l!(N-l)!} = N - l + 1,
$$

$$
\frac{(N-l) N_l}{N_{l+1}} = (N-1) \frac{(l+1)!(N-l-1)!}{l!(N-l)!} = l + 1.
$$

Equation (3.25) with $N + 1$ equations is small compared to 2^N equations in original Crow-Kimura model, so it's much easier to be handled for both analytic and numeric than before.

3.2.2 HJE Method in Crow-Kimura Model

In this section, we apply HJE into Crow-Kimura model to obtain the correction term of $O(\frac{1}{N})$ for the mean fitness and PDF. To investigate the behaviour of p_l, we can use the

following WKB expansion:

$$p_l = p(m,t) = \exp\left[Nu(m,t)\right],$$

$$p_{l+1} = p(m - \frac{2}{N}, t) = \exp\left[Nu(m - \frac{2}{N}, t)\right],$$

$$p_{l-1} = p(m + \frac{2}{N}, t) = \exp\left[Nu(m + \frac{2}{N}, t)\right]. \tag{3.26}$$

The finite population correction can be obtained by the Taylor's expansion of $u(m,t)$:

$$u(m - \frac{2}{N}, t) = u(m,t) - \frac{2}{N}\frac{\partial u(m,t)}{\partial m} + O(\frac{1}{N^2}),$$

$$u(m + \frac{2}{N}, t) = u(m,t) + \frac{2}{N}\frac{\partial u(m,t)}{\partial m} + O(\frac{1}{N^2}),$$

$$p_{l+1} \approx \exp\left[Nu(m,t) - 2\frac{\partial u(m,t)}{\partial m}\right] = \exp\left[-2\frac{\partial u(m,t)}{\partial m}\right]p_l,$$

$$p_{l-1} \approx \exp\left[Nu(m,t) + 2\frac{\partial u(m,t)}{\partial m}\right] = \exp\left[2\frac{\partial u(m,t)}{\partial m}\right]p_l.$$

Put these expansions into Eq. (3.24) and rearrange it to obtain the equation of zero order for p_l:

$$\frac{\partial u(m,t)}{\partial t} = f(m) - \gamma_0 + \gamma_0\left[\frac{1-m}{2}e^{2\frac{\partial u(m,t)}{\partial m}} + \frac{1+m}{2}e^{-2\frac{\partial u(m,t)}{\partial m}}\right].$$

On the other hand, the total probabilities P_l for the l-th Hamming class is:

$$
\begin{aligned}
P_l &= N_l p_l = \exp\left[N(u(m,t) + \frac{\ln N_l}{N})\right] \\
&= \exp\left[N(u(m,t) + h(m))\right] \\
&= \exp\left[NU(m,t)\right],
\end{aligned}
$$

where $h(m) = \frac{\ln N_l}{N}$ and $U(m,t) = u(m,t) + h(m)$. For general case in bio-evolution, l and $N - l$ are both large enough to use Stirling formula. Thus, the approximation of

function $h(m)$ is:

$$
\begin{aligned}
h(m) & = \frac{\ln N_l}{N} = \frac{1}{N} \ln \frac{N!}{l!(N-l)!} \\
& \approx \ln N - (1 - \frac{l}{N}) \ln (N-l) - \frac{l}{N} \ln l \\
& = -\ln (1 - \frac{l}{N}) + \frac{l}{N} \ln [\frac{(N-l)/N}{l/N}] \\
& = -\ln \frac{(1+m)}{2} + \frac{1-m}{2} \ln [(\frac{1+m}{2})/(\frac{1-m}{2})] \\
& = -[\frac{(1+m)}{2} \ln \frac{(1+m)}{2} + \frac{(1-m)}{2} \ln \frac{(1-m)}{2}], \quad (3.27)
\end{aligned}
$$

which is the zero order in $\frac{1}{N}$ approximation. Similarly, we have the following expansions for P_l:

$$
\begin{aligned}
U(m - \frac{2}{N}, t) & \approx U(m,t) - \frac{2}{N} \frac{\partial U(m,t)}{\partial m}, \\
U(m + \frac{2}{N}, t) & \approx U(m,t) + \frac{2}{N} \frac{\partial U(m,t)}{\partial m}, \\
P_{l+1} = P_l(m - \frac{2}{N}, t) & \approx \exp(-2\frac{\partial U}{\partial m}) P_l, \\
P_{l-1} = P_l(m + \frac{2}{N}, t) & \approx \exp(2\frac{\partial U}{\partial m}) P_l,
\end{aligned}
$$

where $\frac{\partial U}{\partial m} = \frac{\partial U(m,t)}{\partial m}$. Put these expansions into Eq. (3.25) and arrange it:

$$
\begin{aligned}
\frac{\partial P_l}{\partial t} & = N \frac{\partial U(m,t)}{\partial t} P_l \\
& \approx N(f(m) - \gamma_0) P_l + \gamma_0 [(N-l+1)e^{2\frac{\partial U}{\partial m}} + (l+1)e^{-2\frac{\partial U}{\partial m}}] P_l,
\end{aligned}
$$

and divide it by P_l to get the equation for $U(m,t)$:

$$
\frac{\partial U(m,t)}{\partial t} = f(m) - \gamma_0 + \gamma_0[(\frac{1+m}{2} + \frac{1}{N})e^{2\frac{\partial U}{\partial m}} + (\frac{1-m}{2} + \frac{1}{N})e^{-2\frac{\partial U}{\partial m}}]. \quad (3.28)
$$

The bulk equation in Eq. (3.28) for $U(m,t)$ turns to:

$$
\frac{\partial U(m,t)}{\partial t} = f(m) - \gamma_0 + \gamma_0[\frac{1+m}{2}e^{2\frac{\partial U}{\partial m}} + \frac{1-m}{2}e^{-2\frac{\partial U}{\partial m}}], \quad (3.29)
$$

which is the exact form of HJE,

$$\frac{\partial U(m,t)}{\partial t} = -H(m, \frac{\partial U}{\partial m}) = -H(m, U'),$$

where $U' = \frac{\partial U}{\partial m}$ and the negative Hamiltonian of system:

$$-H(m, U') = f(m) - \gamma_0 + \gamma_0[\frac{1+m}{2}e^{2U'} + \frac{1-m}{2}e^{-2U'}].$$

To investigate the asymptotic behaviour in a large-scale time for $U(m,t)$, we can assume that $U(m,t) = v(m) + kt$ where k is a constant. This assumption means that the change rate of $U(m,t)$ with respect to t is fixed, and $k = 0$ corresponds to stationary state. Physically, we can imagine that the system energy will not change after a long time. Then we get the ordinary differential equation for k:

$$k = f(m) - \gamma_0 + \gamma_0(\frac{1+m}{2}e^{2v'} + \frac{1-m}{2}e^{-2v'}), \tag{3.30}$$

where $v' = \frac{dv(m)}{dm}$. Let $y = e^{2v'}$ to get the solution of Eq. (3.30) by the following way:

$$k = f(m) - \gamma_0 + \gamma_0[\frac{(1+m)}{2}y + \frac{(1-m)}{2}y^{-1}],$$
$$y = \frac{k + \gamma_0 - f(m) \pm \sqrt{(k+\gamma_0-f(m))^2 - \gamma_0^2(1-m^2)}}{\gamma_0(1+m)},$$
$$v'(m) = \frac{1}{2}\ln\frac{k + \gamma_0 - f(m) \pm \sqrt{(k+\gamma_0-f(m))^2 - \gamma_0^2(1-m^2)}}{\gamma_0(1+m)}. \tag{3.31}$$

Therefore, $v(m)$ is obtained by integrating Eq. (3.31) with respect to m':

$$v(m) = \frac{1}{2}\int_{m_r}^{m}\ln\frac{k + \gamma_0 - f(m') \pm \sqrt{(k+\gamma_0-f(m'))^2 - \gamma_0^2(1-m'^2)}}{\gamma_0(1+m')},$$

where m_r is an appropriate reference point where $v(m_r) = 0$. Assume that the maximum of $v(m)$ is at s where the $v'(s) = 0$ and $v''(s) < 0$, and Eq. (3.30) turns to:

$$k = f(s), \tag{3.32}$$

which gives the equation of zero order in $O\frac{1}{N}$ for k. For the $[s, 1]$ interval, the physical solution for $v'(m)$ in Eq. (3.31) is the $+$ solution. Similarly, the physical solution for $v'(m)$ in Eq. (3.31) is the $'-'$ solution for the $[-1, s]$ interval. Equation (3.32) points that the total probabilities P_l has a maximum at s with mean fitness $R = N[k + O(\frac{1}{N})]$. And the s value is defined as the surplus:

$$s = \sum_{l=0}^{N} m P_l,$$

which gives the general form of mean fitness:

$$
\begin{aligned}
R &= \sum_{l=0}^{N} N f(m) P_l \\
&= N k P_{N(\frac{1-s}{2})} + \sum_{l=0,m\neq s}^{N} N f(m) P_l \\
&\approx N[k + O(\frac{1}{N})].
\end{aligned}
\tag{3.33}
$$

Since the k value corresponds to the negative Hamiltonian of system, we can expect it will reach the maximum or fixed value in a large-scale time. Physically, the bio-evolution process in a large-scale time minimizes or fixes the system energy. We have the following inequality:

$$0 \le \frac{1+m}{2} \le 1, \ 0 \le \frac{1-m}{2} \le 1,$$

and thus the corresponding inequality:

$$
k - f(m) + \gamma_0 = \gamma_0 [\frac{(1+m)}{2} e^{2v'} + \frac{(1-m)}{2} e^{-2v'}],
$$
$$
\to k - f(m) + \gamma_0 \ge 0.
$$

For the maximum condition for k, the partial derivatives of k with respect to v' at v'_0 is zero:

$$\frac{\partial k}{\partial v'}\Big|_{v'=v'_0} = \frac{1}{2}(1+m)e^{-2v'_0}(e^{4v'_0} - \frac{1-m}{1+m}) = 0,$$
$$\rightarrow e^{4v'_0} - \frac{1-m}{1+m} = 0,$$
$$\rightarrow v'_0(m) = \frac{1}{4}\ln\left(\frac{1-m}{1+m}\right). \tag{3.34}$$

Since $v(m)$ must be real in physics, we have the inequality for the square root function in Eq. (3.31):

$$(k + \gamma_0 - f(m))^2 \geq \gamma_0^2(1 - m^2),$$
$$|k + \gamma_0 - f(m)| \geq \gamma_0\sqrt{1 - m^2},$$
$$k \geq f(m) - \gamma_0 + \gamma_0\sqrt{1 - m^2} = V(m), \tag{3.35}$$

where we define the $V(m)$ as the potential of system. In CM, the $V(m)$ corresponds to negative potential energy of the system. Such inequality can be derived from the geometrical inequality:

$$k + \gamma_0 - f(m) = \gamma_0\left(\frac{1+m}{2}e^{2v'} + \frac{1-m}{2}e^{-2v'}\right)$$
$$\geq \gamma_0\sqrt{1 - m^2},$$
$$\rightarrow k \geq f(m) - \gamma_0 + \gamma_0\sqrt{1 - m^2} = V(m). \tag{3.36}$$

Thus, the k value is the maximum of $V(m)$ which corresponds to the minimum energy of system:

$$k = \max_{-1 \leq m \leq 1} V(m), \tag{3.37}$$

which is consistent with the condition for $v_0'(m)$, where the negative Hamiltonian of system:
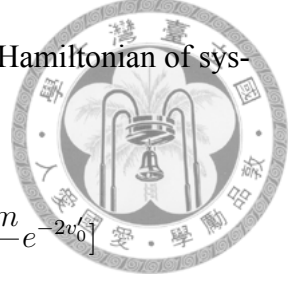
$$
\begin{aligned}
-H(m, v_0'(m)) &= f(m) - \gamma_0 + \gamma_0 \left[\frac{1+m}{2} e^{2v_0'} + \frac{1-m}{2} e^{-2v_0'} \right] \\
&= f(m) - \gamma_0 + \gamma_0 \sqrt{1 - m^2} = V(m).
\end{aligned}
$$

For the $O(\frac{1}{N})$ correction of k, the P_l in a large-scale time can be written as:

$$
P_l = \exp\left[N(k + \frac{k_1}{N})t + Nv(m) + v_1(m) \right], \tag{3.38}
$$

where $v_1(m)$ and k_1 are the correction terms of $O(\frac{1}{N})$ for $v(m)$ and k. Similarly, we have the following Taylor expansions for $v(m)$ and $v_1(m)$:

$$
\begin{aligned}
v(m \pm \frac{2}{N}) &\approx v(m) \pm \frac{2}{N}v'(m) + \frac{2}{N^2}\frac{d^2 v(m)}{dm^2}, \\
v_1(m \pm \frac{2}{N}) &\approx v_1(m) \pm \frac{2}{N}v_1'(m),
\end{aligned}
$$

so the corresponding expansion for P_{l-1} and P_{l+1}:

$$
\begin{aligned}
P_{l-1} &\approx \exp\left[N(k + \frac{k_1}{N})t + Nv(m) + v_1(m) + 2v'(m) + \frac{2}{N}v''(m) + \frac{2}{N}v_1'(m) \right] \\
&= \exp\left[2v'(m) + \frac{2}{N}v''(m) + \frac{2}{N}v_1'(m) \right] P_l, \\
P_{l+1} &\approx \exp\left[N(k + \frac{k_1}{N})t + Nv(m) + v_1(m) - 2v'(m) + \frac{2}{N}v''(m) - \frac{2}{N}v_1'(m) \right] \\
&= \exp\left[-2v'(m) + \frac{2}{N}v''(m) - \frac{2}{N}v_1'(m) \right] P_l,
\end{aligned}
$$

where $v''(m) = \frac{d^2 v(m)}{dm^2}$ and $v'_1(m) = \frac{dv_1(m)}{dm^2}$. Put these expansions into Eq. (3.28) to get the equation of $O(\frac{1}{N})$ for k_1 and $v_1(m)$:

$$
\begin{aligned}
(k + \frac{k_1}{N})P_l &\approx f(m) - \gamma_0 + \gamma_0[(\frac{1+m}{2} + \frac{1}{N})e^{2v'}e^{\frac{2}{N}u''}e^{\frac{2}{N}v'_1} \\
&+ (\frac{1-m}{2} + \frac{1}{N})e^{-2v'}e^{\frac{2}{N}u''}e^{-\frac{2}{N}v'_1}] \\
&\approx f(m) - \gamma_0 + \gamma_0[\frac{1+m}{2}e^{2v'} + \frac{1-m}{2}e^{-2v'} + \frac{1}{N}(e^{2v'} + e^{-2v'})] \\
&+ \frac{2\gamma_0 v''}{N}(\frac{1+m}{2}e^{2v'} + \frac{1-m}{2}e^{-2v'}) + \frac{2\gamma_0 v'_1}{N}(\frac{1+m}{2}e^{2v'} - \frac{1-m}{2}e^{-2v'}) \\
&\rightarrow k_1 = \gamma_0[e^{2v'} + e^{-2v'} + 2v''(\frac{1+m}{2}e^{2v'} + \frac{1-m}{2}e^{-2v'}) \\
&+ 2v'_1(\frac{1+m}{2}e^{2v'} - \frac{1-m}{2}e^{-2v'})], \tag{3.39}
\end{aligned}
$$

where these approximations have been used:

$$
\begin{aligned}
e^{\frac{2}{N}v''} &\approx 1 + \frac{2}{N}v'', \\
e^{\frac{2}{N}v'_1} &\approx 1 + \frac{2}{N}v'_1, \\
e^{-\frac{2}{N}v'_1} &\approx 1 - \frac{2}{N}v'_1.
\end{aligned}
$$

Alternatively, the k_1 value can be defined at point m_0 where the coefficient of v'_1 vanishes, so we have:

$$
\begin{aligned}
\frac{1+m_0}{2}e^{2v'(m_0)} - \frac{1-m_0}{2}e^{-2v'(m_0)} &= 0, \\
\rightarrow e^{4v'(m_0)} &= \frac{1-m_0}{1+m_0}, \\
\rightarrow v'(m_0) &= \frac{1}{4}\ln\left(\frac{1-m_0}{1+m_0}\right), \tag{3.40}
\end{aligned}
$$

which is consistent with the condition defined in Eq. (3.34), where $v'(m_0) = v'_0(m_0)$. Therefore, the k_1 value is:

$$
\begin{aligned}
k_1 &= \gamma_0\{e^{2v'(m_0)} + e^{-2v'(m_0)} + v''(m_0)[(1 + m_0)e^{2v'(m_0)} + (1 - m_0)e^{-2v'(m_0)}]\} \\
&= \gamma_0[\sqrt{\frac{1 - m_0}{1 + m_0}} + \sqrt{\frac{1 + m_0}{1 - m_0}} + v''(m_0)(\sqrt{1 - m_0^2} + \sqrt{1 - m_0^2})] \\
&= \frac{2\gamma_0}{\sqrt{1 - m_0^2}} + 2\gamma_0 v''(m_0)\sqrt{1 - m_0^2}.
\end{aligned}
\tag{3.41}
$$

To find $v''(m_0)$, we can write $-k = H(m, v')$ or $k = V(m)$ and expand it near m_0 up to second order. Remember that the first derivatives of $V(m)$ and $H(m_0, v'(m_0))$ with respect to m and v' at m_0 and $v'(m_0)$ are both zero. We have the following expansions and approximations:

$$
\begin{aligned}
k &\approx V(m_0) + V''(m_0)\frac{(m - m_0)^2}{2}, \\
-k &\approx H(m_0, v'(m_0)) + \frac{d^2 H(m_0, v'(m_0))}{dv'^2}\frac{(v'(m_0) - v_0(m_0))^2}{2}, \\
&\rightarrow V''(m_0)\frac{(m - m_0)^2}{2} + \frac{d^2 H(m_0, v'(m_0))}{dv'^2}\frac{(v'(m_0) - v_0(m_0))^2}{2} \approx 0,
\end{aligned}
\tag{3.42}
$$

where the second derivatives of $V(m)$ and $H(m_0, v'(m))$ at m_0 and $v'_0(m_0)$ are:

$$
\begin{aligned}
V''(m_0) &= f''(m_0) - \frac{\gamma_0}{(1 - m_0^2)^{\frac{3}{2}}}, \\
\left.\frac{d^2 H(m_0, v'(m_0))}{dv'^2}\right|_{v'=v'_0} &= 4\gamma_0\sqrt{1 - m_0^2},
\end{aligned}
\tag{3.43}
$$

where $f''(m_0) = \left.\frac{d^2 f(m)}{dm^2}\right|_{m=m_0}$. Also, we have the following approximations for $v'_0(m)$ near the $m_0 = 1 - \frac{2l_0}{N}$ point:

$$
\begin{aligned}
m - m_0 &= \frac{2(l_0 - l)}{N} = O(\frac{1}{N}), \\
2v''(m_0) &= \frac{-1}{1 - m_0^2} = 2\frac{v'(m) - v'_0(m_0)}{m - m_0} + O(\frac{1}{N}), \\
2[v'(m) - v'_0(m_0)] &\approx [2v''(m_0) + \frac{1}{1 - m_0^2}](m - m_0),
\end{aligned}
$$

where l is near l_0 and $O(\frac{1}{N})$ terms must be neglected for k_1 correction term. Put these approximations into Eq. (3.42) to obtain $v''(m_0)$:
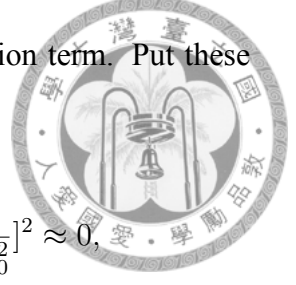
$$
\begin{aligned}
4V''(m_0) \;+\; & \frac{d^2H(m_0, v'(m_0))}{dv'^2}\Big|_{v'=v'_0}[2v''(m_0) + \frac{1}{1-m_0^2}]^2 \approx 0, \\
2v''(m_0) \;\approx\; & -\frac{1}{1-m_0^2} - \sqrt{-\frac{4V''(m_0)}{\frac{d^2H(m_0,v'(m_0))}{dv'^2}\Big|_{v'=v'_0}}} \\
= \; & \frac{-1}{1-m_0^2} - \frac{1}{(1-m_0^2)^{\frac{1}{4}}}\sqrt{\frac{1}{(1-m_0^2)^{3/2}} - \frac{f''(m_0)}{\gamma_0}} \\
= \; & \frac{-1}{1-m_0^2}[1 + \sqrt{1 - \frac{(1-m_0^2)^{\frac{3}{2}}f''(m_0)}{\gamma_0}}].
\end{aligned}
\tag{3.44}
$$

With the known $2v''(m_0)$, we can put it into Eq. (3.41) to obtain k_1:

$$
\begin{aligned}
k_1 \;=\; & \frac{2\gamma_0}{\sqrt{1-m_0^2}} - \frac{\gamma_0}{\sqrt{1-m_0^2}} - \frac{\gamma_0}{\sqrt{1-m_0^2}}\sqrt{1 - \frac{(1-m_0^2)^{\frac{3}{2}}f''(m_0)}{\gamma_0}} \\
= \; & \frac{\gamma_0}{\sqrt{1-m_0^2}}[1 - \sqrt{1 - \frac{(1-m_0^2)^{\frac{3}{2}}f''(m_0)}{\gamma_0}}].
\end{aligned}
\tag{3.45}
$$

And the equation for v'_1 can be obtained:

$$
\begin{aligned}
& 2v'_1(\frac{1+m}{2}e^{2v'} - \frac{1-m}{2}e^{-2v'}) \\
& = \frac{k_1}{\gamma_0} - e^{2v'} - e^{-2v'} - 2v''(\frac{1+m}{2}e^{2v'} + \frac{1-m}{2}e^{-2v'}). \\
& v'_1 = \frac{\frac{k_1}{\gamma_0} - e^{2v'} - e^{-2v'} - v''[(1+m)e^{2v'} + (1-m)e^{-2v'}]}{(1+m)e^{2v'} - (1-m)e^{-2v'}}.
\end{aligned}
\tag{3.46}
$$

Therefore, the correction term v_1 is:

$$
v_1(m) = \int_{m_r}^{m} \frac{\frac{k_1}{\gamma_0} - e^{2v'} - e^{-2v'} - v''[(1+m')e^{2v'} + (1-m')e^{-2v'}]}{(1+m')e^{2v'} - (1-m')e^{-2v'}} dm',
\tag{3.47}
$$

where m_r is an appropriate reference point, where $v_1(m_r) = 0$.

3.2.3 Modified Eigen Model in Hamming Class
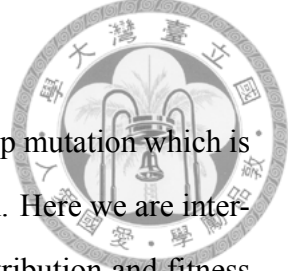
As mentioned before, Eigen model is the evolution of multiple-step mutation which is more complicated than the Crow-Kimura model of one-step mutation. Here we are interested at the Eigen model in Hamming class, where the sequence distribution and fitness function are both symmetrical.

Considering the sequence S_{l-n} with $l - n$ Hamming distance from reference sequence S_0, the S_{l-n} can be generated from S_l through n_1 up and n_2 down, where $n = n_1 - n_2$. This process can be explained by Hamming distance $d_{l0} = l$ in the following way. For the sequence S_l with l number of -1 spin, n_1 up and n_2 down corresponds to the change of Hamming distance:

$$\Delta d = -n_1 + n_2$$
$$\rightarrow d_{l0} + \Delta d = l - (n_1 - n_2) = l - n,$$

where Δd is the change of Hamming distance after n_1 up and n_2 down. And all the possible transitions from S_{l-n} to S_l is:

$$M_n = \frac{l!}{n_1!(l - n_1)!} \times \frac{(N - l)!}{n_2!(N - l - n_2)!}, \tag{3.48}$$

where M_n is the number of all possible transitions, $0 \leq n_1 \leq l$, and $0 \leq n_2 \leq N - l$. Consider the following mutation matrix,

$$Q_{ij} = Q_n = \hat{Q}q^{-n}(1 - q)^n, \tag{3.49}$$

where $n = d_{ij}$ and $\hat{Q}$ is the constant q^N. Thus, we can write down the modified Eigen model without dilution and degradation terms as the following:

$$\frac{dp_l}{dt} = \sum_{n_1=0}^{l} \sum_{n_2=0}^{N-l} M_n Q_{n_1+n_2} r_{l-n} p_{l-n}, \tag{3.50}$$

where p_l is one sequence probability in l-th Hamming class and the number of total mu-

tations from p_{l-n} to p_l is $n_1 + n_2$.

3.3 SMAT Modelling

For common SMAT experiments, 304-steel balls always cover the area of motor top in $20 \sim \% \sim 25\%$. The probability ratio of ball-ball collision to ball-sample collision is very small, and it can be estimated as follows:

$$P_{bb} \propto A_b^2 \times \frac{NV_b}{V_c}, \ P_{bs} \propto A_b A_s,$$
$$\rightarrow \frac{P_{bb}}{P_{bs}} \propto \frac{A_b}{A_s} \frac{NV_b}{V_c} \approx 0,$$

where we have assumed that flying balls are uniformly distributed in the chamber, P_{bb} and P_{bs} are the probability of ball-ball and ball-sample collision, A_b and A_s are the cross-sectional area of ball and sample, V_b and V_c are the volume of ball and chamber, and N is the ball number. Usually, the ratio of $\frac{A_b}{A_s}$ is less than 1% [33, 47]. Based on this fact, the collisions between flying balls is less frequent than collisions between flying balls and sample or flying balls and motor, namely, ball-ball collisions can be neglected without loss of generality. Physically, this means that the ball-ball interaction or potential can be neglected. Thus, we can select a flying ball to stand the whole flying balls as a representative particle, and the motor is regarded as a reservoir providing balls energy. Consequently, these identical-flying balls can be regarded as a system interacting with the sample bottom while ignoring the collisions between these flying balls. For this reason, we can consider the time-averaged value of single representative ball.

3.3.1 The Kinetic Energy of balls

Since the average ratio of horizontal speed to vertical speed for flying balls in common SMAT experiments is abut $0.16 \sim 0.25$ [33], namely, the average angle of both motor and sample surfaces is about $80°$. The kinetic energy ratio of horizontal component to vertical component is about 0.05, which is $<< 1$. Thus, we can assume the angle of both impact

surfaces are normal without loss of generality. The motor-top motion can be characterized as a longitudinal harmonic motion:

$$
\begin{aligned}
v_m &= A\omega sin(\omega t) \\
&= 2\pi\nu A sin(\omega t),
\end{aligned} \tag{3.51}
$$

where A is the oscillation amplitude, ω is the angular frequency, and ν is the oscillation frequency. By the formula in Eq. (2.49), the ball velocity induced initially by motor top is:

$$
\begin{aligned}
v_{b0} &= \frac{2m_m}{m_m + m_b}v_m \\
&= \frac{2}{1 + \frac{m_b}{m_m}}v_m \approx 2v_m,
\end{aligned} \tag{3.52}
$$

where m_m and m_b are the mass of motor and ball. Usually, m_m is millions times m_b in common SMAT experiments. Therefore, the initial velocity of balls is assumed to be:

$$
v_{b0} = \frac{2A\omega}{1 + \frac{m_b}{m_m}} \sin \phi, \tag{3.53}
$$

where ϕ is the phase of sinusoidal function. And flying balls will collide with the sample bottom under the condition:

$$
\frac{1}{2}m_b v_{b0}^2 \geq mg(h - D) \rightarrow \sin \phi \geq \frac{\sqrt{2g(h - D)}}{v_{max}},
$$
$$
v_{max} = \frac{2A\omega}{1 + \frac{m_b}{m_m}}, \; \theta_0 = sin^{-1}(\frac{\sqrt{2g(h - D)}}{v_{max}}), \tag{3.54}
$$

where h is the chamber height, D is the diameter of a flying ball, g is the gravitational acceleration, and v_{max} and θ_0 are parameters defined by Eq. (3.54). This condition states that a flying ball must overcome the gravitational potential between a flying ball and earth to collide with the sample bottom. The time average for initial speed of balls is obtained

by carrying out the integration per one cycle of harmonic motion:

$$\bar{v_{b0}} = \frac{\int_{\theta_0}^{\pi/2} v_{b0}\mathrm{d}\phi}{\int_{\theta_0}^{\pi/2} \mathrm{d}\phi} = \frac{v_{max}\cos\theta_0}{\frac{\pi}{2} - \theta_0},$$

where $\sin\phi$ is symmetrical to $\phi = \frac{\pi}{2}$ and this integration can be carried out over first quadrant. For common SMAT experiments, we are allowed to use the following conditions and approximations:

$$A\omega \gg \sqrt{g(h-D)/2},$$

$$\sin\theta_0 \approx 0, \sin\theta_0 \approx \theta_0,$$

$$\theta_0 \approx (1 + \frac{m_b}{m_m})\sqrt{\frac{g(h-D)}{2A^2\omega^2}}. \tag{3.55}$$

Then the averaged initial speed of these balls turn immediately to:

$$\bar{v_{b0}} \approx \frac{v_{max}(1 - \frac{\theta_0^2}{2})}{\frac{\pi}{2} - \theta_0} \approx \frac{2}{\pi}v_{max},$$

where the following Taylor expansion for cosine function has been used:

$$\cos\phi \approx 1 - \frac{\phi^2}{2!}.$$

Let us define the two parameters for simplicity:

$$\alpha = \theta_0^2 = \frac{2g(h-D)}{v_{max}^2}, \eta = \frac{\alpha}{sin^2\phi}, \tag{3.56}$$

and the flying time of these balls from the motor top to the sample bottom are given by the equation:

$$h - D = v_{b0}t - \frac{1}{2}gt^2.$$

Thus, we have the following approximation for t:

$$
\begin{aligned}
t &= \frac{v_{b0}}{g}\left(1 - \sqrt{1 - \frac{\alpha}{\sin^2\phi}}\right) \\
&= \frac{v_{b0}}{g}(1 - \sqrt{1 - \eta}), \\
&\approx \frac{v_{b0}}{g}\left(\frac{1}{2}\eta + \frac{1}{8}\eta^2 + \frac{1}{16}\eta^3\right) \\
&= \frac{\alpha v_{max}}{2g}\left(\csc\phi + \frac{1}{4}\alpha\csc^3\phi + \frac{1}{8}\alpha^2\csc^5\phi\right),
\end{aligned}
$$

where α and η are both parameters defined in Eq. (3.56) and the binomial expansion has been used:

$$
\begin{aligned}
(1 + x)^n &= \sum_{k=0}^{\infty}\left[\frac{\mathrm{d}^k}{\mathrm{d}x^k}(1+x)^n\right]\Big|_{x=0}\frac{x^k}{k!} = \sum_{k=0}^{\infty}\binom{k}{n}x^n \\
&\approx 1 + nx + \frac{n(n-1)}{2!}x^2 + \frac{n(n-1)(n-2)}{3!}x^3, \ for \ x << 1. \quad (3.57)
\end{aligned}
$$

With the expansion for t, the time-averaged t, τ, can be acquired by carrying out the integration with respect to ϕ over one period of sinusoidal function:

$$
\begin{aligned}
\tau &\approx \frac{\alpha v_{max}}{2g}\frac{\int_{\theta_0}^{\frac{\pi}{2}}(\csc\phi + \frac{1}{4}\alpha\csc^3\phi + \frac{1}{8}\alpha^2\csc^5\phi)\mathrm{d}\phi}{\int_{\theta_0}^{\frac{\pi}{2}}\mathrm{d}\phi} \\
&= \frac{\alpha v_{max}}{g(\pi - 2\theta_0)}I(\theta_0), \quad (3.58)
\end{aligned}
$$

where

$$
\begin{aligned}
I(\theta_0) &= \left(1 + \frac{\theta_0^2}{8} + \frac{3\theta_0^4}{64}\right)\ln(\csc\theta_0 + \cot\theta_0) \\
&+ \frac{\theta_0^2}{8}\left(1 + \frac{3\theta_0^2}{8}\right)\csc\theta_0\cot\theta_0 + \frac{\theta_0^4}{32}\csc^3\theta_0\cot\theta_0.
\end{aligned}
$$

For common SMAT experiments, the scale of $A, \omega, h,$ and D are $40 \sim 80 \ \mu m, 40\pi \ krad/s$, $20 \ mm$, and $1 \sim 3 \ mm$ respectively [33, 47]. The corresponding value of parameters, α and $\sin\theta_0$, are from $8.242 \times 10^{-4} \sim 3.685 \times 10^{-3}$ and $2.871 \times 10^{-2} \sim 6.070 \times 10^{-2}$ respectively, so the higher order terms can be neglected without loss of generality. The relative errors of approximation in Eq. (3.55) are less than 0.1%. The τ in Eq. (3.58)

ranges from $2.413 \sim 4.570 \ ms$. The averaged initial speed of these balls ranges from $6.645 \sim 13.033 \ m/s$. The time-averaged speed of these balls before second collision can be obtained by:

$$
\begin{aligned}
\langle v \rangle &= \frac{\int_{\theta_0}^{\frac{\pi}{2}} \sqrt{v_{b0}^2 - 2g(h - D)} \mathrm{d}\phi}{\int_{\theta_0}^{\frac{\pi}{2}} \mathrm{d}\phi} \\
&= \frac{v_{max}}{\frac{\pi}{2} - \theta_0} \int_{\theta_0}^{\frac{\pi}{2}} \sin\phi \sqrt{1 - \eta} \mathrm{d}\phi \\
&\approx \frac{v_{max}}{\frac{\pi}{2} - \theta_0} \int_{\theta_0}^{\frac{\pi}{2}} \sin\phi (1 - \frac{\eta}{2} - \frac{\eta^2}{8} - \frac{\eta^3}{16}) \mathrm{d}\phi \\
&\approx \bar{v_{b0}} - g\tau \approx \bar{v_{b0}},
\end{aligned}
\tag{3.59}
$$

which gives the averaged-speed of these balls, varying from $6.588 \sim 12.693 \ m/s$ in good agreement with the speed of flying balls in the SMAT experiment measured by high-speed cameras [33]. The variation trends of averaged flying ball speed as a function of SMAT vibration amplitude and frequency are presented in Fig. 3.1. It can be seen that the ball speed would increase in proportional to the SMAT amplitude and frequency.

Thus, the total-averaged kinetic energy of these flying balls before second collision between the sample bottom and flying balls is the sum of kinetic energy of each ball:

$$
\begin{aligned}
E_{k,total} &= \sum_{k=1}^{N} \frac{1}{2} m_b \langle v \rangle^2 \\
&\approx N \times \frac{1}{2} m_b (\bar{v_{b0}} - g\tau)^2 \approx N \times \frac{1}{2} m_b \bar{v_{b0}}^2 \\
&\approx \frac{N}{3\pi} D^3 \rho_b A^2 \omega^2 \propto D A^2 \omega^2,
\end{aligned}
$$

where ρ_b is the density of flying balls. Recall that the balls will cover about 25% area of the chamber bottom,

$$
N \times \pi D^2 \approx 0.25 A_c,
$$
$$
N \approx \frac{A_c}{4\pi D^2} \propto \frac{1}{D^2},
$$

where A_c is the surface area of chamber bottom. Thus, the higher the diameter of ball is,

the lower the total number of balls would be.

3.3.2 The Loss of Kinetic Energy for Balls

On colliding with the sample surface, the kinetic energy of flying balls will not be conserved due to the inelastic collision between flying balls and sample. In the SMAT chamber, we assume that a ball with mass m_b have velocity v_b before colliding with the sample bottom and velocity v_b' after colliding with the sample bottom, and the sample with mass m_s is initially at rest and gains velocity v_s' after colliding with a flying ball. Thus, the corresponding coefficient of restitution (the act of recovering to a former state) is:

$$e = \frac{v_s' - v_b'}{v_b - v_s} = \frac{v_s' - v_b'}{v_b},$$

Considering the inelastic collision, we can use Eq. (2.48) and Eq. (3.59) to calculate the v_b' and v_s':

$$v_b' = \frac{m_b - em_s}{m_b + m_s} v_b = \frac{m_b - em_s}{m_b + m_s} \langle v \rangle,$$
$$v_s' = \frac{(1+e)m_b}{m_b + m_s} v_b = \frac{(1+e)m_b}{m_b + m_s} \langle v \rangle.$$

And the averaged-loss of kinetic energy for flying balls and sample ($\Delta E_{k,loss,b}$ and $\Delta E_{k,loss,s}$) are:

$$
\begin{aligned}
\Delta E_{k,loss,b} &= N(\frac{1}{2}m_b v_b^2 - \frac{1}{2}m_b v_b'^2) \\
&= \frac{N}{2}m_b \langle v \rangle^2 [1 - (\frac{m_b - em_s}{m_b + m_s})^2], \quad (3.60) \\
\Delta E_{k,loss,s} &= N(\frac{1}{2}m_s v_s^2 - \frac{1}{2}m_s v_s'^2) \\
&= \frac{N}{2}m_b \langle v \rangle^2 [\frac{(1+e)m_b}{m_b + m_s}]^2. \quad (3.61)
\end{aligned}
$$

This loss will be converted into the heat energy of sample and flying balls and the internal energy (or so-called the strain energy) of sample and flying balls. And the kinetic energy of sample will be assumed to convert almost into the internal energy of sample. Figure 3.2

60

presents the variation trends of kinetic energy loss of flying balls, sample, and total (the sum of those for balls and sample). It is apparent that the kinetic energy loss will increase with increasing $\frac{m_b}{m_s}$, the loss will reach the maximum at the point $\frac{m_b}{m_s} = e$. Similarly, the average time, τ', of flying balls from the sample bottom to the motor top between second collision of the sample bottom and flying balls and third collision of the motor top and flying balls can be obtained by the following equations:

$$
\begin{aligned}
h - D &= |v_b'|\,\tau' + \frac{1}{2}g\tau'^2, \\
\tau' &= \frac{|v_b'|}{g}\left(-1 + \sqrt{1 + \frac{2g(h-D)}{v_b'^2}}\right) \\
&= \frac{|v_b'|}{g}\left(-1 + \sqrt{1 + \eta'}\right),
\end{aligned}
$$

where the corresponding ball velocity and parameters:

$$
|v_b'| = \left|\frac{\frac{m_b}{m_s} - e}{1 + \frac{m_b}{m_s}}\right| v_b = \left|\frac{\frac{m_b}{m_s} - e}{1 + \frac{m_b}{m_s}}\right| \langle v \rangle = \frac{-\chi + e}{1 + \chi}\langle v \rangle, \tag{3.62}
$$

$$
\eta' = \frac{2g(h-D)}{v_b'^2}, \chi = \frac{m_b}{m_s} = \frac{\pi \rho_b D^3}{6 \rho_s A_s L}. \tag{3.63}
$$

where L is the sample thickness, ρ_s is the sample density, and η' and χ assumed to be smaller than e are parameters defined in Eq. (3.63). Similarly, the average time of these flying balls from the sample bottom to the motor top between second and third collision, τ', can be obtained by the expansion of η':

$$
\tau' \approx \frac{v_b'}{2g}\left(\eta' - \frac{1}{4}\eta'^2 + \frac{1}{8}\eta'^3\right).
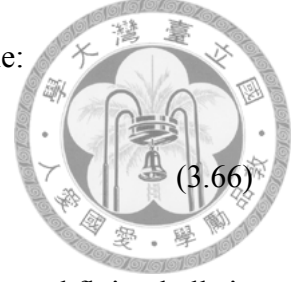$$

Thus, the averaged-time period of flying balls (going up and down between second and third collision) and total-averaged power loss of kinetic energy of balls are

$$
\Delta t = \tau + \tau', \tag{3.64}
$$

$$
P_{loss,b} = N\frac{\Delta E_{k,loss,b}}{\Delta t} = \frac{N}{2}m_b \langle v \rangle^2 \frac{1 - \left(\frac{\chi - e}{\chi + 1}\right)^2}{\tau + \tau'}. \tag{3.65}
$$

And so does the total-averaged power loss of kinetic energy of sample:

$$P_{loss,s} = N \times \frac{\Delta E_{k,loss,s}}{\Delta t} = \frac{N}{2} m_s \langle v \rangle^2 \frac{\left[\frac{(1+e)\chi}{\chi+1}\right]^2}{\tau + \tau'}, \qquad (3.66)$$

where we have assumed that there is N collisions between the sample and flying balls in Δt. Figure 3.3 illustrates the variation trend of averaged-time period of flying balls as a function of the SMAT vibration amplitude and frequency. The trend says that the time period decreases with increasing amplitude and frequency. This is reasonable in physics since the average speed of flying balls is proportional to amplitude and frequency. In addition, Fig. 3.4 shows the variation trends of power loss of flying balls, sample, and total (the sum of those for balls and sample). It is apparent that with increasing $\frac{m_b}{m_s}$ the energy loss will increase, but with different trends.

On the other hand, the phase change of harmonic motion after ball going up and down in the SMAT chamber is:

$$\Delta\phi = 2\pi \times \nu\Delta t,$$

and if $\Delta\phi$ satisfies the condition:

$$\Delta\phi = 2\pi \times n, \ n \in positive \ integer,$$

$$\rightarrow \nu \cdot \Delta t = n,$$

then the sinusoidal function will reach the same value ($\sin(\phi + \Delta\phi) = \sin\phi$), namely, the velocity of flying balls will be steady. In static, the condition make the fluctuation of speed for flying balls independent of time in a large-scale time. With the steady speed of flying balls, each strain caused by a collision in the sample will be uniform.

Chapter 4

Analytical and Numerical Solution

In this chapter, we solve the analytical and numerical solution of CME with Gaussian white and compound Poisson noises, modified Eigen model in Hamming class, and heat equation for SMAT. Analytical solutions of CME and Eigen are well consistent with numerical simulation in a large-scale time. Mathematically, we can say that they are equal to each other. The calculation of analytical solutions and numerical equation is involved in this chapter in a detail.

4.1 CME Solution

We consider two models to describe chemical reactions including the CME with compound Poisson noise and CME with compound Poisson and Gaussian noise. We have calculated the analytical solution of steady-state PDF for the models, and the dynamics of PDF has been simulated by finite difference methods. On reaching the steady state of dynamics for PDF, they are in a good agreement with each other. We at first preferred the Galerkin method which requires fixed boundary conditions (B.C.s) for $x = 0$ and $x = \infty$ to do this simulation, however, the only B.C.s for this case is $P(\infty) = 0$ and $P'(\infty) = 0$. Additionally, it can be expected that the B.C.s of analytical solution at $x = 0$ are not fixed making the Galerkin method failed. Thus, we turn to the forward finite difference method with normalized condition which doesn't need the fixed B.C.s at $x = 0$ to simulate the dynamics state of PDF.

4.1.1 Finite Difference Method
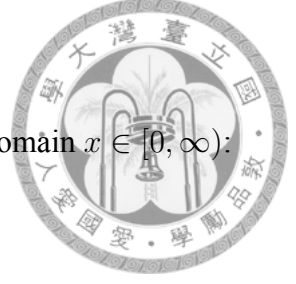
In our CME research, we works with the general CME with the domain $x \in [0, \infty)$:

$$\frac{\partial P(x,t)}{\partial t} = \epsilon \frac{\partial^2 P(x,t)}{\partial x^2} + \frac{\partial}{\partial x}[R(x)P(x,t)]$$
$$+ c\left[\int_0^x P(x-y,t)w(y)dy - P(x,t)\right], \quad (4.1)$$
$$w(y) = k\exp{(-ky)}.$$

From Taylor expansion with finite difference h, we have the following for $f(x+h)$:

$$
\begin{aligned}
f(x+h) &= \sum_{n=0}^{\infty} \frac{f^{(n)}(x)}{n!}h^n \\
&= f(x) + f'(x)h + \frac{f''(x)}{2!}h^2 + \frac{f'''(x)}{3!}h^3 + \cdots \\
&= f(x) + f'(x)h + O(h^2).
\end{aligned}
$$

Therefore, we have the following approximation of $O(h)$ for $f'(x)$:

$$
\begin{aligned}
f'(x) &= \frac{f(x+h) - f(x) - O(h^2)}{h}, \\
&= \frac{f(x+h) - f(x)}{h} + O(h).
\end{aligned}
$$

Similarly, $f(x+2h)$ and $f(x+h)$ can be expanded as:

$$f(x+2h) = f(x) + 2f'(x)h + 2f''(x)h^2 + O(h^3),$$
$$f(x+h) = f(x) + f'(x)h + \frac{f''(x)}{2}h^2 + O(h^3).$$

Thus, the approximation of $O(h)$ for $f''(x)$:

$$f(x+2h) - 2f(x+h) + f(x) = f''(x)h^2 + O(h^3),$$
$$f''(x) = \frac{f(x+2h) - 2f(x+h) + f(x) - O(h^3)}{h^2}$$
$$= \frac{f(x+2h) - 2f(x+h) + f(x)}{h^2} + O(h).$$

These are the forward finite difference with accuracy of $O(h)$ for $f'(x)$ and $f''(x)$. To get the accuracy of high order for $f'(x)$, we can expand $f(x+h)$ into more terms:

$$f(x+h) = f(x) + f'(x)h + \frac{f''(x)}{2!}h^2 + O(h^3),$$

and we have:

$$
\begin{aligned}
f'(x) &= \frac{f(x+h) - f(x) - \frac{f''(x)}{2!}h^2 - O(h^3)}{h} \\
&= \frac{2f(x+h) - 2f(x) - f(x+2h) + 2f(x+h) - f(x) + O(h^3)}{h} \\
&= \frac{-f(x+2h) + 4f(x+h) - 3f(x)}{2h} + O(h^2).
\end{aligned}
$$

Similarly, the accuracy of high order for $f''(x)$ can be derived as:

$$f''(x) = \frac{-f(x+3h) + 4f(x+2h) - 5f(x+h) + 2f(x)}{h^2} + O(h^2).$$

The coefficients of higher order for forward finite difference are listed in the table of Appendix. For the integration of Eq. (4.1), we apply the trapezoid rule with accuracy of $O(h^2)$ to approximate it:

$$
\begin{aligned}
\int_a^b f(x)dx &= \frac{h[f(a) + f(a+h)]}{2} + \frac{h[f(a+h) + f(a+2h)]}{2} \\
&\quad + \ldots + \frac{h[f(a+(N-1)h) + f(b)]}{2} + O(h^2) \\
&= \sum_{l=1}^{N-1} f(a+lh)h + \frac{h[f(a) + f(b)]}{2} + O(h^2),
\end{aligned}
$$

where the discrete space of integration is chose to be equal to that of differentiation, N is the partition number of interval $[a, b]$, and $Nh = b - a$. Put all these approximations into Eq. (4.1) and take the forward finite difference with space H in first order on time axis to obtain the following numerical equation with accuracy of $O(h^2)$ and $O(H)$ at $x = ih$ and

65

$t = jH$:

$$\frac{P(ih, (j+1)H) - P(ih, jH)}{H}$$

$$\approx \; \epsilon \frac{-P((i+3)h, jH) + 4P((i+2)h, jH) - 5P((i+1)h, jH) + 2P(ih, jH)}{h^2}$$

$$+ \; \frac{-R((i+2)h)P((i+2)h, jH) + 4R((i+1)h)P((i+1)h, jH) - 3R(ih)P(ih, jH)}{2h}$$

$$+ \; c[\sum_{l=1}^{i-1} P((i-l)h, jH)w(lh)h + \frac{ckh}{2}[P(0, jH)e^{-ikh} + P(ih, jH)] - P(ih, jH)].(4.2)$$

For sake of simplicity, we can introduce the following notations:

$$P(ih, jH) = P_i^j, R(ih) = R_i.$$

Therefore, Eq. (4.2) can be re-written as:

$$
\begin{aligned}
P_i^{j+1} &= -\frac{\epsilon H}{h^2} P_{i+3}^j + (\frac{4\epsilon H}{h^2} - \frac{H}{2h} R_{i+2}) P_{i+2}^j + (\frac{-5\epsilon H}{h^2} + \frac{2H}{h} R_{i+1}) P_{i+1}^j \\
&+ (1 + \frac{2\epsilon H}{h^2} - \frac{3H}{2h} R_i + \frac{kchH}{2} - cH) P_i^j \\
&+ ckhH \sum_{l=1}^{i-1} P_{i-1}^j e^{-lkh} + \frac{ckHh}{2} P_0^j e^{-ikh}.
\end{aligned}
\tag{4.3}
$$

For $i = 0$ and $j = 0$,

$$P_0^1 = -\frac{\epsilon H}{h^2} P_3^0 + (\frac{4\epsilon H}{h^2} - \frac{H}{2h} R_1) P_0^1 + (1 + \frac{2\epsilon H}{h^2} - \frac{3H}{2h} R_0 - cH) P_0^0,$$

where we have removed the integral term of Eq. (4.3) which makes no contribution (the area is zero) at $i = 0$ and $j = 0$. For $i = 1$ and $j = 0$:

$$
\begin{aligned}
P_1^1 &= -\frac{\epsilon H}{h^2} P_4^0 + (\frac{4\epsilon H}{h} - \frac{H}{2h} R_3) P_3^0 + (\frac{-5\epsilon H}{h^2} + \frac{2H}{h} R_2) P_2^0 \\
&+ (1 + \frac{2\epsilon H}{h^2} - \frac{3H}{2h} R_1 + \frac{kchH}{2} - cH) P_1^0 + \frac{ckHh}{2} e^{-kh} P_1^0.
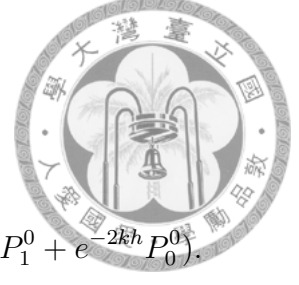\end{aligned}
$$

For $i = 2$ and $j = 0$:

$$
\begin{aligned}
P_2^1 &= -\frac{\epsilon H}{h^2} P_5^0 + (\frac{4\epsilon H}{h^2} - \frac{H}{2h} R_4) P_4^0 + (\frac{-5\epsilon H}{h^2} + \frac{2H}{h} R_3) P_3^0 \\
&+ (1 + \frac{2\epsilon H}{h^2} - \frac{3H}{2h} R_2 + \frac{kchH}{2} - cH) P_2^0 + \frac{ckHh}{2} (2e^{-kh} P_1^0 + e^{-2kh} P_0^0).
\end{aligned}
$$

To simplify the representation of N numerical equations, it can be written as the matrix multiplication:

$$
\begin{pmatrix} P_0^1 \\ P_1^1 \\ \vdots \\ P_{N-2}^1 \\ P_{N-1}^1 \\ P_N^1 \end{pmatrix} = A_{N \times N+3} \begin{pmatrix} P_0^0 \\ P_1^0 \\ \vdots \\ P_{N+1}^0 \\ P_{N+2}^0 \\ P_{N+3}^0 \end{pmatrix}, \tag{4.4}
$$

where A is a N by $N + 3$ non-square matrix. To make A square, the last three elements of right column on the right side of Eq. (4.4) can be neglected without loss of generality. If the system boundary is large enough, the PDF is approximately zero on $x = (N + 1)h \sim (N + 2)h$. Effect of the last three elements is so small that it will make no impact on the dynamical behaviour of PDF. By observing the A elements from $i = 0 \sim 2$ at $j = 0$, A can be written as the general representation in i and j:

$$
\begin{cases}
A_{i,i} = 1 + \frac{2\epsilon H}{h^2} - \frac{3H}{2h} R_i + \frac{kchH}{2}(1 - \delta_{i0}) - cH, \ 0 \le i \le N - 1 \\[2mm]
A_{i,i+1} = \frac{-5\epsilon H}{h^2} + \frac{2H}{h} R_{i+1}, \ 0 \le i \le N - 2 \\[2mm]
A_{i,i+2} = \frac{4\epsilon H}{h^2} - \frac{H}{2h} R_{i+2}, \ 0 \le i \le N - 3 \\[2mm]
A_{i,i+3} = -\frac{\epsilon H}{h^2}, \ 0 \le i \le N - 4 \\[2mm]
A_{i,0} = \frac{1}{2} kchH e^{(1-i)kh}, \ 1 \le i \le N - 1 \\[2mm]
A_{i,j} = chHw((i - j)h), \ for \ i \ge 1 \ and \ i > j
\end{cases} \tag{4.5}
$$

where we have ignored the last three columns of A not affecting the dynamical state of PDF in general if Nh is large enough. Thus, A is a square N by N matrix now. Eventually,

the time-evolution of PDF can be simulated by the algorithm with normalization condition for PDF:

$$P_i^1 = AP_i^0, \, P_i^1 = \frac{P_i^1}{\sum_j P_j^1},$$

$$P_i^2 = AP_i^1, \, P_i^2 = \frac{P_i^2}{\sum_j P_j^2},$$

$$\vdots$$

$$P_i^k = AP_i^{k-1}, \, P_i^k = \frac{P_i^k}{\sum_j P_j^k},$$

where $P_i^k = \frac{P_i^k}{\sum_j P_j^k}$ is the step for normalization. As time past, we can judge whether PDF arrive the steady state or not by the following criteria:

$$\frac{P_i^k}{P_i^{k-1}} \approx 1 \, or \, \frac{P_i^k - P_i^{k-1}}{P_i^{k-1}} \approx 0 \, for \, all \, i.$$

With the $h \to 0^+$ and $H \to 0^+$ condition, A will become a Markov matrix. Physically, each matrix multiplication of A is equivalent to the perturbation of previous state. Since this perturbation is so small that it can be imagined as the adiabatic process in quantum mechanics, initial PDF will finally become one of the eigenvectors of A. Nevertheless, it's very hard to find the eigenvector of A for large N value. As we all know that the total eigenvectors of A is of $O(N)$ and N is normally from $10000 \sim 20000$ in this case. Furthermore, it's also hard to judge which eigenvector is right for the steady state of PDF. Thus, it's better to simulate the dynamical steady of PDF in a large-scale time, namely, the initial PDF is multiplied by A after many times.

4.1.2 Analytical Solution of Van Kampen CME without Diffusion Term

Consider the Van Kampen CME solved by FCX in 2006 [1]:

$$\frac{\partial P(x,t)}{\partial t} = \frac{\partial}{\partial x}[\gamma_2 x P(x,t)] + k_1 [\int_0^x dy P(x-y,t)w(y) - P(x,t)], \qquad (4.6)$$

68

where $w(y)$ is the transition PDF for a mRNA into protein. This partial differential equation (PDE) corresponds to the following scheme for DNA-mRNA-protein process as indicated in Fig. 4.1, where k_1 is the transition rate of a DNA into mRNA, k_2 is the transition rate of a mRNA into protein, and $\gamma_{1,2}$ is the degradation rate of mRNA or protein, respectively. Since the lifetime of mRNAs can be assumed to be short compared to that of proteins, proteins can be considered to be produced in random uncorrelated events. The transition PDF $w(y)$ for a mRNA into protein has been measured in Fig. 4.2 [48].

$$w(y) = \frac{1}{b} \exp\left(-\frac{1}{b}y\right),$$

where $b = \frac{k_2}{\gamma_1}$. Let us at first consider the steady-state solution of PDF, namely,

$$\frac{\partial P(x,t)}{\partial t} = 0,$$

and take the Laplace transform on the both sides of Eq. (4.6):

$$
\begin{aligned}
0 &= s\mathscr{L}[\gamma_2 x P(x)] - [\gamma_2 x P(x)]\big|_{x=0} - k_1\left(\frac{\frac{1}{b}}{s + \frac{1}{b}} - 1\right)\hat{P}(s), \\
0 &= -\gamma_2 s \frac{d\hat{P}(s)}{ds} - k_1 \frac{s}{s + \frac{1}{b}}\hat{P}(s), \\
0 &= \frac{d\hat{P}(s)}{ds} + \frac{a}{s + \frac{1}{b}}\hat{P}(s),
\end{aligned}
\tag{4.7}
$$

where $a = \frac{k_1}{\gamma_2}$, s is a complex constant, and

$$\hat{P}(s) = \mathscr{L}[P(x)] = \int_0^\infty P(t)e^{-st}dt.$$

The $\hat{P}(s)$ solution can be obtained by taking the integration in the method of separation variables:

$$\frac{d\hat{P}(s)}{\hat{P}(s)} = \frac{-a}{s + \frac{1}{b}} ds,$$

$$\int \frac{d\hat{P}(s)}{\hat{P}(s)} = \int \frac{-a}{s + \frac{1}{b}} ds,$$

$$\ln|\hat{P}(s)| = -a \ln|s + \frac{1}{b}| + \ln c,$$

$$\hat{P}(s) = \frac{c}{(s + \frac{1}{b})^a}. \tag{4.8}$$

where c is an integration constant. Finally, the $P(x)$ solution is immediately obtained by taking the inverse Laplace transformation of $\hat{P}(s)$:

$$P(x) = \mathscr{L}^{-1}[\hat{P}(s)] = \frac{c}{\Gamma(a)} x^{a-1} e^{-\frac{x}{b}}, \tag{4.9}$$

where

$$\mathscr{L}^{-1}[\hat{P}(s)] = \frac{1}{2\pi i} \lim_{T \to \infty} \int_{\gamma - iT}^{\gamma + iT} e^{st} \hat{P}(s) ds,$$

and $P(x)$ is a gamma distribution. The c value can be calculated from the normalization condition for $P(x)$:

$$\begin{aligned}
1 &= \int_0^\infty P(x)dx = \frac{c}{\Gamma(a)} \int_0^\infty x^{a-1} e^{\frac{-x}{b}} dx \\
&= \frac{cb^a}{\Gamma(a)} \int_0^\infty x^{a-1} e^{-x} dx = \frac{cb^a}{\Gamma(a)} \Gamma(a) = cb^a, \\
&\Rightarrow c = \frac{1}{b^a}, \; P(x) = \frac{1}{\Gamma(a)b^a} x^{a-1} e^{\frac{-x}{b}}. \tag{4.10}
\end{aligned}$$

To test the validity of our numerical algorithm, we can simulate the dynamical state of PDF by the forward finite difference method with three set of parameters: (i) $a = 0.5$, $b = 5$, (ii) $a = 5$, $b = 5$, (iii) $a = 8$, $b = 8$, and set the initial PDF as exponential distribution which is reasonable for the DNA-mRNA–protein process:

$$P(x, 0) = ke^{-kx} \; or \; P(x, 0) = \frac{2}{\sqrt{\pi}} e^{-x^2}.$$

No matter which initial exponential PDF we set, we can expect that PDF will finally reach the same steady state, namely, the gamma distribution. The Figs. 4.3-5 correspond to the case (i) of dynamical state and steady state for PDF. As indicated in these figures, the dynamical state of PDF in a large-scale time will be consistent with the analytical solution of steady state for PDF, the gamma distribution. For $a < 1$ parameter, the gamma distribution goes to infinity as $x \to 0^+$. For $a > 1$ parameter, the gamma distribution has a global maximum at $x_0 = b(a - 1)$ where $\frac{dP(x)}{dx}\big|_{x=x_0} = 0$. The Figs. 4.6-8 correspond to the case (ii) of dynamical state and steady state for PDF. The Figs. 4.9-10 correspond to the case (iii) of dynamical state and steady state for PDF. As shown in Figs. 4.6-10 the x_0 value increases with increasing a and b.
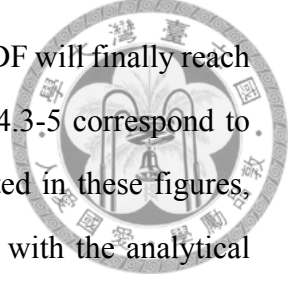
4.1.3 Asymptotic Solution of Van Kampen CME with Diffusion Term

Now we turn to consider the Van Kampen CME added diffusion term, $\epsilon \frac{\partial^2 P(x,t)}{\partial x^2}$, which is so-called intrinsic noise for a given system. This CME has the form:

$$
\begin{aligned}
\frac{\partial P(x,t)}{\partial t} &= \epsilon \frac{\partial^2 P(x,t)}{\partial x^2} + \frac{\partial}{\partial x}[\gamma_2 x P(x,t)] \\
&+ a\gamma_2 [\int_0^x P(x-y,t)w(y)dy - P(x,t)],
\end{aligned}
\tag{4.11}
$$

where the transition PDF $w(y)$ we use is ke^{-ky}. To investigate the steady-state solution of Eq. (4.11), we at first calculate the special cases: (i) $a = 0$ and (ii) x near 0. For $a = 0$ parameter, Eq. (4.11) on reaching steady-state becomes the form:

$$
0 = \epsilon \frac{\partial^2 P(x,t)}{\partial x^2} + \frac{\partial}{\partial x}[\gamma_2 x P(x,t)],
\tag{4.12}
$$

which is the exact form of Fokker-Planck equation. The Eq. (4.12) can be reduced into the ordinary differential equation of first order:

$$
\begin{aligned}
0 &= \frac{\partial}{\partial x}[\frac{\partial P(x)}{\partial x} + \frac{\gamma_2 x}{\epsilon} P(x)], \\
c_1 &= \frac{\partial P(x)}{\partial x} + \frac{\gamma_2 x}{\epsilon} P(x),
\end{aligned}
\tag{4.13}
$$

where c_1 is an integration constant. The integrating factor $I(x)$ of Eq. (4.13) is:

$$I(x) = \exp \int \frac{\gamma_2 x}{\epsilon} dx = \exp\left(\frac{\gamma_2 x^2}{2\epsilon}\right).$$

With this $I(x)$, the general solution of $P(x)$ in Eq. (4.13) is:

$$P(x) = c_1 e^{-\frac{\gamma_2 x^2}{2\epsilon}} \int_c^x e^{\frac{\gamma_2 t^2}{2\epsilon}} dt + c_2 e^{-\frac{\gamma_2 x^2}{2\epsilon}}, \qquad (4.14)$$

where c_2 is an integration constant and c is an appropriate reference point. Physically, we require the B.C.s for PDF: $P(\infty) = 0$ and $P'(\infty) = 0$. We have the following equations for $P(\infty)$ and $P'(\infty)$ in Eq. (4.14):

$$
\begin{aligned}
\lim_{x\to\infty} P(x) &= \lim_{x\to\infty}\left[c_1 e^{-\frac{\gamma_2 x^2}{2\epsilon}} \int_c^x e^{\frac{\gamma_2 t^2}{2\epsilon}} dt + c_2 e^{-\frac{\gamma_2 x^2}{2\epsilon}}\right] \\
&= \lim_{x\to\infty}\left[c_1 e^{-\frac{\gamma_2 x^2}{2\epsilon}} \int_c^x e^{\frac{\gamma_2 t^2}{2\epsilon}} dt\right] \\
&= c_1 \lim_{x\to\infty} \frac{\int_c^x e^{\frac{\gamma_2 t^2}{2\epsilon}} dt}{e^{\frac{\gamma_2 x^2}{2\epsilon}}} \\
&= c_1 \lim_{x\to\infty} \frac{\epsilon}{\gamma_2 x} = 0,
\end{aligned}
$$

$$
\begin{aligned}
\lim_{x\to\infty} P'(x) &= \lim_{x\to\infty}\left[-c_1 \frac{\gamma_2}{\epsilon} x e^{-\frac{\gamma_2 x^2}{2\epsilon}} \int_c^x e^{\frac{\gamma_2 t^2}{2\epsilon}} dt + c_1 - c_2 \frac{\gamma_2}{\epsilon} x e^{-\frac{\gamma_2 x^2}{2\epsilon}}\right] \\
&= c_1 \lim_{x\to\infty}\left[1 - \frac{\gamma_2}{\epsilon} \frac{x \int_c^x e^{\frac{\gamma_2 t^2}{2\epsilon}} dt}{e^{\frac{\gamma_2 x^2}{2\epsilon}}}\right] \\
&= c_1 \lim_{x\to\infty}\left[1 - \frac{\int_c^x e^{\frac{\gamma_2 t^2}{2\epsilon}} dt + x e^{\frac{\gamma_2 t^2}{2\epsilon}}}{x e^{\frac{\gamma_2 t^2}{2\epsilon}}}\right] \\
&= -c_1 \lim_{x\to\infty} \frac{\int_c^x e^{\frac{\gamma_2 t^2}{2\epsilon}} dt}{x e^{\frac{\gamma_2 t^2}{2\epsilon}}} = 0,
\end{aligned}
$$

where the both solutions satisfy the B.C.s of $P(x)$ and $P'(x)$ as $x \to \infty$. Since we have the following asymptotic behaviour for the first solution of $P(x)$ in Eq. (4.14):

$$\lim_{x \to \infty} \frac{\int_c^x e^{\frac{\gamma_2 t^2}{2\epsilon}} dt}{e^{\frac{\gamma_2 t^2}{2\epsilon}}} = \frac{\epsilon}{\gamma_2} \lim_{x \to \infty} \frac{1}{x},$$

$$e^{-\frac{\gamma_2 x^2}{2\epsilon}} \int_c^x e^{\frac{\gamma_2 t^2}{2\epsilon}} dt \sim \frac{1}{x},$$

the first solution violates the normalization condition for $P(x)$:

$$\int_0^\infty dx \, e^{-\frac{\gamma_2 x^2}{2\epsilon}} \int_c^x e^{\frac{\gamma_2 t^2}{2\epsilon}} dt \to \infty \neq 1.$$

Thus, the first solution of $P(x)$ in Eq. (4.14) must be dropped off. By the normalization condition, the c_2 can be obtained by:

$$
\begin{aligned}
1 &= \int_0^\infty P(x) dx \\
&= c_2 \int_0^\infty e^{-\frac{\gamma_2 x^2}{2\epsilon}} dx = c_2 \sqrt{\frac{\pi \epsilon}{2\gamma_2}}, \\
\Rightarrow \quad c_2 &= \sqrt{\frac{2\gamma_2}{\pi \epsilon}}, \, P(x) = \sqrt{\frac{2\gamma_2}{\pi \epsilon}} e^{-\frac{\gamma_2 x^2}{2\epsilon}},
\end{aligned}
$$

where $P(x)$ is a Gaussian distribution with $\sqrt{\frac{2\epsilon}{\pi\gamma_2}}$ expectation value. Physically, this small amount of proteins are created by the intrinsic noise, random collisions in diffusion process. As γ_2 increases, the protein production decreases. The effect of random collisions disappears as $\epsilon \to 0$, and $P(x)$ becomes the delta function at $x = 0$. Without intrinsic noise (ϵ term) and extrinsic noise ($a\gamma_2$ term), protein cannot be synthesised.

We have the following integration by part for the integration term in Eq. (4.11):

$$
\begin{aligned}
\int_0^x P(x-y)w(y)dy &= \int_0^x P(y)w(x-y)dy \\
&= e^{-kx}\int_0^x P(y)ke^{ky}dy = e^{-kx}\int_0^x P(y)de^{ky} \\
&= e^{-kx}\{[e^{ky}P(y)]\big|_0^x - \frac{1}{k}\int_0^x P'(y)de^{ky}\} \\
&= e^{-kx}\{e^{kx}P(x) - P(0) - [\frac{e^{ky}}{k}P'(y)]\big|_0^x + \frac{1}{k^2}\int_0^x P''(y)de^{ky}\} \\
&= e^{-kx}\{e^{kx}P(x) - P(0) - \frac{1}{k}[e^{kx}P'(x) - P'(0)] \\
&+ \frac{1}{k^2}\int_0^x P''(y)de^{ky}\},
\end{aligned}
\tag{4.15}
$$

where we have the following approximations for x near 0:

$$
e^{kx}P(x) - P(0)
$$

$$
\approx (1+kx)[P(0) + P'(0)x] - P(0)
$$

$$
\approx kxP(0) + xP'(0),
$$

$$
e^{kx}P'(x) - P'(0)
$$

$$
\approx (1+kx)[P'(0) + P''(0)x] - P'(0)
$$

$$
\approx kxP'(0) + xP''(0).
$$

Therefore, Eq. (4.15) can be approximated as:

$$
\begin{aligned}
&kxP(0) + xP'(0) - xP'(0) - \frac{x}{k}P''(0) + \frac{1}{k^2}\int_0^x P''(y)de^{ky} \\
&\approx kxP(x) - \frac{x}{k}P''(x) + \frac{P''(x)}{k}\int_0^x e^{ky}dy \\
&= kxP(x) - \frac{x}{k}P''(x) + \frac{P''(x)}{k^2}(e^{kx} - 1) \\
&\approx kxP(x) - \frac{x}{k}P''(x) + \frac{xP''(x)}{k} \approx kxP(x)
\end{aligned}
\tag{4.16}
$$

where we have used the mean value theorem of integral for the integration:

$$
\int_0^x P''(y)e^{ky}dy = P''(c)\int_0^x e^{ky}dy, \ for \ c \in (0, x).
$$

Since x is near 0, the c can be approximated as x. For x near 0 case, the integration term in Eq. (4.11) can be neglected under the condition:

$$kx << \gamma_2 \Rightarrow x << \frac{\gamma_2}{k},$$

and the Eq. (4.11) becomes:

$$\frac{\partial P(x,t)}{\partial t} = \epsilon \frac{\partial^2 P(x,t)}{\partial x^2} + \frac{\partial}{\partial x}[\gamma_2 x P(x,t)] - a\gamma_2 P(x,t). \tag{4.17}$$

For the steady-state $P(x)$ of Eq. (4.17), we have:

$$0 = \frac{d^2 P(x)}{dx^2} + \frac{d}{dx}[\frac{\gamma_2}{\epsilon} x P(x)] - \frac{a\gamma_2}{\epsilon} P(x),$$
$$0 = \frac{d^2 P(x)}{dx^2} + \frac{\gamma_2}{\epsilon} x \frac{dP(x)}{dx} + \gamma_2 \frac{1-a}{\epsilon} P(x). \tag{4.18}$$

Since the solution of Eq. (4.18) with $a = 0$ reduces to Gaussian distribution, we can use the ansatz:

$$P(x) = e^{-\frac{\gamma_2 x^2}{2\epsilon}} H(x) = e^{-\frac{\gamma_2 x^2}{2\epsilon}} x F(x). \tag{4.19}$$

The corresponding derivatives of $P(x)$ in terms of $F(x)$ are:

$$\begin{aligned}
\frac{dP(x)}{dx} &= e^{-\frac{\gamma_2 x^2}{2\epsilon}}[-\frac{\gamma_2}{\epsilon} x H(x) + \frac{dH(x)}{dx}] \\
&= x e^{-\frac{\gamma_2 x^2}{2\epsilon}}[(-\frac{\gamma_2}{\epsilon} x + \frac{1}{x})F(x) + \frac{dF(x)}{dx}], \\
\frac{d^2 P(x)}{dx^2} &= e^{-\frac{\gamma_2 x^2}{2\epsilon}}[(\frac{\gamma_2^2 x^2}{\epsilon^2} - \frac{\gamma_2}{\epsilon})H(x) - 2\frac{\gamma_2}{\epsilon} x \frac{dH(x)}{dx} + \frac{d^2 H(x)}{dx^2}] \\
&= x e^{-\frac{\gamma_2 x^2}{2\epsilon}}[\frac{\gamma_2}{\epsilon}(\frac{\gamma_2}{\epsilon} x^2 - 3)F(x) + 2(\frac{1}{x} - \frac{\gamma_2}{\epsilon})\frac{dF(x)}{dx} + \frac{d^2 F(x)}{dx^2}].
\end{aligned}$$

Put these expressions into Eq. (4.18) to obtain:

$$\frac{d^2 F(x)}{dx^2} + (\frac{2}{x} - \frac{\gamma_2}{\epsilon} x)\frac{dF(x)}{dx} - \frac{\gamma_2}{\epsilon}(1+a)F(x) = 0. \tag{4.20}$$

And set the change of variables:

$$t = \frac{\gamma_2 x^2}{2\epsilon}.$$

The corresponding differential operators with respect to t:

$$\frac{d}{dx} = \frac{\gamma_2}{\epsilon} x \frac{d}{dt},$$
$$\frac{d^2}{dx^2} = \frac{\gamma_2}{\epsilon} \frac{d}{dt} + \frac{\gamma_2^2}{\epsilon^2} x^2 \frac{d^2}{dt^2}.$$

Thus, the Eq. (4.20) is transformed into:

$$t\frac{d^2 F(t)}{dt^2} + (\frac{3}{2} - t)\frac{dF(t)}{dt} - \frac{1+a}{2} F(t) = 0,$$

which is the Kummer's differential equation with the two linear-independent solutions:

$$F(t) = c_1 KummerM(\frac{1+a}{2}, \frac{3}{2}, t) + c_2 KummerU(\frac{1+a}{2}, \frac{3}{2}, t). \qquad (4.21)$$

And the asymptotic behaviour of the two Kummer functions near $t = 0$ is:

$$KummerM(\frac{1+a}{2}, \frac{3}{2}, t) \sim 1,$$
$$KummerU(\frac{1+a}{2}, \frac{3}{2}, t) \sim \frac{1}{\sqrt{t}},$$

where the corresponding behaviour of $P(x)$ near $x = 0$:

$$P(x) = xe^{-\frac{\gamma_2 x^2}{2\epsilon}} F(t) \approx (c_1 x + c_2 \sqrt{\frac{2\epsilon}{\gamma_2}})e^{-\frac{\gamma_2 x^2}{2\epsilon}} \sim \sqrt{\frac{\epsilon}{\gamma_2}}.$$

Thus, the random-collision process or diffusion term with any a value is the dominating factor for $P(x)$ near $x = 0$. No matter what the a value is, the intrinsic noise strongly affects the behaviour of $P(x)$ near $x = 0$, and the non-zero $P(0)$ is proportional to $\sqrt{\frac{\epsilon}{\gamma_2}}$.

4.1.4 Analytical Solution of Van Kampen CME with Diffusion Term
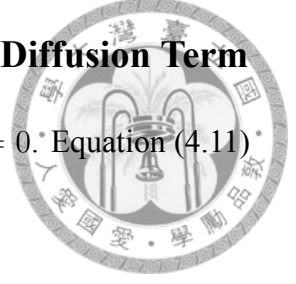
Now we turn to solve the steady state of Eq. (4.11) with $\frac{\partial P(x,t)}{\partial t} = 0$. Equation (4.11) must satisfy the normalization condition for PDF:

$$\int_0^\infty P(x,t)dx = 1.$$

Therefore, we at first take integration on the both sides of Eq. (4.11) with respect to x over the integrand $[0, \infty)$:

$$
\begin{aligned}
0 &= \frac{\partial}{\partial t}\int_0^\infty P(x,t)dx = \int_0^\infty \frac{\partial P(x,t)}{\partial t}dx \\
&= \epsilon\left[\frac{\partial P(x,t)}{\partial x}\right]\Big|_0^\infty + \left[\gamma_2 x P(x,t)\right]\Big|_0^\infty \\
&\quad + a\gamma_2\left[\int_0^\infty\int_0^x ke^{-ky}P(x-y,t)dydx - \int_0^\infty P(x,t)dx\right] \\
&= \epsilon\frac{\partial P(x,t)}{\partial x}\Big|_{x=0} + \left[\gamma_2 x P(x,t)\right]\Big|_{x=0},
\end{aligned}
$$

to investigate the behaviour of $P(x,t)$ at $x = 0$, where the integration for convolution term is:
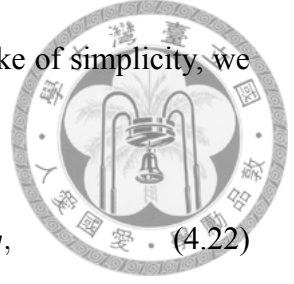
$$
\begin{aligned}
\int_0^\infty\int_0^x ke^{-ky}P(x-y,t)dydx &= \int_0^\infty e^{ky}P(y,t)\int_y^\infty ke^{-kx}dxdy \\
&= \int_0^\infty e^{ky}P(y,t)[-e^{-kx}]\Big|_y^\infty dy \\
&= \int_0^\infty P(y,t)dy = 1.
\end{aligned}
$$

Since we have $P(\infty,t) = 0$ and $\frac{\partial P(x,t)}{\partial x}\Big|_{x=\infty} = 0$, we can chose the reasonable boundary conditions for $P(x,t)$:

$$
\lim_{x\to 0}[xP(x,t)] = 0,
$$
$$
\frac{\partial P(x,t)}{\partial x}\Big|_{x=0} = 0,
$$

where the last condition is the zero flux for $P(x, t)$ at $x = 0$. For sake of simplicity, we can set the change of variables for the steady-state $P(x)$:

$$y(x) = \int_0^x P(x - y)e^{-ky}dy = e^{-kx}\int_0^x P(x)e^{ky}dy, \quad (4.22)$$

where the corresponding derivatives of $P(x)$ in terms of $y(x)$ are:

$$P(x) = \frac{dy(x)}{dx} + ky(x),$$
$$\frac{dP(x)}{dx} = \frac{d^2y(x)}{dx^2} + k\frac{dy(x)}{dx},$$
$$\frac{d^2P(x)}{dx^2} = \frac{d^3y(x)}{dx^3} + k\frac{d^2y(x)}{dx^2}.$$

And the corresponding initial conditions for $y(x)$ at $x = 0$:

$$\begin{cases} y(0) = 0, \\ y'(0) = P(0), \\ y''(0) = -kP(0), \end{cases} \quad (4.23)$$

where recall that we have the zero flux for PDF at $x = 0$. Therefore, we have the following ordinary differential equation of third order for $y(x)$:

$$\frac{\epsilon}{\gamma_2}\frac{d^3y(x)}{dx^3} + (x + \frac{\epsilon}{\gamma_2}k)\frac{d^2y(x)}{dx^2} + (1 - a + kx)\frac{dy(x)}{dx} + ky(x) = 0, \quad (4.24)$$

which is a linear homogeneous equation. Since the Eq. (4.24) is linear homogeneous and third order equation, the solution of Eq. (4.24) can be expressed as the sum of three linear-independent functions:

$$y(x) = c_1y_1(x) + c_2y_2(x) + c_3y_3(x), \quad (4.25)$$

where c_{1-3} are all undetermined constants determined by the initial conditions of Eq. (4.23) and normalization condition for $P(x, t)$ and $y_{1-3}(x)$ is the homogeneous solution

of Eq. (4.24). Since the solution of Eq. (4.24) without diffusion term is a gamma function, we can expect that $y(x)$ is proportional to e^{-kx}. To simplify Eq. (4.24), we can let $y(x)$ in term of:

$$y(x) = e^{-kx}H(x),$$

where the corresponding derivatives of $y(x)$ are:

$$\frac{dy(x)}{dx} = -ky(x) + e^{-kx}\frac{dH(x)}{dx},$$
$$\frac{d^2y(x)}{dx^2} = -k\frac{dy(x)}{dx} - e^{-kx}(k\frac{dH(x)}{dx} + \frac{d^2H(x)}{dx^2}),$$
$$\frac{d^3y(x)}{dx^3} = -k\frac{d^2y(x)}{dx^2} + e^{-kx}(k^2\frac{dH(x)}{dx} - 2k\frac{d^2H(x)}{dx^2} + \frac{d^3H(x)}{dx^3}).$$

Put all these derivatives of $y(x)$ in term of $H(x)$ into Eq.(4.24) and rearrange it:

$$0 = e^{-kx}[\frac{\epsilon}{\gamma_2}\frac{d^3H}{dx^3} + (x - 2\frac{\epsilon}{\gamma_2}k)\frac{d^2H}{dx^2} + (\frac{\epsilon}{\gamma_2}k^2 + 1 - a - kx)\frac{dH}{dx} + akH],$$
$$0 = \frac{\epsilon}{\gamma_2}\frac{d^3H}{dx^3} + (x - 2\frac{\epsilon}{\gamma_2}k)\frac{d^2H}{dx^2} + (\frac{\epsilon}{\gamma_2}k^2 + 1 - a - kx)\frac{dH}{dx} + akH. \qquad (4.26)$$

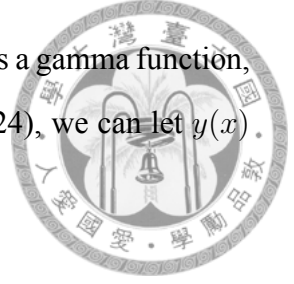Set $c = \frac{\epsilon}{\gamma_2}k$ and the change of variable:

$$s = x - \frac{\epsilon}{\gamma_2}k = x - c,$$

and then the Eq. (4.26) becomes:

$$\frac{\epsilon}{\gamma_2}\frac{d^3H}{ds^3} + (s - c)\frac{d^2H}{ds^2} + (1 - a - ks)\frac{dH}{ds} + akH = 0. \qquad (4.27)$$
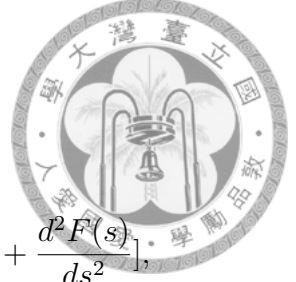
As we did in previous section, we can let:

$$H(s) = e^{-\frac{\gamma_2 s^2}{2\epsilon}}sF(s),$$

where the corresponding derivatives of $H(s)$:

$$
\frac{dH(s)}{ds} = se^{-\frac{\gamma_2 s^2}{2\epsilon}}[(-\frac{\gamma_2}{\epsilon}s + \frac{1}{s})F(s) + \frac{dF(s)}{ds}],
$$

$$
\frac{d^2 H(s)}{ds^2} = se^{-\frac{\gamma_2 s^2}{2\epsilon}}[\frac{\gamma_2}{\epsilon}(\frac{\gamma_2}{\epsilon}s^2 - 3)F(s) + 2(\frac{1}{s} - \frac{\gamma_2}{\epsilon})\frac{dF(s)}{ds} + \frac{d^2 F(s)}{ds^2}],
$$

$$
\frac{d^3 H(s)}{ds^3} = se^{-\frac{\gamma_2 s^2}{2\epsilon}}\{\frac{d^3 F(s)}{ds^3} + 3(\frac{1}{s} - \frac{\gamma_2}{\epsilon}s)\frac{d^2 F(s)}{ds^2}
$$

$$
+ \ 3(\frac{\gamma_2^2}{\epsilon^2}s^2 - 3\frac{\gamma_2}{\epsilon})\frac{dF(s)}{ds} + [(-\frac{\gamma_2^3}{\epsilon^3}s^3 + 6\frac{\gamma_2^2}{\epsilon^2})s - 3\frac{\gamma_2}{\epsilon}\frac{1}{s}]F(s)\}.
$$

Put all these derivatives into Eq. (4.27) to obtain the equation for $F(s)$:

$$
\frac{\epsilon}{\gamma_2}\frac{d^3 F}{ds^3} + (3\frac{\epsilon}{\gamma_2}\frac{1}{s} - \frac{\epsilon k}{\gamma_2} - 2s)\frac{d^2 F}{ds^2} + [\frac{\gamma_2}{\epsilon}s^2 + ks + 2\frac{\epsilon k}{\gamma_2 s} - (a+6)]\frac{dF}{ds}
$$

$$
+ (a+2)(\frac{\gamma_2}{\epsilon}s - \frac{1}{s} + k)F = 0. \qquad (4.28)
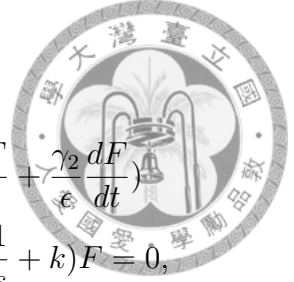$$

Similarly, we can set the change of variable:

$$
t = \frac{\gamma_2 s^2}{2\epsilon},
$$

where the corresponding differential operators with respect to t:

$$
\frac{d}{ds} = \frac{\gamma_2}{\epsilon}s\frac{d}{dt},
$$

$$
\frac{d^2}{ds^2} = \frac{\gamma_2}{\epsilon}\frac{d}{dt} + \frac{\gamma_2^2}{\epsilon^2}s^2\frac{d^2}{dt^2},
$$

$$
\frac{d^3}{ds^3} = 3\frac{\gamma_2^2}{\epsilon^2}s\frac{d^2}{dt^2} + \frac{\gamma_2^3}{\epsilon^3}s^3\frac{d^3}{dt^3}.
$$

Put all these operators into Eq. (4.28) to obtain the equation:

$$\frac{\epsilon}{\gamma_2}(\frac{\gamma_2^3}{\epsilon^3}s^3\frac{d^3F}{dt^3} + 3\frac{\gamma_2^2}{\epsilon^2}s\frac{d^2F}{dt^2}) + (3\frac{\epsilon}{\gamma_2}\frac{1}{s} - \frac{\epsilon k}{\gamma_2} - 2s)(\frac{\gamma_2^2}{\epsilon^2}s^2\frac{d^2F}{dt^2} + \frac{\gamma_2}{\epsilon}\frac{dF}{dt})$$

$$+[\frac{\gamma_2}{\epsilon}s^2 + ks + 2\frac{\epsilon k}{\gamma_2 s} - (a+6)]\frac{\gamma_2}{\epsilon}s\frac{dF}{dt} + (a+2)(\frac{\gamma_2}{\epsilon}s - \frac{1}{s} + k)F = 0,$$

$$\frac{\gamma_2^2}{\epsilon^2}s^3\frac{d^3F}{dt^3} + \frac{\gamma_2}{\epsilon}s(6 - 2\frac{\gamma_2}{\epsilon}s^2 - ks)\frac{d^2F}{dt^2} + [3(\frac{1}{s} - k)$$

$$+\frac{\gamma_2}{\epsilon}s(-8 + \frac{\gamma_2}{\epsilon}s^2 + ks - a)]\frac{dF}{dt} + (a+2)[\frac{\gamma_2}{\epsilon}s(1 - \frac{\epsilon}{\gamma_2 s^2}) + k]F = 0,$$

$$\frac{\gamma_2}{\epsilon}s[2t\frac{d^3F}{dt^3} + (6 - 4t)\frac{d^2F}{dt^2} + (-8 + 2t - a + \frac{\frac{3}{2}}{t})\frac{dF}{dt} - \frac{a+2}{2t}F]$$

$$+k[-2t\frac{d^2F}{dt^2} + (2t - 3)\frac{dF}{dt} + (a+2)F] = 0. \tag{4.29}$$

Since the solution of $F(x)$ is Kummer function near $x = 0$, we can assume that $F(x)$ may be related to Kummer function for $x \neq 0$. We have the solutions $KummerM(\mu, \nu, t)$ and $KummerU(\mu, \nu, t)$ to Kummer's differential equation:

$$t\frac{d^2F}{dt^2} + (\nu - t)\frac{dF}{dt} - \mu F = 0,$$

where μ and ν are both constants, and the following equivalent equations:

$$2t\frac{d^3F}{dt^3} + (2 + 2\nu - 2t)\frac{d^2F}{dt^2} - 2(\mu + 1)\frac{dF}{dt} = 0,$$

$$\frac{d^2F}{dt^2} + (\frac{\nu}{t} - 1)\frac{dF}{dt} - \frac{\mu}{t}F = 0,$$

$$-2kt\frac{d^2F}{dt^2} + (2kt - 2k\nu)\frac{dF}{dt} + 2k\mu F = 0,$$

$$-2t\frac{d^2F}{dt^2} + (2t - 2\nu)\frac{dF}{dt} + 2\mu F = 0.$$

These equations give us the direction to write Eq. (4.29) in terms of t as:

$$\{\frac{\gamma_2}{\epsilon}s[2t\frac{d^3F}{dt^3} + (5-2t)\frac{d^2F}{dt^2} - 2(\frac{a}{2}+2)\frac{dF}{dt}]\}$$

$$-k\{2t\frac{d^2F}{dt^2} + (3-2t)\frac{dF}{dt} + (a+2)F\}$$

$$+\{\frac{\gamma_2}{\epsilon}s[\frac{d^2F}{dt^2} + (\frac{\frac{3}{2}}{t}-1)\frac{dF}{dt} - \frac{\frac{a}{2}+1}{t}F]\}$$

$$+\{\frac{\gamma_2}{\epsilon}s[-2t\frac{d^2F}{dt^2} + (2t-3)\frac{dF}{dt} + (a+2)F]\} = 0. \qquad (4.30)$$

By observation, the solutions to Eq. (4.30) are $KummerM(1+\frac{a}{2}, \frac{3}{2}, t)$ and $KummerU(1+\frac{a}{2}, \frac{3}{2}, t)$ which make all four terms zero in Eq. (4.30). Thus, we already have two solutions to Eq. (4.24). And the two solutions is choose as:

$$y_1(x) = e^{-kx}(x - \frac{\epsilon k}{\gamma_2})e^{-\frac{\gamma_2}{2\epsilon}(x-\frac{\epsilon k}{\gamma_2})^2} KummerM(1+\frac{a}{2}, \frac{3}{2}, \frac{\gamma_2}{2\epsilon}(x-\frac{\epsilon k}{\gamma_2})^2),$$

$$y_2(x) = e^{-kx}(x - \frac{\epsilon k}{\gamma_2})e^{-\frac{\gamma_2}{2\epsilon}(x-\frac{\epsilon k}{\gamma_2})^2} KummerU(1+\frac{a}{2}, \frac{3}{2}, \frac{\gamma_2}{2\epsilon}(x-\frac{\epsilon k}{\gamma_2})^2).$$

To simplify the expression of Eq. (4.30), we can introduce the variable $Y = Y(F(t), t)$ as:

$$Y = 2t\frac{d^2F}{dt^2} + (3-2t)\frac{dF}{dt} - (a+2)F,$$

$$\frac{dY}{dt} = 2t\frac{d^3F}{dt^3} + (5-2t)\frac{d^2F}{dt^2} - (a+4)\frac{dF}{dt},$$

where $Y = 0$ corresponds to the $y_1(x)$ and $y_2(x)$ solution. With the introduction of Y, Eq. (4.30) can be written as:

$$\frac{\gamma_2}{\epsilon}s\frac{dY}{dt} + (-k + \frac{\gamma_2}{\epsilon}s\frac{1}{2t} - \frac{\gamma_2}{\epsilon}s)Y = 0,$$

$$\Rightarrow \frac{dY}{ds} + (\frac{1}{s} - k - \frac{\gamma_2}{\epsilon}s)Y = 0. \qquad (4.31)$$

Therefore, the $y_3(x)$ can be found by the Eq. (4.31) with $Y \neq 0$. For $Y \neq 0$, we have:

$$\frac{dY}{ds} = (k + \frac{\gamma_2}{\epsilon}s - \frac{1}{s})Y,$$

$$\frac{dY}{Y} = (k + \frac{\gamma_2}{\epsilon}s - \frac{1}{s})ds,$$

$$\Rightarrow Y(s) = c_3'\frac{1}{s}e^{ks+\frac{\gamma_2}{2\epsilon}s^2}, \tag{4.32}$$

where c_3' is an integration constant. We should transform $Y(t)$ into $Y(s)$ by the relation between t and s differential operators:

$$\frac{d}{dt} = \frac{\epsilon}{\gamma_2}\frac{1}{s}\frac{d}{ds},$$

$$\frac{d^2}{dt^2} = -\frac{\epsilon^2}{\gamma_2^2}\frac{1}{s^3}\frac{d}{ds} + \frac{\epsilon^2}{\gamma_2^2}\frac{1}{s^2}\frac{d^2}{ds^2},$$

$$Y(s) = \frac{\gamma_2}{\epsilon}s^2(\frac{\epsilon^2}{\gamma_2^2}\frac{1}{s^2}\frac{d^2F}{ds^2} - \frac{\epsilon^2}{\gamma_2^2}\frac{1}{s^3}\frac{dF}{ds}) + (3 - \frac{\gamma_2}{\epsilon}s^2)\frac{\epsilon}{\gamma_2}\frac{1}{s}\frac{dF}{ds} - (a+2)F$$

$$= \frac{\epsilon}{\gamma_2}\frac{d^2F}{ds^2} + (2\frac{\epsilon}{\gamma_2}\frac{1}{s} - s)\frac{dF}{ds} - (a+2)F.$$

Now we turn to solve the non-homogeneous equation:

$$\frac{\epsilon}{\gamma_2}\frac{d^2F}{ds^2} + (2\frac{\epsilon}{\gamma_2}\frac{1}{s} - s)\frac{dF}{ds} - (a+2)F = c_3'\frac{1}{s}e^{ks+\frac{\gamma_2}{2\epsilon}s^2},$$

$$\frac{d^2F}{ds^2} + (\frac{2}{s} - \frac{\gamma_2}{\epsilon}s)\frac{dF}{ds} - \frac{\gamma_2}{\epsilon}(a+2)F = c_3'\frac{\gamma_2}{\epsilon}\frac{1}{s}e^{ks+\frac{\gamma_2}{2\epsilon}s^2}. \tag{4.33}$$

Since we have the two homogeneous solutions to Eq. (4.33), the particular solution to Eq. (4.33) can be solved by the variation of parameters. For sake of simplicity, we can set:

$$\begin{cases} Y_1 = Y_1(t) = KummerM(1 + \frac{a}{2}, \frac{3}{2}, \frac{\gamma_2}{2\epsilon}s^2) \\ Y_2 = Y_1(t) = KummerU(1 + \frac{a}{2}, \frac{3}{2}, \frac{\gamma_2}{2\epsilon}s^2) \end{cases}.$$

Thus, the particular solution, Y_3, to Eq. (4.33) is:

$$
\begin{aligned}
Y_3 &= -Y_1 \int \frac{Y_2}{W(Y_1,Y_2)} c_3' \frac{\gamma_2}{\epsilon} \frac{1}{s} e^{ks+\frac{\gamma_2}{2\epsilon}s^2} ds + Y_2 \int \frac{Y_1}{W(Y_1,Y_2)} c_3' \frac{\gamma_2}{\epsilon} \frac{1}{s} e^{ks+\frac{\gamma_2}{2\epsilon}s^2} ds \\
&= c_3' \frac{\gamma_2}{\epsilon} \left(-Y_1 \int \frac{Y_2}{W(Y_1,Y_2)} \frac{1}{s} e^{ks+\frac{\gamma_2}{2\epsilon}s^2} ds + Y_2 \int \frac{Y_1}{W(Y_1,Y_2)} \frac{1}{s} e^{ks+\frac{\gamma_2}{2\epsilon}s^2} ds \right) \\
&= c_3 \left(-Y_1 \int Y_2 s e^{ks} ds + Y_2 \int Y_1 s e^{ks} ds \right),
\end{aligned}
\tag{4.34}
$$

where $c_3 = -(\frac{\gamma_2}{2\epsilon})^{\frac{3}{2}} c_3'$, W is the Wronskian determinant, and we have used the formula [49]:

$$
\begin{aligned}
W(Y_1,Y_2) &= \frac{dt}{ds}\left[Y_1(t) \frac{dY_2(t)}{dt} - \frac{dY_1(t)}{dt} Y_2(t) \right] \\
&= -\frac{\gamma_2}{\epsilon} s \left(\frac{\gamma_2}{2\epsilon} s^2 \right)^{-\nu} e^{\frac{\gamma_2}{2\epsilon}s^2} \frac{\Gamma(\nu)}{\Gamma(\mu)} \Big|_{\mu=1+\frac{a}{2}, \nu=\frac{3}{2}} \\
&= -2\sqrt{2} \left(\frac{\gamma_2}{\epsilon} \right)^{-\frac{1}{2}} \frac{1}{s^2} e^{\frac{\gamma_2}{2\epsilon}s^2} \frac{\Gamma(\frac{3}{2})}{\Gamma(1+\frac{a}{2})}.
\end{aligned}
\tag{4.35}
$$

With the Y_3, the $y_3(x)$ is:

$$
\begin{aligned}
y_3(x) &= e^{-kx} \Big[-KummerM\left(1+\frac{a}{2}, \frac{3}{2}, \frac{\gamma_2}{2\epsilon}s^2\right) \int KummerU\left(1+\frac{a}{2}, \frac{3}{2}, \frac{\gamma_2}{2\epsilon}s^2\right) s e^{ks} ds \\
&+ KummerU\left(1+\frac{a}{2}, \frac{3}{2}, \frac{\gamma_2}{2\epsilon}s^2\right) \int KummerM\left(1+\frac{a}{2}, \frac{3}{2}, \frac{\gamma_2}{2\epsilon}s^2\right) s e^{ks} ds \Big] s e^{-\frac{\gamma_2}{2\epsilon}s^2},
\end{aligned}
$$

where $s = x - \frac{\epsilon k}{\gamma_2}$. From Eq. (4.25) and normalization condition for $P(x)$, the values of c_{1-3} and $P(0)$ can be evaluated numerically by the following equation:

$$
\begin{cases}
c_1 y_1(0) + c_2 y_2(0) + c_3 y_3(0) = 0 \\
c_1 y_1'(0) + c_2 y_2'(0) + c_3 y_3'(0) = P(0) \\
c_1 y_1''(0) + c_2 y_2''(0) + c_3 y_3''(0) = -kP(0) \\
c_1 \int_0^\infty y_1(x)dx + c_2 \int_0^\infty y_2(x)dx + c_3 \int_0^\infty y_3(x)dx = \frac{1}{k}[1 + c_1 y_1(0) + c_2 y_2(0)]
\end{cases}
.
$$

After getting $y(x)$, the steady-state PDF of Eq. (4.11) is determined by:

$$
P(x) = \frac{dy(x)}{dx} + ky(x).
$$

The Fig. 4.11 shows the variation trend of $P(x)$ with fixed k, a, and γ_2 for different ϵ values. The larger the ϵ value is , the more $P(x)$ is diffused and so does the fluctuation of $P(x)$. The Fig. 4.12 shows the variation trend of $P(x)$ with fixed ϵ, a, and γ_2 for different k parameters. The larger the k value is, the more the maximum of $P(x)$ is close near $x = 0$. Physically, the transition PDF decreases rapidly wit increasing k.
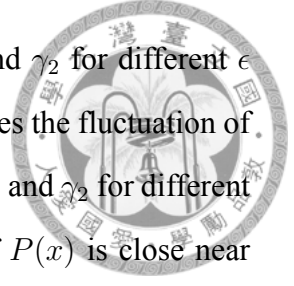
4.1.5 Dynamic Simulation of Van Kampen CME with Diffusion Term

The simulation of Eq. (4.11) uses the forward finite difference introduced in Ch. 4.1.1, but the algorithm must be modified at the $x = 0$. Since the $\frac{\partial P(x,t)}{\partial x}\big|_{x=0}$ in Eq. (4.11) is zero, the condition of zero flux must be added to the algorithm. The modified algorithm is described as follows:

$$
\begin{aligned}
P_i^1 &= A P_i^0, P_i^1 = \frac{P_i^1}{\sum_j P_j^1}, \frac{\partial P_0^1}{\partial x} = 0, \\
P_i^2 &= A P_i^1, P_i^2 = \frac{P_i^2}{\sum_j P_j^2}, \frac{\partial P_0^2}{\partial x} = 0, \\
&\vdots \\
P_i^k &= A P_i^{k-1}, P_i^k = \frac{P_i^k}{\sum_j P_j^k}, \frac{\partial P_0^k}{\partial x} = 0.
\end{aligned}
$$

For $x = 0$ point, we have used the central difference of $O(h^2)$ for $\frac{\partial P(0,t)}{\partial x}$:

$$
\begin{aligned}
\frac{\partial P_0^k}{\partial x} &\approx \frac{P_0^1 - P_0^{-1}}{2h}, \\
P_0^{-1} &= P_0^1, \; for \; zero \; flux,
\end{aligned}
\tag{4.36}
$$

which modifies the two of A matrix element: $A_{0,0}$ and $A_{0,1}$ in Ch. 4.1.1. With zero flux at $x = 0$ for the forward finite difference of $O(h^3)$, we can write $\frac{\partial P_0^k}{\partial x} = 0$ in $O(h^3)$ as:

$$
\begin{aligned}
-\frac{11}{6} P_0^k + 3 P_1^k - \frac{3}{2} P_2^k + \frac{1}{3} P_3^k &= 0, \\
\Rightarrow P_0^k = \frac{8}{11} P_1^k - \frac{9}{11} P_2^k + \frac{2}{11} P_3^k.
\end{aligned}
$$

In a large-scale time, the Figs. 4.13-18 show that the dynamical state of PDF is consistent with the steady-state of PDF. Mathematically, we can say they are equal to each other. For a larger k value, the maximum position of PDF approaches the $x = 0$. The fluctuation of PDF increases with the increasing ϵ value. No matter what a and ϵ values are, the steady-state or dynamical PDF is strongly affected by diffusion term at $x = 0$.
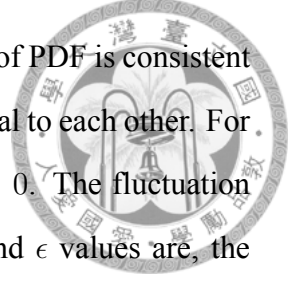
4.2 Finite correction of Modified Eigen Model in Hamming Class

Modified Eigen Model in Hamming class in Ch. 3.2.3 is described as the following:

$$\frac{\partial p_l}{\partial t} = \sum_{n_1=0}^{l} \sum_{n_2=0}^{N-l} M_n Q_{n_1+n_2} r_{l-n} p_{l-n}, \qquad (4.37)$$

where p_l is a sequence probability in l-th Hamming class,

$$M_n = \frac{l!}{n_1!(l-n_1)!} \frac{(N-l)!}{n_2!(N-l-n_2)!}, r_l = f(m),$$

and

$$Q_{n_1+n_2} = \hat{Q} q^{-(n_1+n_2)} (1-q)^{n_1+n_2}.$$

In this chapter, we derive the mean fitness and probability distribution of $O(\frac{1}{N})$ by HJE method, where N is the genome length. The numerical simulation is well consistent with our analytical results in a relative errors less than 1%.

4.2.1 The derivation for Hamilton-Jacobi equation

At first, we can apply the WKB expansion for p_l:

$$p_l = \exp[Nu(m,t) + u_1(m)],$$

where $u(m,t)$ is the HJE solution with the bulk Hamiltonian, u_1 is the correction term of $O(\frac{1}{N})$ for the steady-state probability distribution. The u_1 calculation is our main goal of this work. Since we want to investigate the finite correction of $O(\frac{1}{N})$, each variable should be related to N. All our work is to calculate the correction of $O(\frac{1}{N})$, so all the $O(\frac{1}{N^2})$ and higher order terms are neglected. Then we can expand the $u(m_{l-n})$ and $u_1(m_{l-n})$ at m till all correction terms are of $O(\frac{1}{N})$:

$$
\begin{aligned}
m_{l-n} &= 1 - \frac{2(l-n)}{N} = m_l + \frac{2n}{N} \equiv m + \frac{2n}{N}, \\
u(m_{l-n},t) &= u(m,t) + \frac{2n}{N}u'(m,t) + 2\left(\frac{n}{N}\right)^2 u''(m,t) + \ldots, \\
u_1(m_{l-n}) &= u_1(m) + \frac{2n}{N}u_1{}'(m) + \ldots, \\
p_{l-n} &\approx p_l \exp(2nu' + 2\frac{n^2}{N}u'' + \frac{2n}{N}u_1{}'),
\end{aligned}
\tag{4.38}
$$

where $u'(m,t) = \frac{\partial u(m,t)}{\partial m}$, $u''(m,t) = \frac{\partial^2 u(m,t)}{\partial m^2}$, and $u_1{}'(m) = \frac{du_1(m)}{dm}$. The r_{l-n} can be expanded at m:

$$
r_{l-n} = f(m_{l-n}) \approx f(m) + \frac{2n}{N}f'(m),
\tag{4.39}
$$

where $f'(m) = \frac{df(m)}{dm}$. The element of mutation matrix can be expressed by the parameter:

$$
\gamma = N(1-q).
\tag{4.40}
$$

For $N >> 1$, we have the following approximations and notation:

$$
\begin{aligned}
Q_n &= \hat{Q}(\frac{\gamma}{N})^n(1 - \frac{\gamma}{N})^{-n} = \hat{Q}(\frac{\gamma}{N-\gamma})^n, \\
\gamma_0 &\equiv \frac{N\gamma}{N-\gamma} = \gamma(1-\frac{\gamma}{N})^{-1} \approx \gamma(1+\frac{\gamma}{N}), \\
\hat{Q} &= (1-\frac{\gamma}{N})^N \approx (e^{\frac{\gamma}{N}} - \frac{\gamma^2}{2N^2})^N \approx e^{-\gamma}(1 - \frac{\gamma^2}{2N}).
\end{aligned}
\tag{4.41}
$$

With all these expansions, we turn to derive the Hamilton-Jacobi equation now. We have the approximation equation for modified Eigen model in Hamming class:

$$\frac{\partial p_l}{\partial t} \approx \hat{Q} \sum_{n_1=0}^{l} \sum_{n_2=0}^{N-l} \frac{l!}{n_1!(l-n_1)!} \frac{(N-l)!}{n_2!(N-l-n_2)!}$$
$$\times \ (\frac{\gamma_0}{N})^{n_1+n_2} [f(m) + \frac{2(n_1-n_2)}{N} f'(m)]$$
$$\times \ e^{2(n_1-n_2)u' + \frac{2}{N}(n_1-n_2)^2 u'' + \frac{2}{N}(n_1-n_2)u_1'} p_l. \tag{4.42}$$

Similarly, the exponential term can be approximated as:

$$e^{2(n_1-n_2)u' + \frac{2}{N}(n_1-n_2)^2 u'' + \frac{2}{N}(n_1-n_2)u_1'}$$
$$\approx \ e^{2nu'}(1 + \frac{2}{N}n^2 u'')(1 + \frac{2}{N}nu_1')$$
$$\approx \ e^{2(n_1-n_2)u'}[1 + \frac{2}{N}((n_1-n_2)^2 u'' + (n_1-n_2)u_1')]. \tag{4.43}$$

And note that the multiplicative number M_n is the product of two binomial coefficients:

$$M_n = \frac{l!}{n_1!(l-n_1)!} \frac{(N-l)!}{n_2!(N-l-n_2)!}$$
$$= \binom{l}{n_1} \binom{N-l}{n_2}.$$

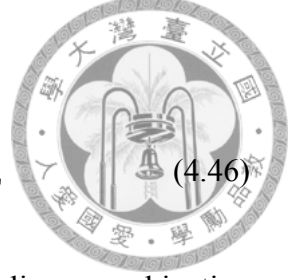Holding till the second order terms for Eq. (4.42), we get:

$$\frac{\partial p_l}{\partial t} \approx \hat{Q} p_l f(m) \sum_{n_1=0}^{l} \sum_{n_2=0}^{N-l} \binom{l}{n_1} \binom{N-l}{n_2} (\frac{\gamma_0}{N})^{n_1+n_2}$$
$$\cdot e^{2(n_1-n_2)u'}[1 + \frac{2}{N}((n_1-n_2)^2 u'' + (n_1-n_2)u_1')]$$
$$+ \hat{Q} p_l f'(m) \sum_{n_1=0}^{l} \sum_{n_2=0}^{N-l} \binom{l}{n_1} \binom{N-l}{n_2}$$
$$\cdot (\frac{\gamma}{N})^{n_1+n_2} e^{2(n_1-n_2)u'} \frac{2(n_1-n_2)}{N}. \tag{4.44}$$

By the binomial theorem, we can use the formula for summation:

$$(1+a)^n = \sum_{k=0}^{n} \binom{l}{k} a^k. \tag{4.45}$$

88

With these expansions, the Eq. (4.44) divided by p_l turns to

$$\frac{\partial u(m,t)}{\partial t} + \hat{H}(m,u') + H_3(m,u',u_1,u'',f') = 0, \tag{4.46}$$

where we have rescaled $t \to \frac{t}{N}$ ($\frac{d}{dt} \to \frac{1}{N}\frac{d}{dt}$), $H_3(m,u',u_1,u'',f')$ is a linear combination of correction terms including u_1, u'', and f' terms, and

$$
\begin{aligned}
-\hat{H} &= \hat{Q}f(m) \sum_{n_1=0}^{l} \sum_{n_2=0}^{N-l} \binom{l}{n_1}\binom{N-l}{n_2}(\frac{\gamma_0}{N})^{n_1+n_2}e^{2(n_1-n_2)u'} \\
&= \hat{Q}f(m) \sum_{n_1=0}^{l} \binom{l}{n_1}(\frac{\gamma_0}{N}e^{2u'})^{n_1} \sum_{n_2=0}^{N-l} \binom{N-l}{n_2}(\frac{\gamma_0}{N}e^{-2u'})^{n_2} \\
&= \hat{Q}f(m) \sum_{n_1=0}^{l} \binom{l}{n_1}x_0^{n_1} \sum_{n_2=0}^{N-l} \binom{N-l}{n_2}y_0^{n_2} \\
&= \hat{Q}f(m)(1+x_0)^l(1+y_0)^{N-l}, \tag{4.47}
\end{aligned}
$$

where we have denoted the two notations:

$$x_0 = \frac{\gamma_0}{N}e^{2u'}, y_0 = \frac{\gamma_0}{N}e^{-2u'},$$

and the corresponding notations:

$$
\begin{aligned}
\alpha_{10} &= lx_0 = \gamma_0\frac{1-m}{2}e^{2u'}, \\
\alpha_{20} &= (N-l)y_0 = \gamma_0\frac{1+m}{2}e^{-2u'}.
\end{aligned}
$$

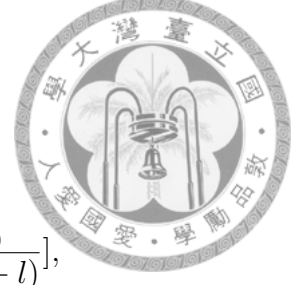Without H_3 term in Eq. (4.46), Eq. (4.46) becomes the HJE form:

$$\frac{\partial u(m,t)}{\partial t} + \hat{H}(m,u') = 0,$$

where $\hat{H}(m,u')$ is the fictitious Hamiltonian of system. Recall that we have the approximation for $N \gg 1$,

$$(1+\frac{\alpha}{N})^N = e^\alpha(1 - \frac{\alpha^2}{2N}).$$

With the largeness of $l >> 1$ and $N - l >> 1$, then

$$(1 + x_0)^l = (1 + \frac{\alpha_{10}}{l})^l \approx e^{\alpha_{10}}(1 - \frac{\alpha_{10}^2}{2l}),$$

$$(1 + y_0)^{N-l} = (1 + \frac{\alpha_{20}}{N - l})^{N-l} \approx e^{\alpha_{20}}[1 - \frac{\alpha_{20}^2}{2(N - l)}],$$

$$(1 + x_0)^l(1 + y_0)^{N-l} \approx e^G[1 - \frac{\alpha_{10}^2}{2l} - \frac{\alpha_{20}^2}{2(N - l)}]$$

$$= e^G[1 - \frac{\gamma_0}{2N}(\alpha_{10}e^{2u'} + \alpha_{20}e^{-2u'})],$$

where $G = \alpha_{10} + \alpha_{20}$. Therefore, the bulk term and $O(\frac{1}{N})$ term in Eq. (4.47) can be re-written as:

$$\hat{Q}f(m)e^G[1 - \frac{\gamma_0}{2N}(\alpha_{10}e^{2u'} + \alpha_{20}e^{-2u'})]$$

$$= -H_0(\gamma_0) - H_2(\gamma_0), \qquad (4.48)$$

where

$$-H_0(\gamma_0) = \hat{Q}f(m)e^G,$$

$$-H_2(\gamma_0) = \frac{\gamma_0}{2N}(\alpha_{10}e^{2u'} + \alpha_{20}e^{-2u'})H_0(\gamma_0).$$

Taking the simple expansion of γ_0 in $\frac{1}{N}$, the Hamiltonian in terms of γ can be represented as:

$$-\hat{H} = \hat{Q}f(m)e^G = (1 - \frac{\gamma}{N})^N f(m)e^{(1+\frac{\gamma}{N})\gamma(\frac{1-m}{2}e^{2u'} + \frac{1+m}{2}e^{-2u'})}$$

$$\approx -(1 - \frac{\gamma^2}{2N})H_0(1 + \frac{\gamma}{N}z) \approx -H_0 - H_1,$$

$$-H_1 = -H_0(-\frac{\gamma^2}{2N} + \frac{\gamma}{N}z),$$

$$-H_2 = -H_0[\frac{-\gamma}{2N}(\alpha_1 e^{2u'} + \alpha_2 e^{-2u'})], \qquad (4.49)$$

90

where we have denoted the following notations:

$$\alpha_1 = \gamma \frac{1-m}{2} e^{2u'}, \alpha_2 = \gamma \frac{1+m}{2} e^{-2u'},$$

$$z = \alpha_1 + \alpha_2, H_0 = H_0(\gamma) = -e^{-\gamma} f(m) e^z.$$

And the other approximations for $-H_3$ term:

$$
\begin{aligned}
-H_3 &= \frac{2\hat{Q}}{N} \sum_{n_1=0}^{l} \sum_{n_2=0}^{N-l} \binom{l}{n_1} \binom{N-l}{n_2} (\frac{\gamma}{N})^{n_1+n_2} e^{2(n_1-n_2)u'} \\
&\times \{[(n_1-n_2)^2 u'' + (n_1-n_2)u_1']f(m) + (n_1-n_2)f'(m)\}. \quad (4.50)
\end{aligned}
$$

For sake of simplicity, let us denote $a = 2u'$ and define the function:

$$
\begin{aligned}
J(a) &= \sum_{n_1=0}^{l} \sum_{n_2=0}^{N-l} \binom{l}{n_1} (\frac{\gamma}{N} e^a)^{n_1} \binom{N-l}{n_2} (\frac{\gamma}{N} e^{-a})^{n_2} \\
&= (1+x)^l (1+y)^{N-l}, \quad (4.51)
\end{aligned}
$$

where we have denoted:

$$x = \frac{\gamma}{N} e^a, y = \frac{\gamma}{N} e^{-a}.$$

Then the differentiation of $J(a)$ with respect to a is:

$$
\begin{aligned}
J'(a) &= \frac{\partial J(a)}{\partial x} \frac{dx}{da} + \frac{\partial J(a)}{\partial y} \frac{dy}{da} \\
&= lx(1+x)^{l-1}(1+y)^{N-l} - (N-l)y(1+x)^l(1+y)^{N-l-1} \\
&= J(a)(\frac{\alpha_1}{1+x} - \frac{\alpha_2}{1+y}) \\
&\approx J(a)[(1-x)\alpha_1 - (1-y)\alpha_2] \approx J(a)(\alpha_1 - \alpha_1),
\end{aligned}
$$

where the x and y of $O(\frac{1}{N})$ can be ignored since H_3 is proportional to $\frac{1}{N}$. And the differentiation of $J'(a)$ with respect to a is:

$$
\begin{aligned}
J''(a) &= \frac{dJ'(a)}{da} = \frac{\partial J'(a)}{\partial \alpha_1}\frac{d\alpha_1}{da} + \frac{\partial J'(a)}{\partial \alpha_2}\frac{d\alpha_2}{da} \\
&\approx J'(a)(\alpha_1 - \alpha_2) + J(a)(\alpha_1 + \alpha_2) \\
&\approx J(a)[z + (\alpha_1 - \alpha_2)^2].
\end{aligned}
\tag{4.52}
$$

Since H_3 is a linear combination of $J'(a)$ and $J''(a)$, H_3 can be obtained by the following steps:

$$
\begin{aligned}
H_3 &= \frac{2}{N}\hat{Q}\sum_{n_1=0}^{l}\sum_{n_2=0}^{N-l}\binom{l}{n_1}(\frac{\gamma}{N}e^a)^{n_1}\binom{N-l}{n_2}(\frac{\gamma}{N}e^{-a})^{n_2} \\
&\times \{[(n_1-n_2)^2 u'' + (n_1-n_2)u_1']f(m) + (n_1-n_2)f'(m)\} \\
&= \frac{2}{N}\hat{Q}\{[u'' J''(a) + u_1' J'(a)]f(m) + J'(a)f'(m)\} \\
&\approx \frac{2}{N}e^{-\gamma}f(m)J(a)\{u''[z+(\alpha_1-\alpha_2)^2] + (\alpha_1-\alpha_2)(u_1' + \frac{f'(m)}{f(m)})\} \\
&\approx \frac{2}{N}H_0[(\alpha_1-\alpha_2)(u_1 + \frac{f'}{f}) + u''(z+(\alpha_1-\alpha_2)^2)].
\end{aligned}
\tag{4.53}
$$

Thus, the Hamilton-Jacobi equation with $O(\frac{1}{N})$ correction terms, H_{1-3}, has the form:

$$
\frac{\partial u(m,t)}{\partial t} + H_0 + (H_1 + H_2 + H_3) = 0.
\tag{4.54}
$$

On reaching the steady state, we can imagine that this fictitious Hamiltonian arrives the minimum energy without time-dependence. Thus, we can assume that

$$
Nu(m,t) + u_1(m) = N[u(m) + kt] + u_1(m),
$$

where remember that we have rescaled t to $\frac{t}{N}$. Mathematically, this assumption for $u(m,t)$ is reasonable since H_{0-3} are all independent of time t. As we did in Ch. 3.2.2, we can

define the potential $V(m)$ for H_0 by the following way:

$$
\begin{aligned}
-H_0 &= e^{-\gamma} f(m) \exp\left[\gamma\left(\frac{1-m}{2} e^{2u'} + \frac{1+m}{2} e^{-2u'}\right)\right] \\
&\geq f(m) e^{\gamma(-1+\sqrt{1-m^2})} = V(m).
\end{aligned}
$$

Thus, the zero order and first order of $\frac{1}{N}$ for $k \approx k_0 + \frac{k_1}{N}$ are:

$$
\begin{aligned}
k_0 &= \max_{-1 \leq m \leq 1}[V(m)], \\
k_1 &= -N[H_1(m_0) + H_2(m_0) + H_3(m_0)],
\end{aligned} \tag{4.55}
$$

where the k_0 will reach the minimum energy at steady state while $V(m)$ reaches the maximum, and m_0 is the maximum point for $V(m)$. The first order k_1 can be also defined at m_0 where the coefficient of u_1' and f' is zero as shown in Ch. 3.2.2, so we have:

$$
\begin{aligned}
u'(m_0) &= \frac{1}{4} \ln\left(\frac{1+m_0}{1-m_0}\right), \\
k_1 &= H_0(m_0)[2u''(m_0)z + \gamma(z(m_0) - \gamma)].
\end{aligned} \tag{4.56}
$$

Since we are working with a sequence in l-th Hamming class, the total probability of l-th Hamming class is

$$
P_l = N_l p_l = \exp[Nu(m) + u_1(m) + \ln N_l], \tag{4.57}
$$

where N_l is the multiplicative number of l-th Hamming class,

$$
N_l = \frac{N!}{l!(N-l)!}.
$$

For general case of $N - l >> 1$ and $l >> 1$, it is allowed to apply Stirling formula to approximate these logarithms:

$$\ln N! \approx N \ln N - N + \frac{1}{2} \ln (2\pi N),$$

$$\ln l! \approx l \ln l - l + \frac{1}{2} \ln (2\pi l),$$

$$\ln (N - l)! \approx (N - l) \ln (N - l) - (N - l) + \frac{1}{2} \ln [2\pi(N - l)].$$

For the zero order term of $\frac{1}{N}$, it was derived in Ch. 3.2.2:

$$h(m) = -[\frac{1 + m}{2} \ln (\frac{1 + m}{2}) + \frac{1 - m}{2} \ln (\frac{1 - m}{2})].$$

Therefore, the approximation of $\ln N_l$ up to first order can be written as:

$$
\begin{aligned}
\ln N_l &\approx Nh(m) + \frac{1}{2} \ln (2\pi N) - \frac{1}{2} \ln (2\pi l) - \frac{1}{2} \ln [2\pi(N - l)] \\
&= Nh(m) - \frac{1}{2} \ln (2\pi N) - \frac{1}{2} \ln (2\pi \frac{l}{N}) - \frac{1}{2} \ln (2\pi \frac{N - l}{N}) \\
&= Nh(m) - \frac{1}{2}[\ln (1 + m) + \ln (1 - m) + \ln (2N\pi)] \\
&= Nh(m) + h_1(m),
\end{aligned}
\tag{4.58}
$$

where we have denoted:

$$h_1(m) = -\frac{1}{2}[\ln (\frac{1 + m}{2}) + \ln (\frac{1 - m}{2}) + \ln (2N\pi)].$$

Thus, the expression of P_l in $O(\frac{1}{N})$ in Eq. (4.57) can be approximated as:

$$P_l \approx \exp[N(u(m) + h(m)) + u_1(m) + h_1(m)], \tag{4.59}$$

and the relation between the single sequence u and the class v in Ch. 3.2.2 is:

$$v = u + h(m), u'' = v'' - \frac{d^2 h(m)}{dm^2} = v'' + \frac{1}{1 - m^2}.$$

Therefore, we can use the previous results of Crow-Kimura model in Ch. 3.2.2 by the mapping:

$$f \to \ln f, \qquad (4.60)$$

and the $u''(m_0)$ value is:

$$
\begin{aligned}
2u''(m_0) &= 2v''(m_0) + \frac{2}{1-m_0^2} \\
&= \frac{1}{1-m_0^2}[1 - \sqrt{1 - (1-m_0^2)^{3/2}\frac{(\ln f(m_0))''}{\gamma}}]. \qquad (4.61)
\end{aligned}
$$

With the Eq. (4.61) aid, the k_1 value of Eq. (4.56) is:

$$
\begin{aligned}
k_1 &= \gamma^2 e^{z(m_0)-\gamma} f(m_0) \{ \frac{1}{z(m_0)}[1 - \sqrt{1 - \frac{z^3(m_0)}{\gamma^4}(\ln f(m_0))''}] - 1 + \frac{z(m_0)}{\gamma} \} \\
&= \gamma^2 f_0 e^{z_0-\gamma} \{ \frac{1}{z_0}[\sqrt{1 - \frac{z_0^3}{\gamma^4}(\ln f)''}] - 1 + \frac{z_0}{\gamma} \}, \qquad (4.62)
\end{aligned}
$$

where we have let

$$f_0 = f(m_0), \; z_0 = \gamma\sqrt{1-m_0^2}.$$

With the known $u''(m_0)$ and k_1, the u_1' can be obtained by the Eq. (4.55). Thus, we have:

$$
\begin{aligned}
&- \; 2u_1'(\alpha_1 - \alpha_2)H_0 \\
&= \; k_1 + 2u''[z + (\alpha_1 - \alpha_2)^2]H_0 + 2\frac{f'}{f}(\alpha_1 - \alpha_2)H_0 \\
&+ \; \frac{\gamma}{2}[2z - (\alpha_1 e^{2u'} + \alpha_2 e^{-2u'}) - \gamma]H_0, \\
&(\alpha_1 - \alpha_2)u_1' = \frac{k_1}{2f}e^{-z+\gamma} - u''[z + (\alpha_1 - \alpha_2)^2] \\
&- \; (\alpha_1 - \alpha_2)\frac{f'}{f} + \frac{\gamma}{4}(\alpha_1 e^{2u'} + \alpha_2 e^{-2u'}) + \frac{\gamma^2}{4} - \frac{\gamma}{2}z,
\end{aligned}
$$

or

$$
\begin{aligned}
u_1' &= \frac{1}{\alpha_1 - \alpha_2}\{ \frac{k_1}{2f}e^{-z+\gamma} - u''[z + (\alpha_1 - \alpha_2)^2] \\
&- \; (\alpha_1 - \alpha_2)\frac{f'}{f} + \frac{\gamma}{4}(\alpha_1 e^{2u'} + \alpha_2 e^{-2u'}) + \frac{\gamma^2}{4} - \frac{\gamma}{2}z \}. \qquad (4.63)
\end{aligned}
$$

95

Therefore, u_1 can be obtained from Eq. (4.63) by integrating u_1' with respect to m:

$$
\begin{aligned}
u_1(m) &= \int_{m_r}^{m} \frac{dm'}{\alpha_1 - \alpha_2} \{ \frac{k_1}{2f} e^{-z+\gamma} - u''[z + (\alpha_1 - \alpha_2)^2] \\
&- (\alpha_1 - \alpha_2)\frac{f'}{f} + \frac{\gamma}{4}(\alpha_1 e^{2u'} + \alpha_2 e^{-2u'}) + \frac{\gamma^2}{4} - \frac{\gamma}{2}z \},
\end{aligned} \tag{4.64}
$$

where m_r is an appropriate reference point where $u_1(m_r) = 0$. The $u'(m)$ and $u(m)$ we have used in Eq. (4.64) is obtained from H_0 by the following steps:

$$
k_0 = H_0(m) = e^{-\gamma+z} f,
$$

$$
\ln k_0 = -\gamma + z + \ln f
$$

$$
= -\gamma + \gamma(\frac{1-m}{2}e^{2u'} + \frac{1+m}{2}e^{-2u'}) + \ln f,
$$

$$
e^{2u'} = \frac{\ln k_0 + \gamma - \ln f - \sqrt{(\ln k_0 + \gamma - \ln f)^2 - \gamma^2(1 - m^2)}}{\gamma(1-m)},
$$

$$
u'(m) = \frac{1}{2} \ln \frac{\ln k_0 + \gamma - \ln f - \sqrt{(\ln k_0 + \gamma - \ln f)^2 - \gamma^2(1 - m^2)}}{\gamma(1-m)},
$$

$$
u(m) = \frac{1}{2} \int_{m_r'}^{m} \ln \frac{\ln k_0 + \gamma - \ln f - \sqrt{(\ln k_0 + \gamma - \ln f)^2 - \gamma^2(1 - m'^2)}}{\gamma(1-m')} dm',
$$

where we only take the $+$ solution for $u'(m)$ since we are interested in the interval $[m_0, 1]$, and m_r' is an appropriate reference point where $u(m_r') = 0$. Therefore, the probability distributions of Hamming class for zero and first order of $\frac{1}{N}$ are:

$$
\left\{
\begin{aligned}
P(m) &= \exp\left[N(u(m) + h(m))\right], \\
P_1(m) &= P(m)\exp\left[u_1(m) + h_1(m)\right]
\end{aligned}
\right. , \tag{4.65}
$$

where $P(m)$ and $P_1(m)$ are the probability distributions of zero and first order of $\frac{1}{N}$.

4.2.2 Comparison with Numerics

To test the validity of our analytic solution in Eq. (4.65), we use Runge-Kutta method to simulate the Eq. (3.50) for different values of γ and functions of $f(m)$. The probability distributions of Hamming class for the zero order, the first order, and numerics are

shown in Figs. 4.19 to 4.21. Some probability values for correction and numerics near the maximum point are listed in tables 4.1-3. As shown in the figures and tables, our results of $P_1(m)$ are well consistent with numerics. The relative error of probability distribution between numerics and first order is less than $1\ \%$.
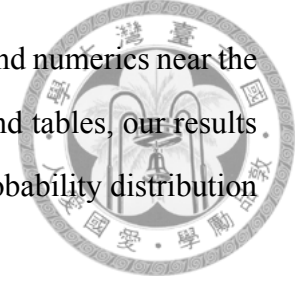
4.3   Solution of Heat Equation in SMAT

Considering the one-dimensional heat equation, where the sample temperature, T, is described by the partial differential equation (PDE) derived in Ch. 2.4.2:

$$\frac{\partial}{\partial z}k_0\frac{\partial T}{\partial z} + \dot{q} = \rho_s C\frac{\partial T}{\partial t}, \tag{4.66}$$

where z is the distance from the sample bottom, t is the time, k_0 is the thermal conductivity of sample at $300\ K$, the heat source, $\dot{q}$, is the heat energy generation per unit volume per unit time, C is the specific heat of sample, and ρ_s is the sample density.

4.3.1   The Heat Source

We can count the collisions between the sample bottom and flying balls as the heat source, where the loss of kinetic energy converts into the heat and internal energy of sample and flying balls. Experimentally, the balls in SMAT acts on a effective depth within $100\ \mu m$. With this idea, the heat source can be thought as uniformly distributed in some effective depth of sample and it can be described as

$$\dot{q} = q[u(z) - u(z - l)],$$

where l is the effective depth with heat source within it, and $u(z)$ is the unit step function since it has the following property

$$\int_0^l q[u(z) - u(z - l)]\mathrm{d}z = ql,$$

and q is heat coming from the power loss of averaged kinetic energy of sample and flying balls,

$$q = r\frac{P_{k,loss,s} + P_{k,loss,b}}{A_s l},$$

where r is the conversion ratio of kinetic energy loss to heat energy and A_s is the cross-sectional area of sample.
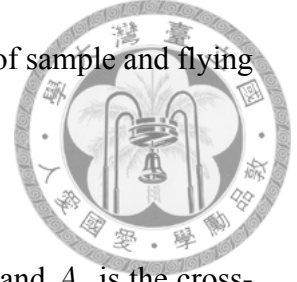
4.3.2 The Temperature Distribution of Steady State

On reaching the steady state, the changing rate of sample temperature with respect to time will become zero, $\frac{\partial T}{\partial t} = 0$, the Eq. (4.66) can be simplified as:

$$\frac{\mathrm{d}}{\mathrm{d}z}k_0\frac{\mathrm{d}T}{\mathrm{d}z} + \dot{q} = 0. \tag{4.67}$$

Eq. (4.67) can be solved by the following steps:

$$\int_0^z \frac{\mathrm{d}}{\mathrm{d}z'}k_0\frac{\mathrm{d}T}{\mathrm{d}z'}\mathrm{d}z' = -\int_0^l \dot{q}\mathrm{d}z' - \int_l^z \dot{q}\mathrm{d}z',$$

$$\frac{\mathrm{d}T}{\mathrm{d}z} = \begin{cases} -\frac{q}{k_0}z + c_1, \ z < l \\[2mm] c_2 - \frac{ql}{k_0}, \ z \geq l \end{cases},$$

$$T(z) = \begin{cases} -\frac{q}{2k_0}z^2 + c_1 z + c_3, \ 0 \leq z < l \\[2mm] (c_2 - \frac{ql}{k_0})z + c_4, \ l \leq z \leq L \end{cases}, \tag{4.68}$$

where c_{1-4} are all integration constants. Assume that the equilibrium temperature of bottom surface of sample is T_b and the equilibrium temperature of top surface of sample is T_t. We have the boundary conditions for $T(z)$ and $\frac{\mathrm{d}T(z)}{\mathrm{d}z}$ at $z = l$ to determine the c_{1-4} values:

$$\begin{cases} T(l^-) = T(l^+) \\[2mm] \frac{\mathrm{d}T(z)}{\mathrm{d}z}\Big|_{z=l^-} = \frac{\mathrm{d}T(z)}{\mathrm{d}z}\Big|_{z=l^+} \end{cases}.$$

Thus, we have the system equation for c_{1-4}:

$$\begin{cases} -\frac{ql}{k_0} + c_1 = c_2 - \frac{ql}{k_0} \\ -\frac{q}{2k_0}l^2 + c_1 l + c_3 = (c_2 - \frac{ql}{k_0})l + c_4 \\ T(0) = T_b = c_3 \\ T(L) = T_t = (c_2 - \frac{ql}{k_0})L + c_4 \end{cases},$$

and the c_{1-4} values are:

$$\begin{cases} c_1 = \frac{T_t - T_b}{L} + \frac{ql}{k_0}(1 - \frac{l}{2L}) \\ c_2 = c_1 \\ c_3 = T_b \\ c_4 = T_b + \frac{ql^2}{2k_0} \end{cases},$$

where L is the sample thickness along z direction. Therefore, the temperature distribution of sample is:

$$T(z) = \begin{cases} -\frac{q}{2k_0}l^2 + [\frac{T_t - T_b}{L} + \frac{ql}{k_0}(1 - \frac{l}{2L})]z + T_b, \ 0 \le z < l \\ (\frac{T_t - T_b}{L} - \frac{ql^2}{2k_0})z + T_b + \frac{ql^2}{2k_0}, \ l \le z \le L \end{cases}. \qquad (4.69)$$

The temperature drop predicted by Eq. (4.69) from the surface (subject to SMAT bombarding) to the inner portion is presented in Fig. 4.22 for pure Cu and 304 stainless steel, for the region near the surface (less than 0.05 mm) and the overall depth (up to 1 mm). Near the surface region, there exists a small hump, and then the temperature continues to drop all the way into the inner portion. With the known temperature distribution, we can calculate the heat energy of sample by integration:

$$\begin{aligned} \Delta Q &= C \int_0^L \Delta T(z) \mathrm{d}m_s \\ &= \rho_s A_s L C \int_0^L (T(z) - T_0) \mathrm{d}z, \end{aligned} \qquad (4.70)$$

where m_s is the sample mass and T_0 is the initial temperature of sample with isothermal-distributed temperature. Normally, T_0 can be set to room temperature, $300 \ K$. Now we turn to consider the case in which the thermal conductivity has temperature dependence, namely,

$$k = k_0[1 + \beta(T - T_0)],$$

where β is a temperature-independent constant. We can apply the change of variables into Eq. (4.67), $T_v = T - T_0$, to do the integration:

$$\int_0^z \frac{\mathrm{d}}{\mathrm{d}z'} k_0(1 + \beta T_v) \frac{\mathrm{d}T_v}{\mathrm{d}z'} \mathrm{d}z' = -\int_0^l \dot{q} \mathrm{d}z' - \int_l^z \dot{q} \mathrm{d}z'.$$

Then we can immediately obtain:

$$(1 + \beta T_v) \frac{\mathrm{d}T_v}{\mathrm{d}z} = \begin{cases} -\frac{q}{k_0} z + c_1, \ 0 \leq z \ < \ l \\ \\ c_2 - \frac{ql}{k_0}, \ l \leq z \ \leq \ L \end{cases},$$

$$T_v + \frac{1}{2} \beta T_v{}^2 = \begin{cases} -\frac{q}{2k_0} z^2 + c_1 z + c_3, \ 0 \leq z < l \\ \\ (c_2 - \frac{ql}{k_0})z + c_4, \ l \leq z \leq L, \end{cases} \qquad (4.71)$$

Similarly, we have the boundary conditions for $T_v(z)$ and $\frac{\mathrm{d}T_v(z)}{dz}$:

$$\begin{cases} T_v(l^-) = T_v(l^+) \\ \\ \frac{\mathrm{d}T_v(z)}{\mathrm{d}z}\Big|_{z=l^-} = \frac{\mathrm{d}T_v(z)}{\mathrm{d}z}\Big|_{z=l^+} \end{cases}.$$

And the system equation for c_{1-4}:

$$\begin{cases} -\frac{ql}{k_0} + c_1 = c_2 - \frac{ql}{k_0} \\ \\ -\frac{q}{2k_0} l^2 + c_1 l + c_3 = (c_2 - \frac{ql}{k_0})l + c_4 \\ \\ T_v(0) = (T_b - T_0)(1 + \beta \frac{T_b - T_0}{2}) = c_3 \\ \\ T_v(L) = (T_t - T_0)(1 + \beta \frac{T_t - T_0}{2}) = (c_2 - \frac{ql}{k_0})L + c_4 \end{cases},$$

and the c_{1-4} values:

$$
\begin{cases}
c_1 = \frac{T_t - T_b}{L}[1 + \beta(\frac{T_b + T_t}{2} - T_0)] + \frac{ql}{k_0}(1 - \frac{l}{2L}) \\[2mm]
c_2 = c_1 \\[2mm]
c_3 = (T_b - T_0)(1 + \beta\frac{T_b - T_0}{2}) \\[2mm]
c_4 = (T_b - T_0)(1 + \beta\frac{T_b - T_0}{2}) + \frac{ql^2}{2k_0}
\end{cases}
,
$$

The temperature drop predicted by Eq. (4.71) from the surface (subject to SMAT bombarding) to the inner portion is presented in Fig. 4.23 for pure Cu and 304 stainless steel, for the region near the surface (less than $0.1\ mm$) and the overall depth (up to $1\ mm$). With small changes in the temperature of sample and small β for general metal, the solution will be returning to the solution of Eq. (4.67). Similarly, the heat energy of sample can be obtained by Eq. (4.70) with T_v:

$$
\Delta Q = \rho_s A_s L C \int_0^L T_v(z)\mathrm{dz}. \tag{4.72}
$$

4.3.3 The internal energy of sample

The power for internal energy (or so-called the strain energy) of sample is denoted as:

$$
P_{int,s} = \frac{\Delta U_{int,s}}{\Delta t},
$$

where $\Delta U_{int,s}$ is the change of internal energy of sample in Δt. The energy conservation can be used to estimate the internal energy of sample acquired per unit time in SMAT:

$$
P_{loss,s} + P_{loss,b} = \frac{\Delta Q}{\Delta t} + P_{int,s},
$$
$$
P_{int,s} = P_{loss,s} + P_{loss,b} - \frac{\Delta Q}{\Delta t}, \tag{4.73}
$$

where we have ignored the sonic energy and heat energy of speeding balls because the volume and mass of chamber is much higher than those of balls. By Ch. 3.3, the collision probability is proportional to their cross section area, and the probability ratio of ball-

ball to ball-sample should be proportional to $\frac{\pi D^2}{4 A_s}$. For the common ball size of $2\ mm$ in diameter and SMAT sample area of $40 \times 20\ mm^2$, the ratio value is less than 1%. In this case, the collisions between the balls is not so frequent and the heat energy of balls is also small compared to that of chamber and sample.
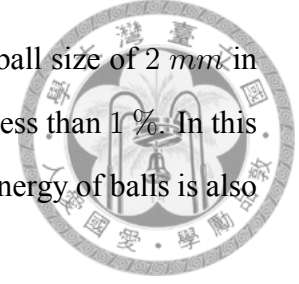
4.3.4   Experimental Methods

In order to compare with the proposed model, an AISI 304 stainless steel was adopted as the tested material with chemical compositions of (in $wt\%$): 0.049 C, 18.20 Cr, 8.66 Ni, 0.58 Si, 1.04 Mn, 0.021 P, 0.007 S, and the balanced Fe. A plate measuring $40 \times 20 \times 1\ mm$ was set on the top of the SMAT chamber, with a cylindrical chamber measuring $70\ mm$ in diameter and $20\ mm$ in height. The SUJ2 bearing steel balls with smooth surface and high hardness in the R_C scale of 62 are applied as the energy deliverer and are placed in a reflecting chamber that is vibrated by a vibration generator with a fixed vibration frequency $\nu = 20\ kHz$. The vibration amplitude, A, was chosen to vary in three levels: 40, 60, and $80\ \mu m$. Three sizes of the balls selected are 1, 2, and $3\ mm$ in diameter. All these balls with different sizes have the same density ρ_b, which is $7.8\ g/cm^3$. To maintain the fixed ball coverage area of 25% inside the chamber, the $1\ mm$ ball case would install $5\ g$ of the total ball weight, the $2\ mm$ ball case for $10\ g$, and the $3\ mm$ ball case for $15\ g$. Throughout the SMAT experiment, the working temperature is controlled and traced to be below $150\ ℃$, which is about $0.2\ T_m$ (melting temperature) of the 304 stainless steel and is considered to be relatively low for the 304 stainless steel samples. After careful mechanical grinding and polishing of the cross section of SMAT samples, the sample surface roughness and the morphology level were sufficient for nano-indentation to extract the hardness variation from the free surface (subject to SMAT) into the inner portion. The SEM observations were performed using a Zeiss Supra 55 field-emission scanning electron microscope. With a low acceleration energy at $5\ kV$ and a low working distance at $5 \sim 7\ mm$, it is able to visualize the distinguishable grains from the back-scattering images (BEIs). The cross-sectional transmission electron microscopy (TEM) foils of SMAT samples were fabricated using the dual-beam focused-ion-beam (FIB) system (Seiko, SMI3050) with an operating

voltage of $30\ kV$ and an ion beam current of $1\ pA$. The TEM foils were examined by the Tecnai G20 field emission transmission electron microscopy with an operating voltage of $200\ kV$. The hardness of SMAT specimens from the cross-sectional surface was measured by the MTS Nano Indenter XP System. The tests were operated with a displacement rate about $10\ nm/s$, and the allowable vibration drift of environment was controlled under $0.05\ nm/s$. The indented depth limit was set to be $1200\ nm$.
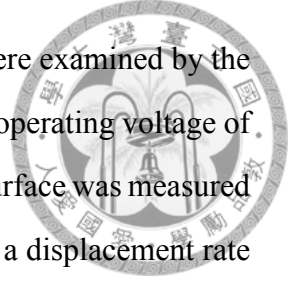
4.3.5 Relating strain rate and temperature with sample micro-structure in SMAT

For metallic materials, it is almost a universal rule that the sample micro-structure would be related to the processing parameters by the Zener-Holloman relationship. In general, the average grain sizes would decrease with decreasing working temperature and increasing working strain rate. The Zener-Holloman Z parameter is defined as:

$$Z = \dot{\varepsilon}exp(Q/RT), \tag{4.74}$$

where $\dot{\varepsilon}$ is the strain rate, Q is the activation energy, T is the absolute temperature, and R is the gas constant. The accumulative strain ε by the successive bombarding cycles can be approximately expressed by

$$\varepsilon_i = \frac{\Delta x}{x} \approx 0.2, \tag{4.75}$$

where ε_i is each strain by each ball bombarding incident, Δx is each compressed depth by each ball bombarding incident, and x is the sample depth experiencing the bombarding impact. The precise strain is difficult to be calculated since the bombarding can be induced by the flying balls from various directions and the induced strain would be different for bombarding from different directions. The average is estimated to be about 0.2 in Eq. (4.75). But in general larger balls are expected to induce a higher degree of strain per bombarding, it is thus postulated that the 1, 2, and $3\ mm$ balls would induce an av-

erage strain about 0.15, 0.20, and 0.25, respectively. The overall strain accumulated by numerous ball bombarding events is simply expressed by:

$$\varepsilon_t = n \cdot \varepsilon_i, \tag{4.76}$$

where n is a statistic evaluation of the overall ball bombarding events during the SMAT time duration t. Since the balls in the chamber can fly randomly in all $3D$ directions, the probability P that one ball will bombard on the sample can be rationalized by the sample flat surface divided by the total surface area including the chamber wall and sample surfaces. This probability can be varied for different SMAT machine system designs. If the sample surface occupies 10% of the overall surface area, then P is assumed to be 0.1. For a vibration frequency ν and overall SMAT time t, the bombarding event onto the sample surface will be:

$$n = \nu t \cdot P. \tag{4.77}$$

Thus, the strain rate is equal to the accumulative strain divided by the SMAT time duration t,

$$\dot{\varepsilon} = \frac{\varepsilon_t}{t} = \frac{\nu t P \varepsilon_i}{t} = \nu P \varepsilon_i. \tag{4.78}$$

The SMAT working temperature T may or may not be measured with reasonable accuracy, depending on the chamber design. Also, even the temperature can be measured from the sample surface, the temperature should be a gradient profile from the outer surface to the inner portion of sample. Since the grain sizes in many SMAT metals or alloys are in the nano- to micro-scale with no pronounced grain growth, the experienced temperature is thought to be around or less than $0.2\,T_m$, where T_m is the melting temperature of metallic sample. With the activation energy Q for the involved major diffusion species, Z can be calculated. And then it is hoped that the grain size can be related to the Z parameter.
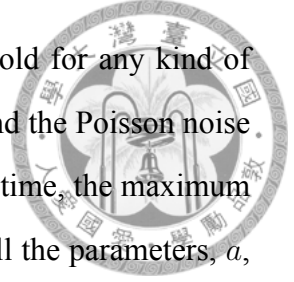
Chapter 5

Conclusion

5.1 Van Kampen CME with Gaussian White Noise

The model with the particle under the influence of Gaussian and Poisson noises has been considered, and we have solved the exact steady-state PDF of the model with the transition PDF, ke^{kx}. Namely, we have considered the related integro-differential Fokker-Planck equation and mapped it into a third order PDE. For the simplest case of drift term, $b(x) = -\gamma_2 x$, we have found the exact steady-state PDF supported by the direct numerics very well. Furthermore, the convergence to the steady-state can be proved analytically. The exact steady-state PDF can be found for any values of $a > 0$, $\epsilon > 0$, and $k > 0$. However, the PDF is expressed by Kummer functions, a special function. We have to solve a transcendental equation to obtain the formula for the exact position of the maximum for PDF, and thus it cannot be derived. Therefore, our main question is transferred to whether the diffusion term can move the position of maximum for PDF from the $x = 0$ point or not. Following from the properties of functions $y_i(x)$ for $i = 1 \sim 3$, the value of $P(0)$ is finite, it depends on ϵ, k, and a. As we can see from Figs. 4.3-18, the limit behaviour of PDF at $x = 0$ is that of PDF for $\epsilon = 0$, the gamma distribution, namely $P(0) \to \infty$ for $a < 1$ and $P(0) \to 0$ for $a > 1$. This means that the maximum point of PDF moves from $x = 0$ if $a > 1$, where this result is independent of any k and γ_2 value. Following from the analytical solution of steady-state PDF, the result holds for any values of ϵ, not necessarily small. In a more general case of the drift term, $b(x) = \gamma_2 x$, the threshold

value is $a = \gamma_2$. Moreover, under basic assumptions this should hold for any kind of transition PDF. Thus, the drift term shifts the particle to the origin, and the Poisson noise acting in the opposite manner competes with drift term. At the same time, the maximum point and decay rate as $x \to \infty$ of PDF and $P(0)$ value depend on all the parameters, a, ϵ, γ_2, and k. For example, $P(0) \sim (\sqrt{\epsilon}k)^{a-1}$ is the ratio of variances of Gaussian and exponential PDF. Figures 4.13-18 present a series of numerical simulations intending to prove that the solution of Eq. (4.11) converges to the steady-state PDF for different values of parameters. Figures 4.11-12 illustrate the maximum position is at the origin for $a < 1$ and outside of the origin for $a > 1$. For $a < 1$ the value of the maximum increases as $\epsilon \to 0$; for $a > 1$ the value of maximum for PDF and the PDF value at $x = 0$ decrease as $\epsilon \to 0$. Regarding the level of compound Poisson noise below the critical value, the Gaussian noise can strongly affect the behaviour of the solution removing the singularity of distribution at $x = 0$, as shown in fig. 4.13-14, while for the stronger Poisson noise above the critical value $a > 1$, the effect of the Gaussian noise is not drastic as shown in fig. 4.15-18. The results can be interpreted as follows. In the case of Gaussian noise, there is a finite maximum of distribution at $x = 0$; in the case of both Gaussian and weak Poisson noises, the distribution also has a finite maximum at zero, but this maximum tends to be infinite as the Gaussian component vanishes. If the Poisson noise is sufficiently large, then the maximum moves from the origin for any values of ϵ and k. Thus, the maximum position of PDF depends only on the Poisson component of noise. We can look at our results from the following point of view: a large noise, due to a finite number of molecules, can strongly influence the biological processes, while up to a certain level of this noise the situation is rather stable. This phenomenon is important for cell biology [50], where the systems can be shaped during the evolution to suppress some finite molecular number fluctuations. Moreover, sometimes the fluctuations can be suppressed, even for single molecule reactions, which yields a highly intriguing experimental result.
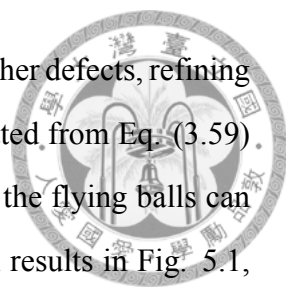
5.2 Finite Correction of Eigen Model
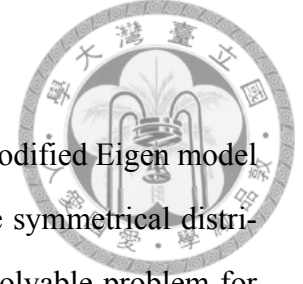
In conclusion, we have used HJE method to get the solution of modified Eigen model in Hamming class. Based on the two symmetrical assumptions, the symmetrical distribution and fitness function, the modified Eigen model becomes a solvable problem for large genome length. In this approach, the steady-state probability of Hamming class with $O(1/N)$ relative accuracy has been obtained by working carefully with the combinatorial problems during the calculation process, where N is the genome length. These calculations are much harder than the corresponding calculations for the Crow-Kimura case [51]. The properties for the $O(\frac{1}{N})$ correction terms have been investigated completely in these calculations. The analytical results for the steady-state probability of Hamming class is well consistent with the numerical results simulated by Runge-Kutta method, where the relative errors between the analytical and numerical results are less than 1% as shown in Figs. 4.19-21 and table 4.1-3. Our formula for the $O(\frac{1}{N})$ correction of probability in Hamming class, Eq. (4.64), is not the special case, and one can apply this formula for any symmetrical distribution and fitness function. Furthermore, our results can be applied to get accurate expression for the steady-state probability of Hamming class for the case of large genome length, where the numerics cannot give the accurate results. In our model we work with the mutation parameter $\gamma = N(1-q)$, while in [52] the mutation parameter $\mu = N(1-q)/q$ has been considered. Our expressions for the corrections of zero and first order in $\frac{1}{N}$ for the mean fitness is identical to the results derived in [52] by quantum field theory.

5.3 SMAT Modelling

Experimentally, it is observed that the grain size is appreciably refined by SMAT, from the initially about $20\ \mu m$ down to less than $100\ nm$, as shown in Fig. 5.1(a) with a gradient trend as viewed from the sample cross-section [47]. In parallel, the hardness increases from the initial about $2.7\ GPa$ up to about $6.0\ GPa$, as shown in Fig. 5.1(b) [47]. The kinetic energy from the flying balls appear to effectively induce substantial internal or

strain energy into the sample surface, increasing the dislocations and other defects, refining the grain size, and raising the hardness. The ball speed can be estimated from Eq. (3.59) to be within the range of $5 \sim 10 \ m/s$, and the kinetic energy for all the flying balls can also be estimated to be about $10 \sim 120 \ mJ$. From the experimental results in Fig. 5.1, coupled with the estimated values based on the current analytical model, it appears that the optimum speed for the 304 stainless steel might be around $8 \sim 10 \ m/s$ and the optimum kinetic energy might be around $70 \sim 75 \ mJ$. The adjustment of the SMAT parameters will influence accordingly the speed (in Fig. 3.1), kinetic energy (in Fig. 3.2), flying time period (in Fig. 3.3), power (in Fig. 3.4), and temperature profiles within the experienced range of the samples (in Figs. 4.22-23).

In this model, we have made efforts in evaluating the temperature profile from the bombarded surface to the sample inner portion (Figs. 4.22-23). This profile can be used as a reference in assessing the experienced temperature at the particular sample depth. For example, based on the calculated temperature in Fig. 4.23 for the 304 stainless steel, the temperature at the depth of $200 \ \mu m$ from the surface would be $365 \ K$ or $92 \ ℃$.

The other parameter left would be the strain rate. In accordance with Eq. (4.78), the strain rate would vary from $3 \times 10^2 \sim 5 \times 10^2 \ s^{-1}$. Taking the $4 \times 10^2 \ s^{-1}$ as the mean value, and $92 \ ℃$ as the experienced temperature, we can incorporate into Eq. (4.74) to extract the Zener-Holloman Z parameter, which is useful for estimate the materials microstructure properties. For 304 stainless steel, the governing activation energy Q should be related to the Fe diffusion, and $Q \sim 220 \ kJ/mol$ is a logical value [53, 54]. With the above information and the gas constant $R = 8.3 \ J/K$, Z can be calculated to be $1.4 \times 10^{34} \ s^{-1}$. With the same calculation manner, we can estimate all values for various cross-sectional positions of the SMAT sample, and plot the measured grain size and Zener-Holloman Z parameter, as presented in Fig. 5.2.

Thus, for SMAT researchers, we can first design the SMAT working parameters (based on the needs), and can calculate the resulting speed, temperature, strain rate, and energy based on this model in Figs. 3.1-4 and Figs. 4.22-23. With all the information, we can estimate the grain size from the Zener-Holloman Z parameter based on Fig. 5.2. The current

approach and modelling nicely establish the link between the physics and the engineering material surface modifications.
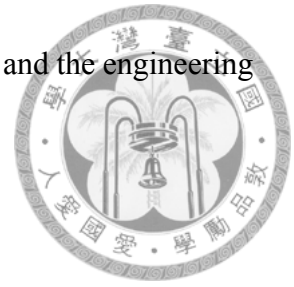
Appendix

.1 The Coefficient of Finite Difference

The following tables present the coefficients of the forward finite difference with space h for several order accuracy in h.

Table 1: The coefficient table for the forward finite difference of $f'(x)$.

Accuracy	$f(x)$	$f(x+h)$	$f(x+2h)$	$f(x+3h)$	$f(x+4h)$	$f(x+5h)$
$O(h)$	-1	1				
$O(h^2)$	$-3/2$	2	$-1/2$			
$O(h^3)$	$-11/6$	3	$-3/2$	$1/3$		
$O(h^4)$	$-25/12$	4	-3	$4/3$	$-1/4$	
$O(h^5)$	$-137/60$	5	-5	$10/3$	$-5/4$	$1/5$

Table 2: The coefficient table for the forward finite difference of $f''(x)$.

Accuracy	$f(x)$	$f(x+h)$	$f(x+2h)$	$f(x+3h)$	$f(x+4h)$	$f(x+5h)$
$O(h)$	1	-2	1			
$O(h^2)$	2	-5	4	-1		
$O(h^3)$	$35/12$	$-26/3$	$19/2$	$-14/3$	$11/12$	
$O(h^4)$	$15/4$	$-77/6$	$107/6$	-13	$61/12$	$-5/6$

For example, the first derivative of $f(x)$ with $O(h^3)$ accuracy is:

$$f'(x) \approx \frac{\frac{-11}{6}f(x) + 3f(x+h) - \frac{3}{2}f(x+2h) + \frac{1}{3}f(x+3h)}{h},$$

and the second derivative of $f(x)$ with $O(h^2)$ accuracy is:

$$f''(x) \approx \frac{2f(x) - 5f(x+h) + 4f(x+2h) - f(x+3h)}{h^2}.$$

.2   The Power Series Expansion of Kummer's Function

The expansion in power series for $KummerM(a, b, x)$ with $a > 0$ and $b > 0$ near $x = 0$:

$$
\begin{aligned}
& KummerM(a, b, x) \\
= \ & 1 + \frac{a}{b}x + \frac{a(a+1)}{2b(b+1)}x^2 + \frac{a(a+1)(a+2)}{6b(b+1)(b+2)}x^3 \\
+ \ & \frac{a(a+1)(a+2)(a+3)}{24b(b+1)(b+2)(b+3)}x^4 + \frac{a(a+1)(a+2)(a+3)(a+4)}{120b(b+1)(b+2)(b+3)(b+4)}x^5 + O(x^6).
\end{aligned}
$$

The expansion in power series for $KummerU(a, b, x)$ with $b \neq \mathbf{Z}$ near $x = 0$:

$$
\begin{aligned}
KummerU(a, b, x) \ = \ & \frac{\Gamma(1-b)}{\Gamma(a-b+1)}[1 + \frac{a}{b}x + \frac{a(a+1)}{2b(b+1)}x^2 + \cdots] \\
+ \ & \frac{\Gamma(b-1)}{\Gamma(a)}x^{1-b}[1 + \frac{1+a-b}{2-b}x + \frac{(1+a-b)(2+a-b)}{2(2-b)(3-b)}x^3 + \cdots].
\end{aligned}
$$

Bibliography

[1] Nir Friedman, Long Cai Long Cai, and X. Sunney Xie. Linking stochastic dynamics to population distribution: An analytical framework of gene expression. *Phys. Rev. Lett.*, 97(168302), 2006.

[2] Richard Losick and Claude Desplan. Stochasticity and cell fate. *Science*, 320(5872): 65–68, 2008.

[3] Leo P. Kadanoff. Hip bone is connected to ... *Physicstoday*, 62:8, 2009.

[4] Hao Ge and Hong Qian. Thermodynamic limit of a nonequilibrium steady state: Maxwell-type construction for a bistable biochemical system. *Phys. Rev. Lett.*, 103(148103), 2009.

[5] Paul J. Choi, X. Sunney Xie, and Eugene I. Shakhnovich. Stochastic switching in gene networks can occur by a single-molecule event or many molecular steps. *Journal of Molecular Biology*, 396:230–244, 2010.

[6] Yao-Chen Hung and Chin-Kun Hu. Constructive role of noise in p53 regulatory network. *Computer Physics Communications*, 182:249–250, 2011.

[7] K. Ito. Stochastic integral. *Proc. Imperial Acad. Tokyo*, 20:519–524, 1944.

[8] L. Onsager and S. Machlup. Fluctuations and irreversible process. *Phys. Rev.*, 91:1505–1512, 1953.

[9] H. Haken. Generalized onsager-machlup function and classes of path integral solutions of the fokker-planck equation and the master equation. *Zeit. Physik. B*, 24:321–326, 1976.

[10] H. Dekker. Functional integration and the onsager-machlup lagrangian for continuous markov processes in riemannian geometries. *Phys. Rev. A*, 19:2102–2111, 1979.

[11] G. Hu. *Chinese Phys. Letters*, 2(217), 1988.

[12] M. I. Dykman, Eugenia Mori, John Ross, and P. M. Hunt. Large fluctuations and optimal paths in chemical kinetics. *J. Chem. Phys.*, 100:5735–5750, 1994.

[13] C. Escudero and A. Kamenev. Switching rates of multistep reactions. *Phys. Rev. E*, 79(041149), 2009.

[14] M. Assaf and B. Meerson. Extinction of metastable stochastic populations. *Phys. Rev. E*, 81(021116), 2010.

[15] A. Martirosyan and D. B. Saakian. Exact results in the large system size limit for the dynamics of the chemical master equation, a one dimensional chain of equations. *Phys. Rev. E*, 84(021122), 2011.

[16] S. Karlin and H.M. Taylor. *A First Course in Stochastic Processes*. Academic Press, New York, 2nd edition, 1975.

[17] S. Karlin and H.M. Taylor. *A Second Course in Stochastic Processes*. Academic Press, New York, 2nd edition, 1980.

[18] H. Ge and H.Qian. Analytical mechanics in stochastic dynamics: Most probable path, large-deviation rate function and hamilton-jacobi equation. 2011.

[19] Van Kampen N. G. *Stochastic processes in Physics and Chemistry*. North-Holland, Elsevier Science, 2007.

[20] E. Baake and W. Gabriel. Biological evolution through mutation, selection, and drift: An introductory review. *Annu. Rev. Comput. Phys.*, 7:203–264, 2000.

[21] M. Eigen. Selforganization of matter and the evolution of biological macromolecules. *Naturwissenschaften*, 58(10):465–523, 1971.

[22] M. Eigen, J. McCaskill, and P. Schuster. The molecular quasispecies. *Adv. Chem. Phys.*, 75:149–263, 1989.

[23] D. B. Saakian and C.-K. Hu. Eigen model as a quantum spin chain: Exact dynamics. *Phys. Rev. E*, 69(021913), 2004.

[24] J. F. Crow and M. Kimura. *An Introduction to Population Genetics Theory*. Harper Row, New York, 1970.

[25] E. Baake, M. Baake, and H. Wagner. Ising quantum chain is equivalent to a model of biological evolution. *Phys. Rev. Lett.*, 78(559), 1997.

[26] D. B. Saakian and C.-K. Hu. Solvable biological evolution model with a parallel mutation-selection scheme. *Phys. Rev. E*, 69(046121), 2004.

[27] M. Eigen. Error catastrophe and antiviral strategy. *Proc. Natl. Acad. Sci. USA*, 99:13374–13376, 2002.

[28] Bocharov G, Ford NJ, Edwards J, Breinig T, Wain-Hobson S, and Meyerhans A. A genetic-algorithm approach to simulating human immunodeficiency virus evolution reveals the strong impact of multiply infected cells and recombination. *J. Gen. Virol.*, 86:3109–18, 2005.

[29] S.A. Meguid, G. Shagal, J.C. Stranart, and J. Daly. Three-dimensional dynamic finite element analysis of shot-peening induced residual stresses. *Finite Elements in Analysis and Design*, 31:179–191, 1999.

[30] M Kobayashi, T Matsui, and Y Murakami. Mechanism of creation of compressive residual stress by shot peening. *International Journal of Fatigue*, 20(5):351–357, 1998.

[31] N. R. Tao, M. L. Sui, J. Lu, and K Lua. Surface nanocrystallization of iron induced by ultrasonic shot peening. *Nanostruct. Mater.*, 11(4):433–440, 1999.

[32] G. Liu, J. Lu, and K. Lu. Surface nanocrystallization of 316l stainless steel induced by ultrasonic shot peening. *Mater Sci Eng A.*, 286:91–95, 2000.

[33] H.L. Chan, H.H. Ruan, A.Y. Chen, and J. Lu. Optimization of the strain rate to achieve exceptional mechanical properties of 304 stainless steel using high speed ultrasonic surface mechanical attrition treatment. *Acta Materialia*, 58(15):5086–5096, 2010.

[34] N.R. Tao, Z.B. Wang, W.P. Tong, M.L. Sui, J. Lu, and K. Lu. An investigation of surface nanocrystallization mechanism in fe induced by surface mechanical attrition treatment. *Acta Mater.*, 50(4603-4616), 2002.

[35] N.W. Zhang, Z.K. Hei, G. Liu, J. Lu, and K. Lu. Formation of nanostructured surface layer on aisi 304 stainless steel by means of surface mechanical attrition treatment. *Acta Mater.*, 51(1871-1881), 2003.

[36] K. Wang, N.R. Tao, G. Liu, J. Lu, and K. Lu. Plastic strain-induced grain refinement at the nanometer scale in copper. *Acta Mater.*, 54:5281–5291, 2006.

[37] K. Lu and J. Lu. Nanostructured surface layer on metallic materials induced by surface mechanical attrition treatment. *Mater. Sci. Eng. A*, 375:38–45, 2004.

[38] X. Wu, N. Tao, Y. Hong, B. Xu G. Liu, J. Lu, and K. Lu. Strain-induced grain refinement of cobalt during surface mechanical attrition treatment. *Acta Mater.*, 53:681–691, 2005.

[39] K.Y. Zhu, A. Vassel, F. Brisset, K. Lu, and J. Lu. Nanostructure formation mechanism of £titanium using smat. *Acta Mater.*, 52:4101–4110, 2004.

[40] X. Wu, N. Tao, B. Xu Y. Hong, J. Lu, and K. Lu. Microstructure and evolution of mechanically-induced ultrafine grain in surface layer of al-alloy subjected to ussp. *Acta Mater.*, 50:2075–2084, 2002.

[41] N. R. Tao, J. Lu, and K. Lu. Surface nanocrystallization by surface mechanical attrition treatment. *Materials Science Forum*, 579:91–108, 2008.

[42] Cynthia L. Kelchner, S. J. Plimpton, and J. C. Hamilton. Dislocation nucleation and defect structure during surface indentation. *Phys. Rev. B*, 58(11085), 1998.

[43] H. Van Swygenhoven and P. M. Derlet. Grain-boundary sliding in nanocrystalline fcc metals. *Phys. Rev. B*, 64(224105), 2001.

[44] Y. H. Zhao, K. Lu, and K. Zhang. Microstructure evolution and thermal properties in nanocrystalline cu during mechanical attrition. *Phys. Rev. B*, 66(085404), 2002.

[45] H. Goldstein. *Classical Mechanics*. Addison-Wesley, 3rd edition, 2000.

[46] S. R. S. Varadhan. Asymptotic probabilities and differential equations. *Comm. Pure Appl. Math.*, 19:261–286, 1966.

[47] W. Y. Tsai, J. C. Huang, Yu Jia Gao, Y. L. Chung, and Guan-Rong Huang. Relationship between microstructure and properties for ultrasonic surface mechanical attrition treatment. *Scripta Mater.*, 103:45–48, 2015.

[48] L.Cai, N. Friedman, and X.S. Xie. Stochastic protein expression in individual cells at the single molecule level. *Nature*, 440(7082):358–362, 2006.

[49] Harry Bateman. *Higher Transcendental Functions*, volume 1. McGraw-Hill, 1953.

[50] Pahle J, Challenger J D, Mendes P, and McKane A J. Biochemical fluctuations, optimisation and the linear noise approximation. *BMC Syst. Biol.*, 6:86, 2012.

[51] Z. Kirakosyan, D. B. Saakian, and C.-K. Hu. Finite genome length corrections for the mean fitness and gene probabilities in evolution models. *J. Stat. Phys.*, 144:198–212, 2011.

[52] J.-M. Park and M. W. Deem. Schwinger boson formulation and solution of the crow-kimura and eigen models of quasispecies theory. *J. Stat. Phys.*, 125:975–1015, 2006.

[53] R. Wurschum, S. Herth, and U. Brossmann. Diffusion in nanocrystalline metals and alloys-a status report. *Adv. Eng. Mater.*, 5:365–372, 2003.

[54] P. Shewmon. *Diffusion in Solids*. John Wiley & Sons, Inc,, 2nd edition, 1989.

Figures and Tables
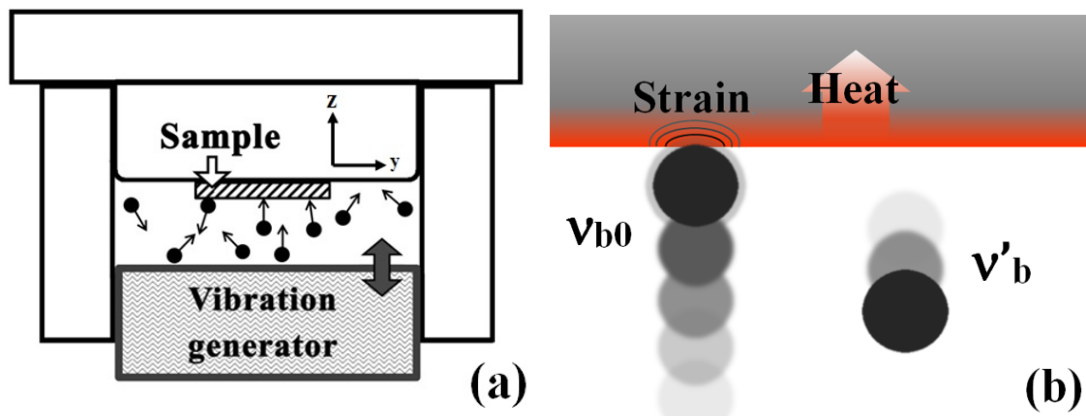
Figure 1.1: (a) The desiged-dimension of chamber in the SMAT experiment. (b) The schematic drawing showing that the sample material gains the heat and strain energy from the kinetic energy loss of sample and flying balls.
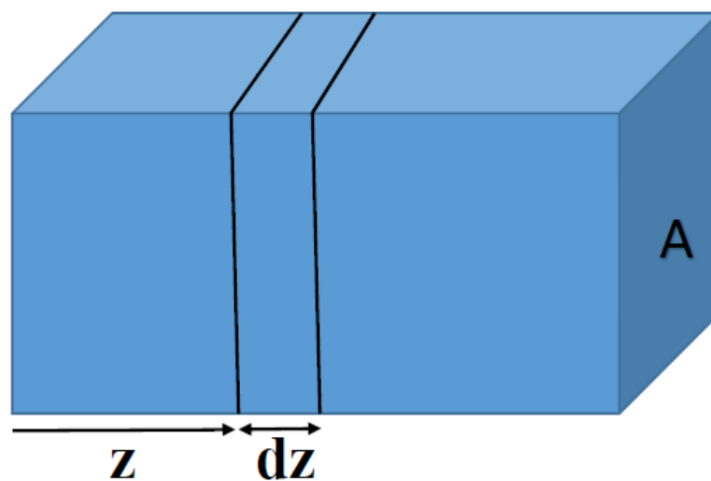
Figure 2.1: The Schematic of sample configuration.
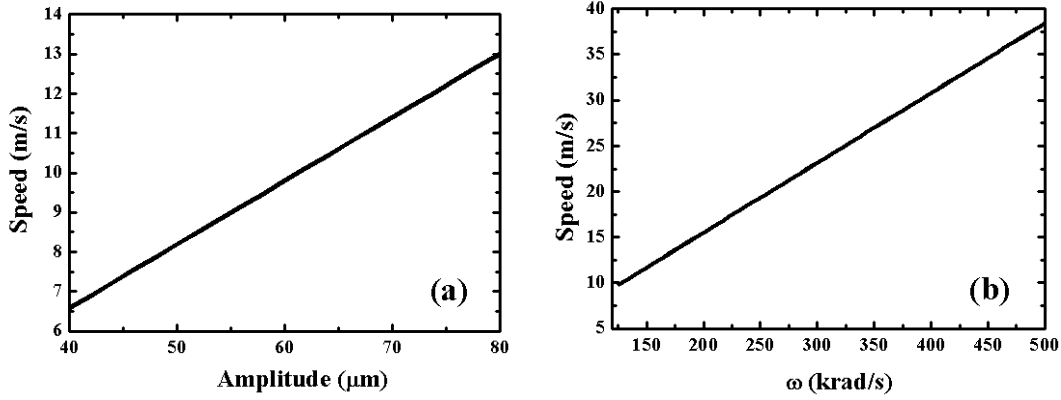
Figure 3.1: (a) The average speed of flying balls (in Eq. (3.59)) versus the SMAT amplitude for the parameters, $H = 20\ mm$, $D = 3\ mm$, $\omega = 40\pi\ krad/s$, and $\frac{m_b}{m_m} = 10^{-6}$. (b) The average speed of flying balls (in Eq. (3.59)) versus the SMAT angular frequency for the parameters, $H = 20\ mm$, $D = 3\ mm$, $A = 60\ \mu m$, and $\frac{m_b}{m_m} = 10^{-6}$.
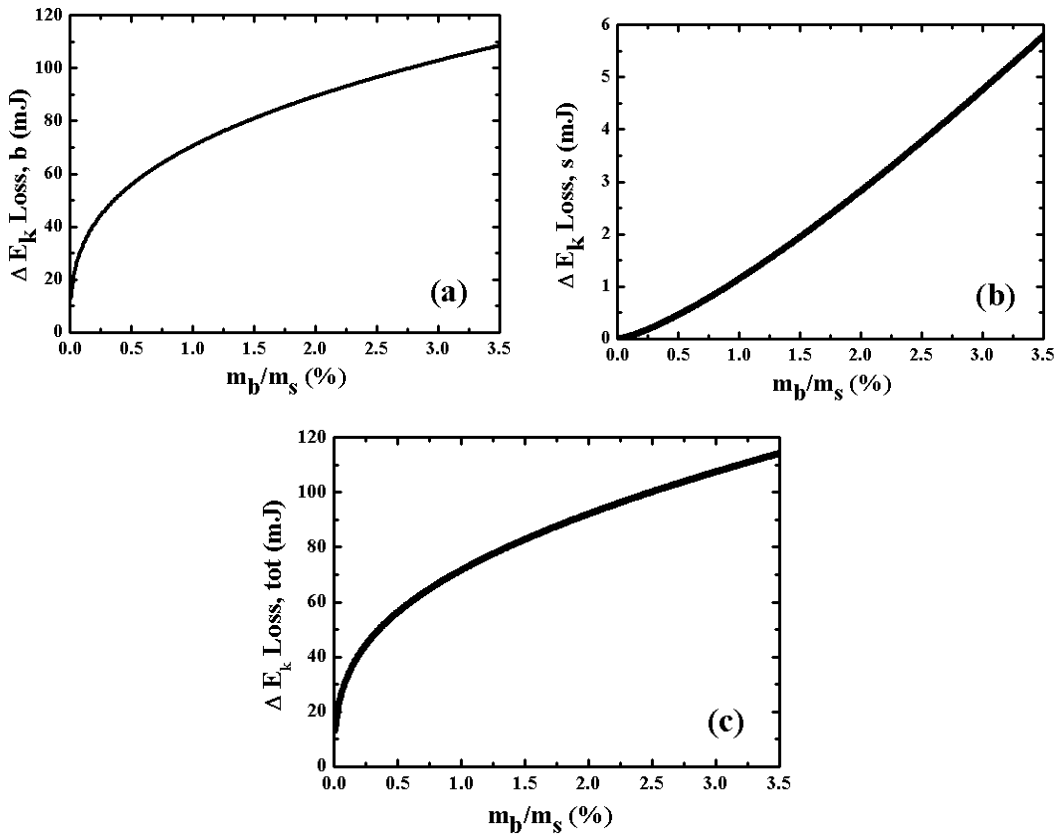
Figure 3.2: (a) The variation trend of $\Delta E_{k,loss,b}$ predicted by Eq. (3.60) as a function of $\frac{m_b}{m_s}$ for the parameters $H = 20\ mm$, $A = 60\ \mu m$, $\omega = 40\pi\ krad/s$, $\frac{m_b}{m_m} = 10^{-6}$, and $e = 0.25$, (b) the variation trend of $\Delta E_{k,loss,s}$ predicted by Eq. (3.61) as a function of $\frac{m_b}{m_s}$ for the parameters $H = 20\ mm$, $A = 60\ \mu m$, $\omega = 40\pi\ krad/s$, $\frac{m_b}{m_m} = 10^{-6}$, and $e = 0.25$, (c) the variation trend of total energy loss, i.e., the sum of $\Delta E_{k,loss,b}$ and $\Delta E_{k,loss,s}$ as a function of $\frac{m_b}{m_s}$ for the parameters $H = 20\ mm$, $A = 60\ \mu m$, $\omega = 40\pi\ krad/s$, $\frac{m_b}{m_m} = 10^{-6}$, and $e = 0.25$.

118
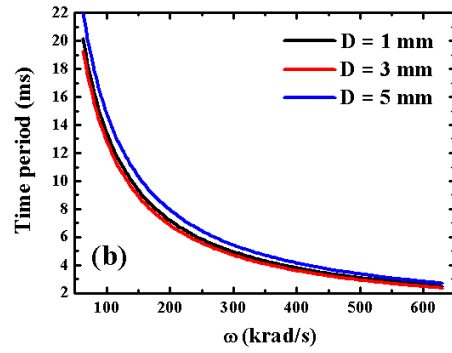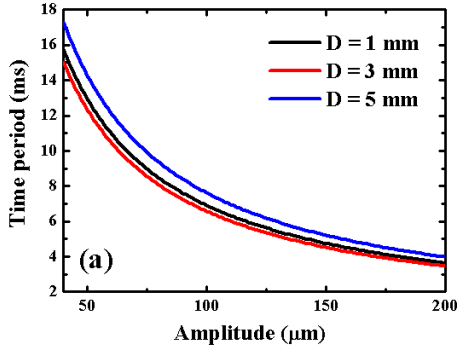
Figure 3.3: (a) The averaged time period of flying balls predicted by Eq. (3.64) versus the SMAT amplitude for the parameters $H = 20\ mm$, $\omega = 40\pi\ krad/s$, $\frac{m_b}{m_m} = 10^{-6}$, and $e = 0.25$. (b) The averaged time period of flying balls predicted by Eq. (3.64) versus the SMAT angular frequency for the parameters $H = 20\ mm$, $A = 60\ \mu m$, $\frac{m_b}{m_m} = 10^{-6}$, and $e = 0.25$.
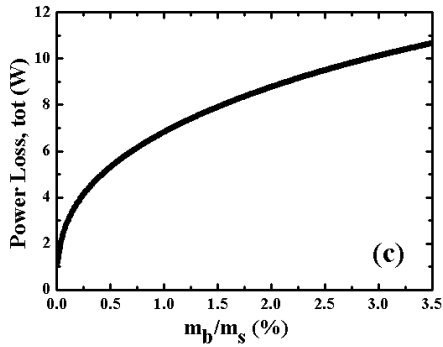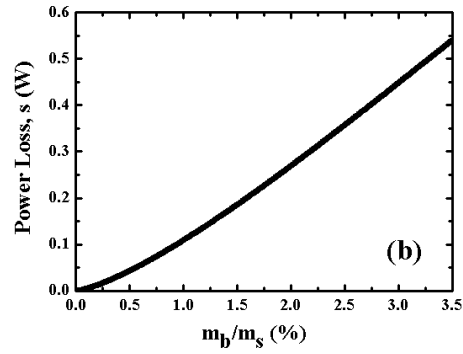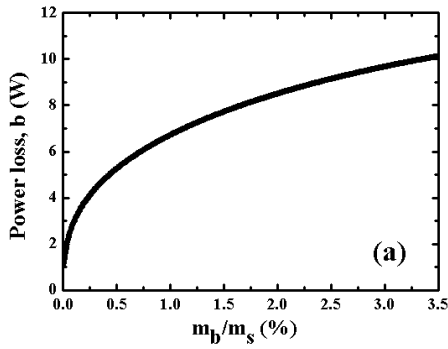
Figure 3.4: (a) The variation trend of $P_{loss,b}$ predicted by Eq. (3.65) as a function of $\frac{m_b}{m_s}$ for the parameters $H = 20\ mm$, $A = 60\ \mu m$, $\omega = 40\pi\ krad/s$, $\frac{m_b}{m_m} = 10^{-6}$, and $e = 0.25$. (b) The variation trend of $P_{loss,s}$ predicted by Eq. (3.66) as a function of $\frac{m_b}{m_s}$ for the parameters $H = 20\ mm$, $A = 60\ \mu m$, $\omega = 40\pi\ krad/s$, $\frac{m_b}{m_m} = 10^{-6}$, and $e = 0.25$. (c) The variation trend of the total power loss, i.e., the sum of $P_{loss,b}$ and $P_{loss,s}$ as a function of $\frac{m_b}{m_s}$ for the parameters $H = 20\ mm$, $A = 60\ \mu m$, $\omega = 40\pi\ krad/s$, $\frac{m_b}{m_m} = 10^{-6}$, and $e = 0.25$.
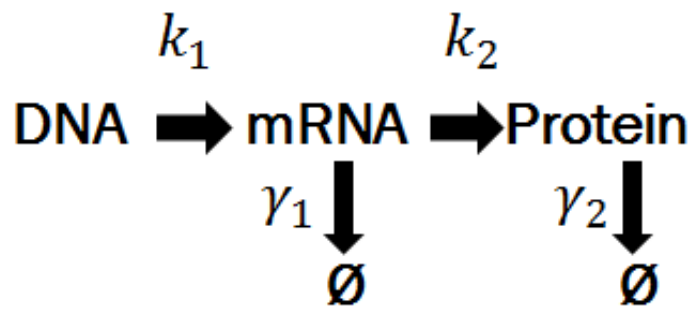
Figure 4.1: The mechanism for DNA-mRNA-protein process.
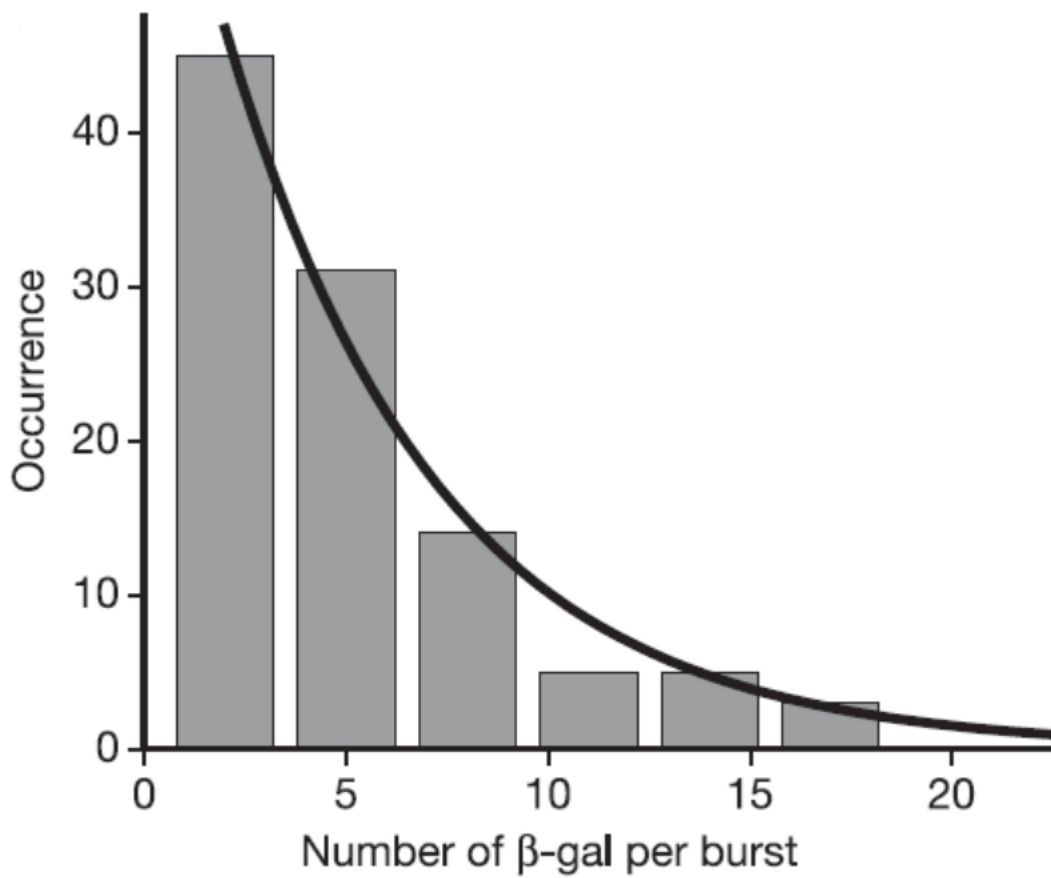
Figure 4.2: The transition PDF for mRNA-protein process.
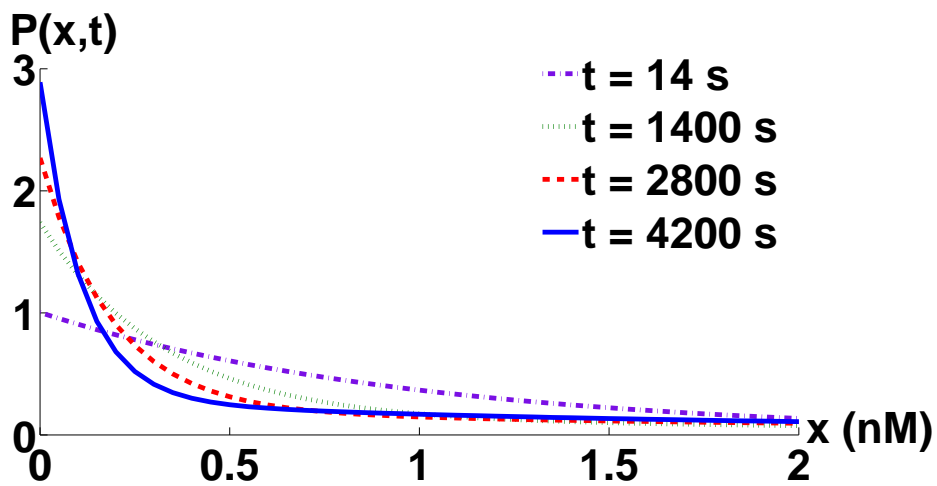
Figure 4.3: The simulation for the dynamical state of PDF with parameters: $a = 0.5$ and $b = 5$ from $t = 14\ s \sim 4200\ s$.
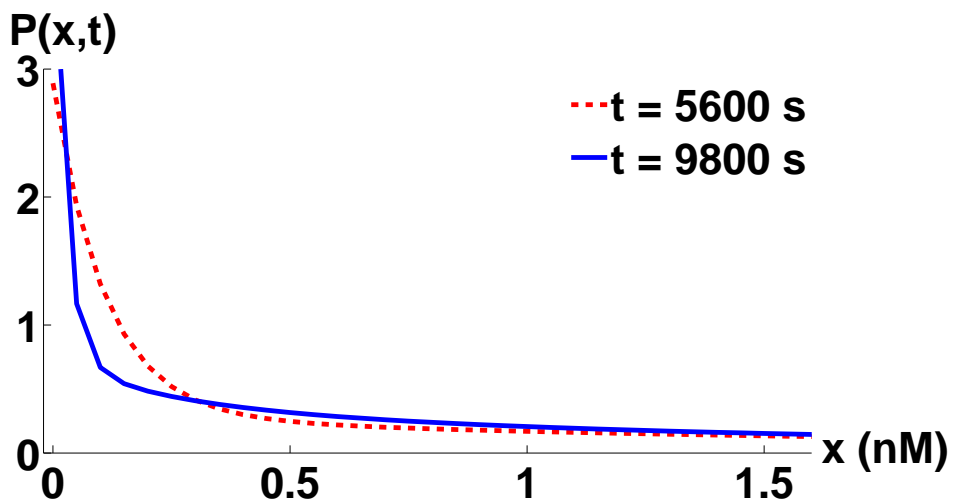
Figure 4.4: The simulation for the dynamical state of PDF with parameters: $a = 0.5$ and $b = 5$ from $t = 5600\ s \sim 9800\ s$.
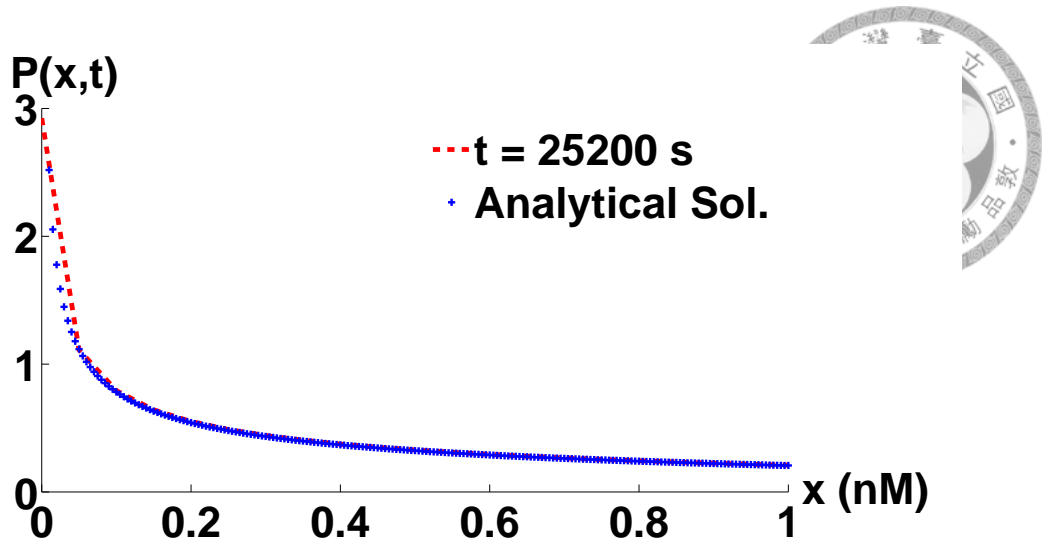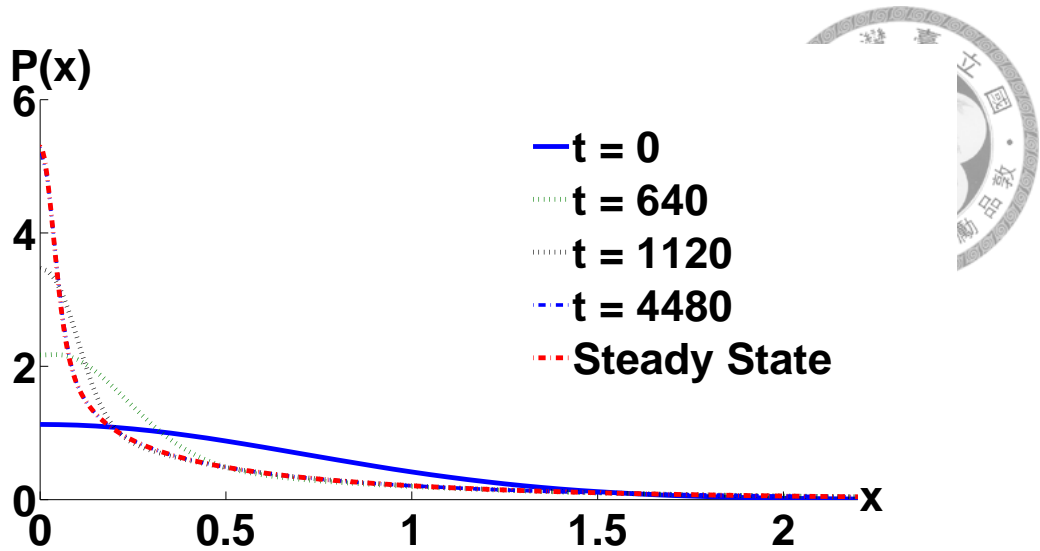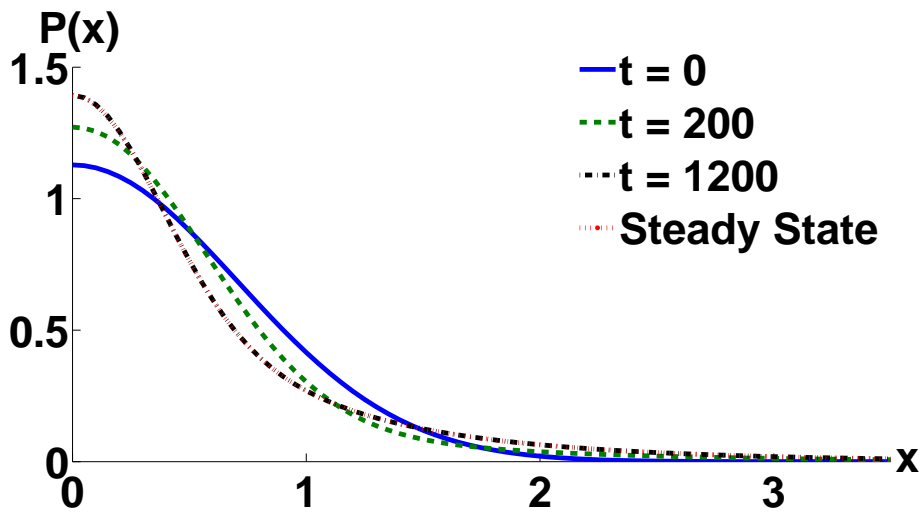
Figure 4.5: The simulation at $t = 25200\ s$ for the dynamical state of PDF and analytical solution with parameters: $a = 0.5$ and $b = 5$.
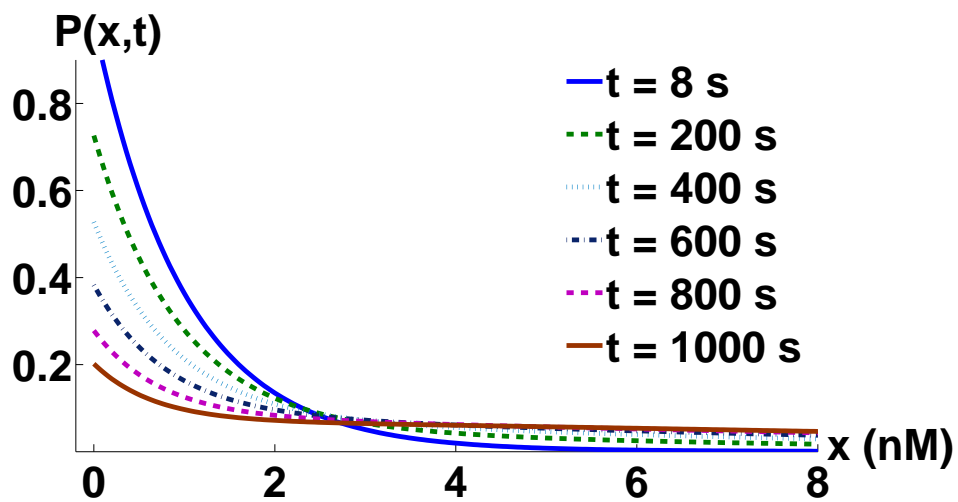
Figure 4.6: The simulation from $t = 8\ s \sim 1000\ s$ for the dynamical state of PDF with parameters: $a = 5$ and $b = 5$.
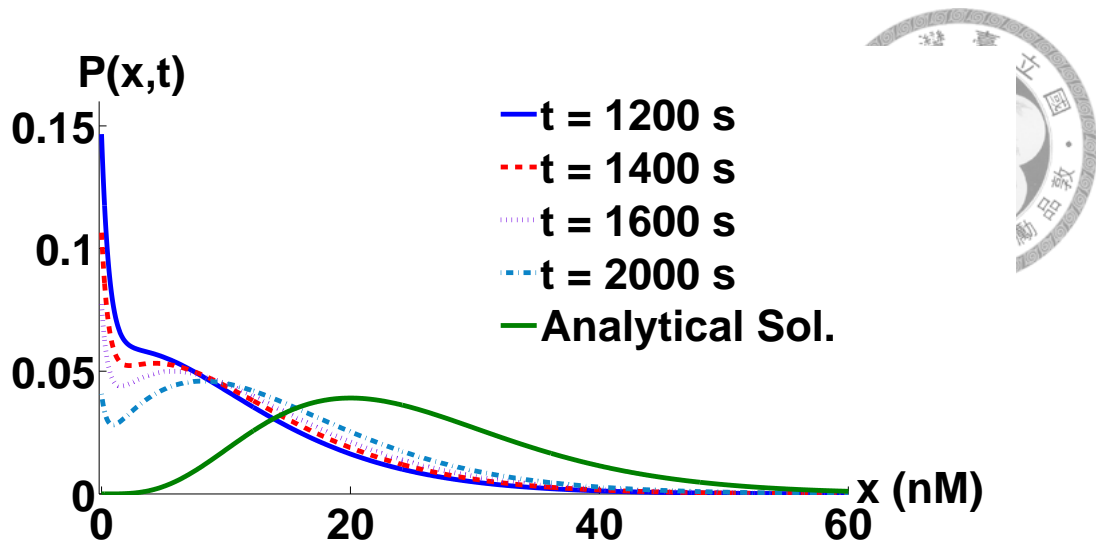
Figure 4.7: The simulation from $t = 1200\ s \sim 2000\ s$ for the dynamical state of PDF and analytical solution with parameters: $a = 5$ and $b = 5$.
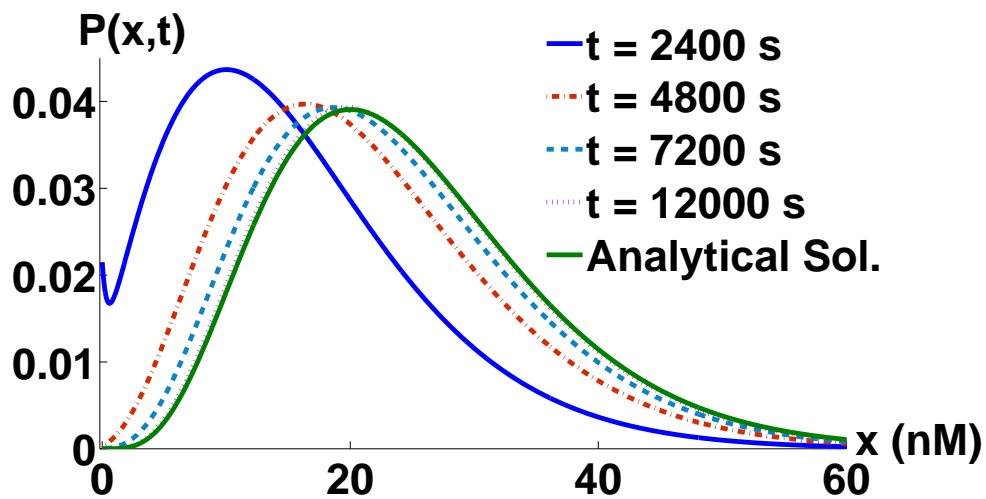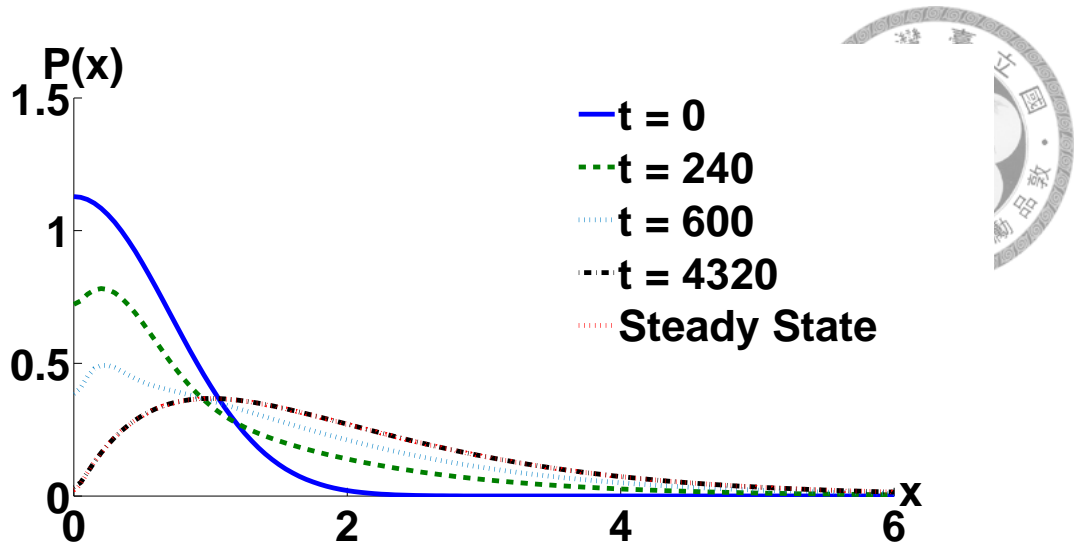

Figure 4.8: The simulation from $t = 2400\ s \sim 12000\ s$ for the dynamical state of PDF and analytical solution with parameters: $a = 5$ and $b = 5$.
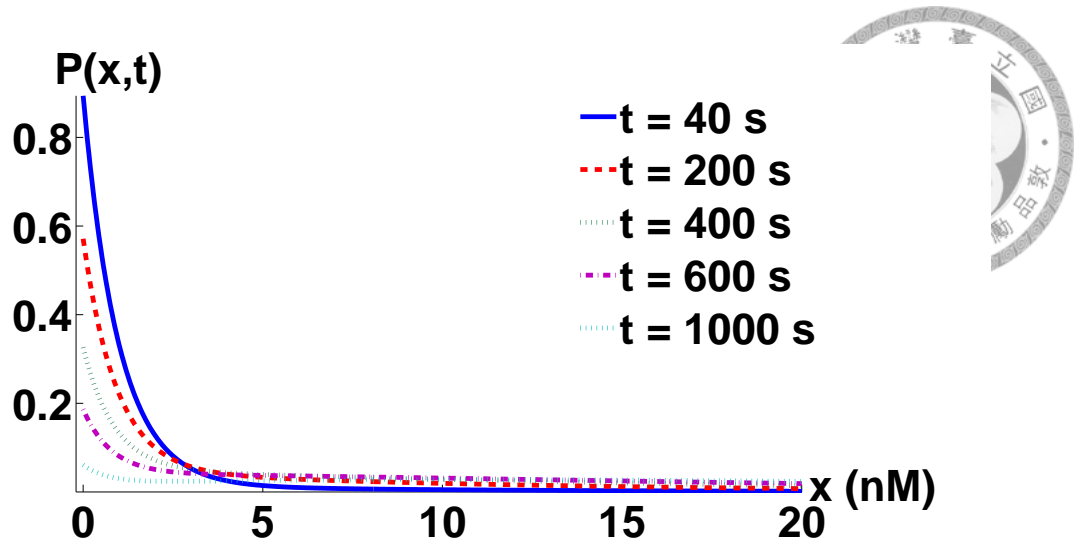
Figure 4.9: The simulation from $t = 40\ s \sim 1000\ s$ for the dynamical state of PDF with parameters: $a = 8$ and $b = 8$.
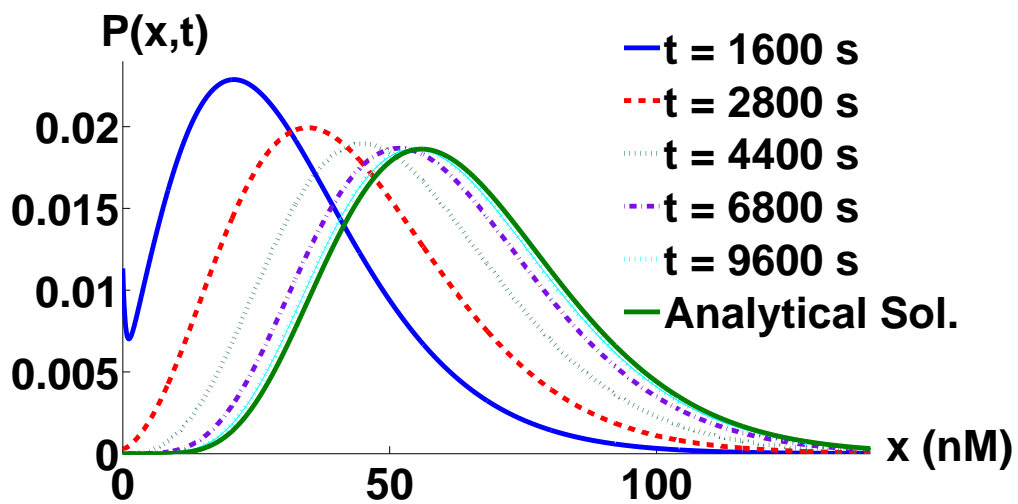
Figure 4.10: The simulation from $t = 1600\ s \sim 9600\ s$ for the dynamical state of PDF and analytical solution with parameters: $a = 8$ and $b = 8$.
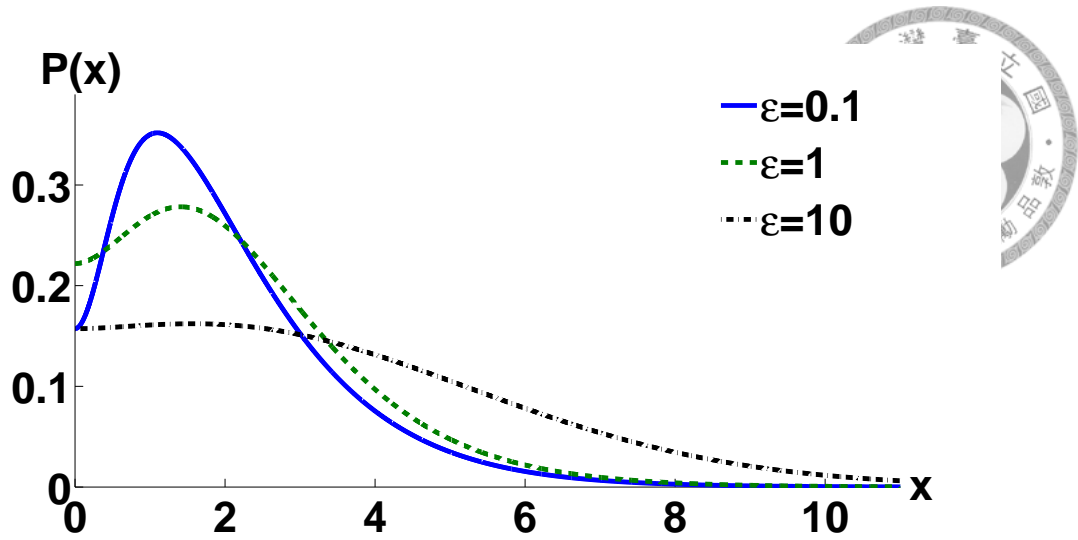
Figure 4.11: The steady-state of PDF for Eq. (4.11) with parameters: $a = 2$, $k = 1$, and $\gamma_2 = 1$.
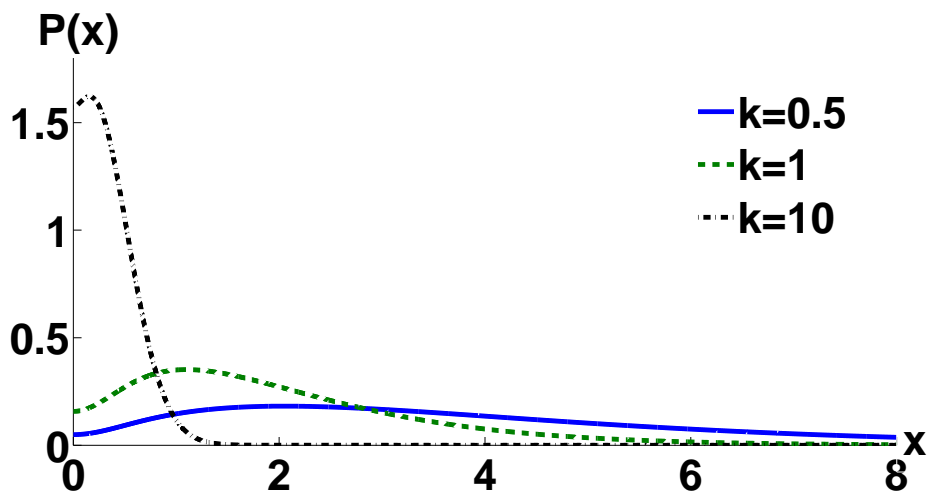
Figure 4.12: The steady-state of PDF for Eq. (4.11) with parameters: $a = 2$, $\epsilon = 0.1$, and $\gamma_2 = 1$.

Figure 4.13: The simulation from $t = 0 \sim 4480$ for the dynamical state of PDF and analytical solution with parameters: $a = 0.5$, $\epsilon = 2 \times 10^{-6}$, $\gamma_2 = 2 \times 10^{-3}$, and $k = 1$.
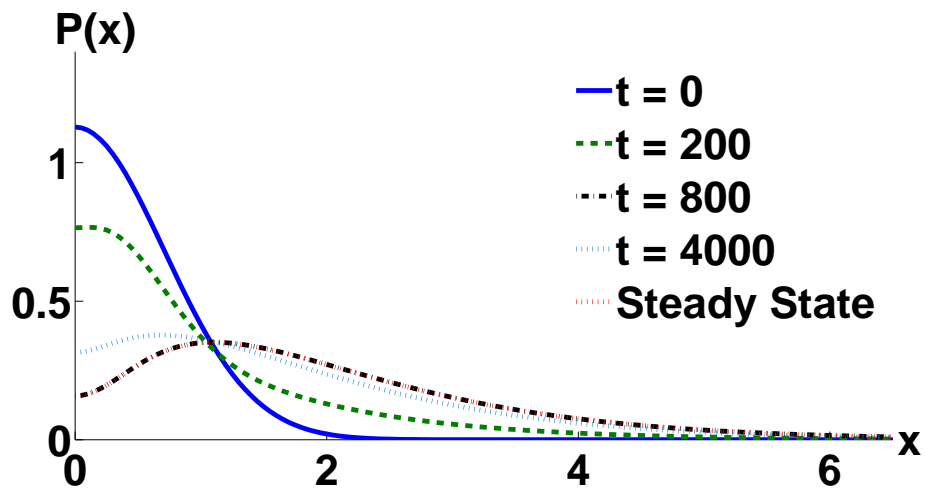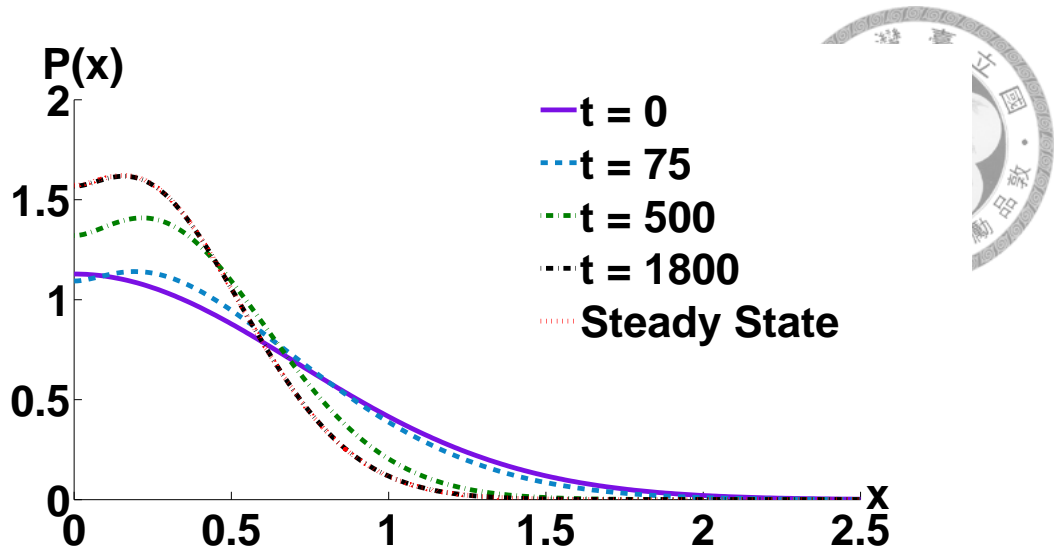

Figure 4.14: The simulation from $t = 0 \sim 1200$ for the dynamical state of PDF and analytical solution with parameters: $a = 0.5$, $\epsilon = 2 \times 10^{-4}$, $\gamma_2 = 2 \times 10^{-3}$, and $k = 1$.

Figure 4.15: The simulation from $t = 0 \sim 4320$ for the dynamical state of PDF and analytical solution with parameters: $a = 2$, $\epsilon = 2 \times 10^{-6}$, $\gamma_2 = 2 \times 10^{-3}$, and $k = 1$.
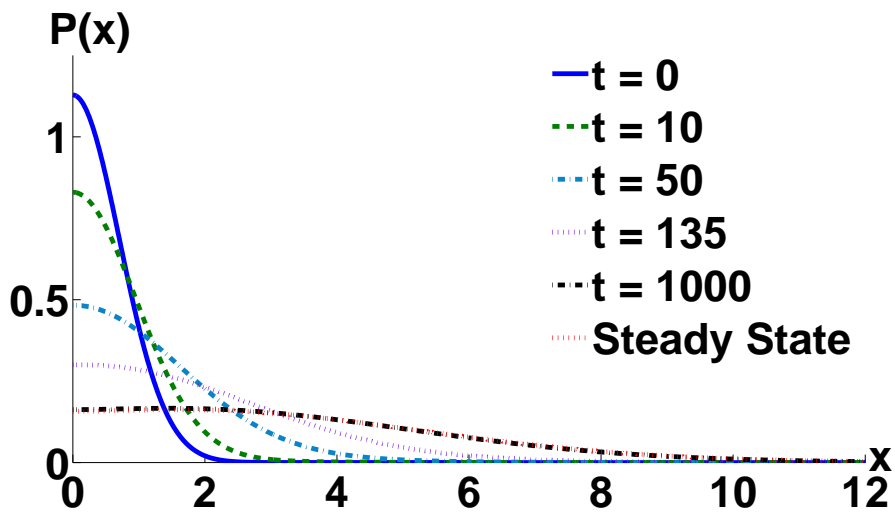

Figure 4.16: The simulation from $t = 0 \sim 4000$ for the dynamical state of PDF and analytical solution with parameters: $a = 2$, $\epsilon = 2 \times 10^{-4}$, $\gamma_2 = 2 \times 10^{-3}$, and $k = 1$.

Figure 4.17: The simulation from $t = 0 \sim 1800$ for the dynamical state of PDF and analytical solution with parameters: $a = 2$, $\epsilon = 2 \times 10^{-4}$, $\gamma_2 = 2 \times 10^{-3}$, and $k = 10$.

Figure 4.18: The simulation from $t = 0 \sim 1000$ for the dynamical state of PDF and analytical solution with parameters: $a = 2$, $\epsilon = 0.02$, $\gamma_2 = 2 \times 10^{-3}$, and $k = 1$.
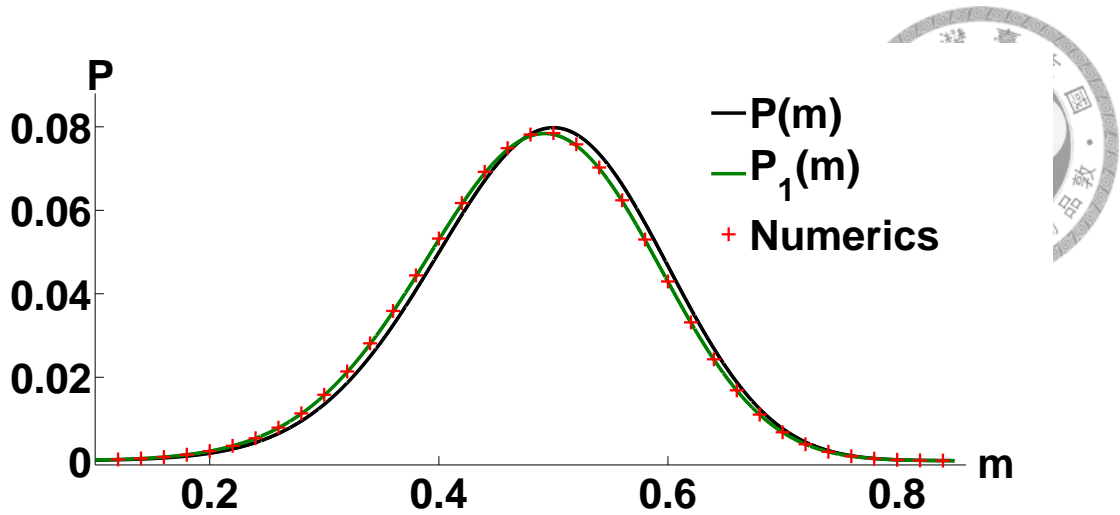
Figure 4.19: The probability distributions predicted by Eq. (4.65) and numerical results with the fitness function and parameters: $N = 100$, $f(m) = e^{m^2}$, and $\gamma = 1$.
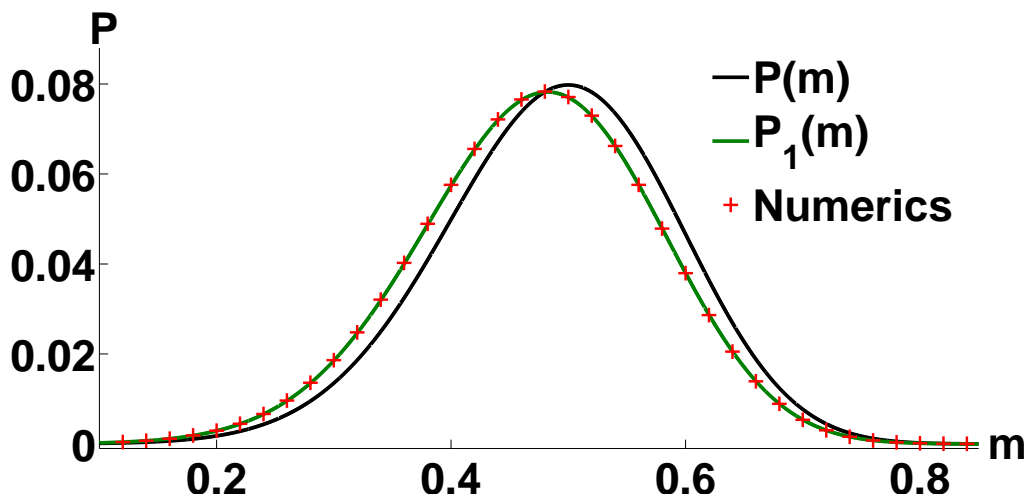

Figure 4.20: The probability distributions predicted by Eq. (4.65) and numerical results with the fitness function and parameters: $N = 100$, $f(m) = e^{2m^2}$, and $\gamma = 2$.
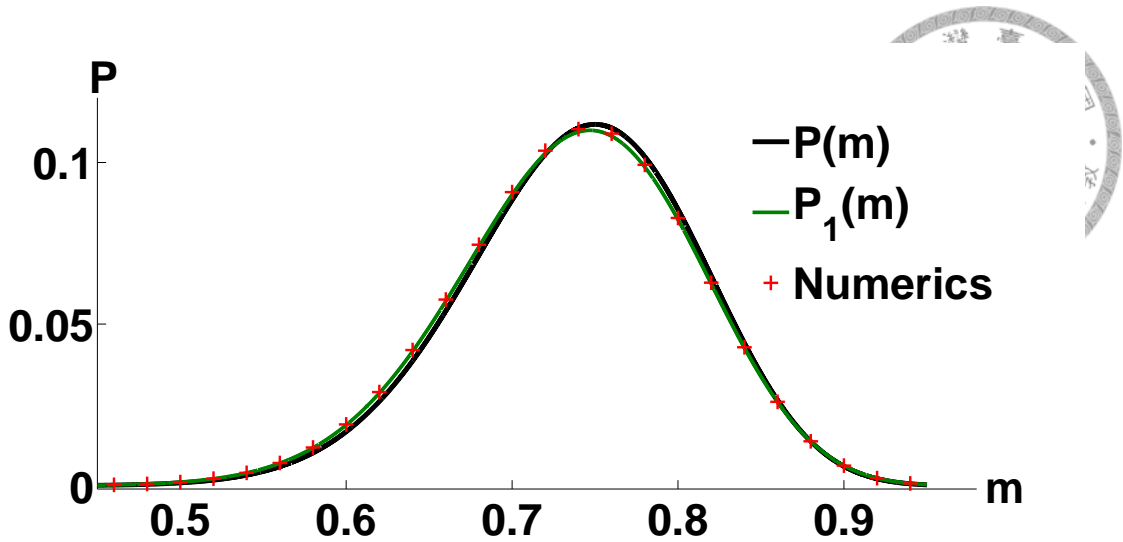
Figure 4.21: The probability distributions predicted by Eq. (4.65) and numerical results with the fitness function and parameters: $N = 100$, $f(m) = e^{2m^2}$, and $\gamma = 1$.

Table 4.1: The comparison of our results among $P(m)$, $P_1(m)$, and numerics for the fitness function and parameters: $f(m) = e^{m^2}, \gamma = 1, N = 100$.

m	0.44	0.46	0.48	0.50	0.52	0.54
$P(m)$	0.0672	0.0738	0.0782	0.0798	0.0782	0.0735
$P_1(m)$	0.0691	0.0748	0.0780	0.0784	0.0757	0.0702
Numerics	0.0692	0.0749	0.0781	0.0785	0.0758	0.0703

Table 4.2: The comparison of our results among $P(m)$, $P_1(m)$, and numerics for the fitness function and parameters: $f(m) = e^{2m^2}, \gamma = 2, N = 100$.

m	0.44	0.46	0.48	0.50	0.52	0.54
$P(m)$	0.0672	0.0738	0.0782	0.0798	0.0782	0.0735
$P_1(m)$	0.0720	0.0764	0.0782	0.0771	0.0730	0.0663
Numerics	0.0721	0.0766	0.0783	0.0771	0.0730	0.0662

Table 4.3: The comparison of our results among $P(m)$, $P_1(m)$, and numerics for the fitness function and parameters: $f(m) = e^{2m^2}, \gamma = 1, N = 100$.

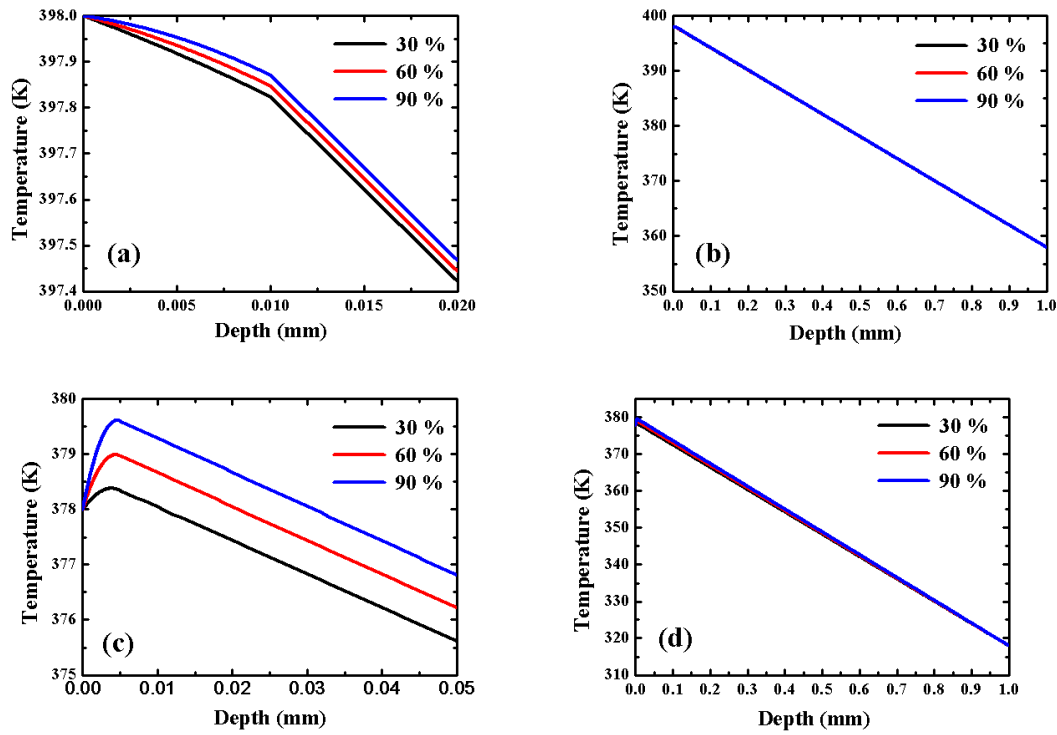| m	0.68	0.70	0.72	0.74	0.76	0.78
$P(m)$	0.0722	0.0894	0.1036	0.1118	0.1117	0.1028
$P_1(m)$	0.0744	0.0906	0.1033	0.1099	0.1086	0.0991
Numerics	0.0746	0.0908	0.1036	0.1103	0.1089	0.0993

Figure 4.22: The temperature distributions for pure Cu predicted by Eq. (4.69) for narrow region near the surface in (a) and for wider region in (b) with the parameters $k_0 = 401\ W/m \cdot K$, $q = 0.772 \times 10^3 \sim 2.28 \times 10^3\ W/mm^3$, $A_s = 800\ mm^2$, $L = 1\ mm$, $l = 5\ \mu m$, $T_b = 398\ K$, and $T_t = 358\ K$. The temperature distributions for 304 stainless steel predicted by Eq. (4.69) for narrow region near the surface in (c) and for wider region in (d) with the parameters $k = 14.9\ W/m \cdot K$, $q = 0.773 \times 10^3 \sim 2.28 \times 10^3\ W/mm^3$, $A_s = 800\ mm^2$, $L = 1\ mm$, $l = 5\ \mu m$, $T_b = 378\ K$, and $T_t = 318\ K$. The different colored lines correspond to various percentages of kinetic energy loss which is converted into the heat energy of sample.
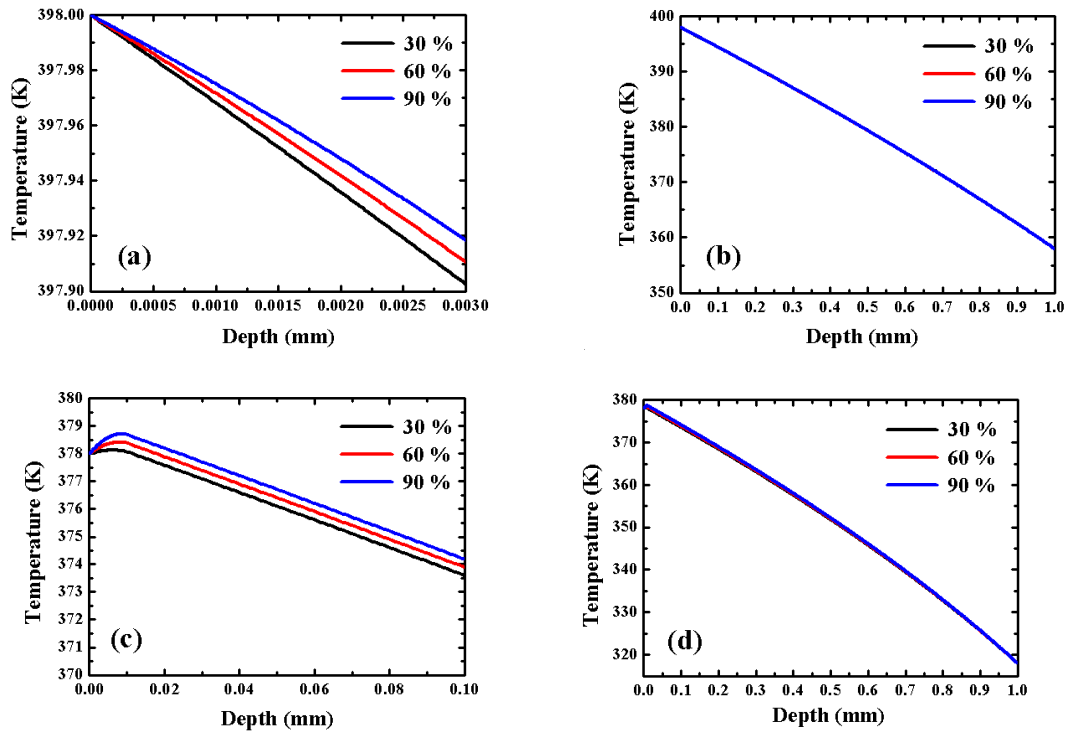
Figure 4.23: The temperature distributions for pure Cu predicted by Eq. (4.71) for narrow region near the surface in (a) and for wider region in (b) with the parameters $k_0 = 401 \ W/m \cdot K$, $q = 0.772 \times 10^3 \sim 2.28 \times 10^3 \ W/mm^3$, $A_s = 800 \ mm^2$, $L = 1 \ mm$, $l = 5 \ \mu m$, $T_b = 398 \ K$, and $T_t = 358 \ K$. The temperature distributions for 304 stainless steel predicted by Eq. (4.71) for narrow region near the surface in (c) and for wider region in (d) with the parameters $k = 14.9 \ W/m \cdot K$, $q = 0.773 \times 10^3 \sim 2.28 \times 10^3 \ W/mm^3$, $A_s = 800 \ mm^2$, $L = 1 \ mm$, $l = 5 \ \mu m$, $T_b = 378 \ K$, and $T_t = 318 \ K$. The different colored lines corresponds to various percentages of kinetic energy loss which is converted into the heat energy of sample.
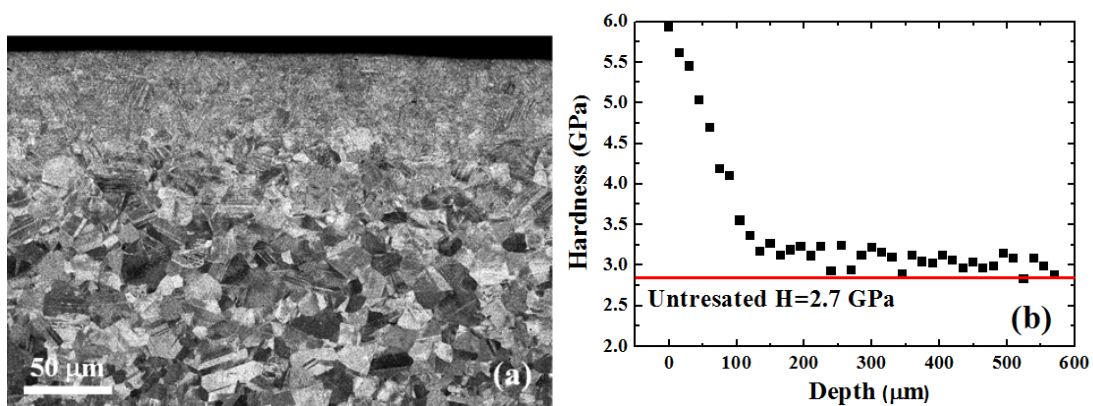

Figure 5.1: (a) The cross-sectional SEM micrograph taken from the sample subject to SMAT with the $2 \ mm$ flying balls and $40 \ \mu m$ SMAT amplitude. (b) The gradient variation trend of hardness of selected SMAT 304 SS samples.
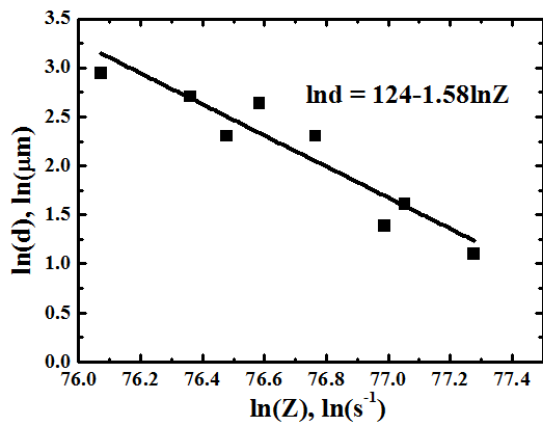
Figure 5.2: The relationship between the resulting grain size and Zener-Holloman parameter with the sample processed by different SMAT conditions.